NEAR-INFRARED ABSORBING PHTHALOCYANINES: SECOND-GENERATION OF PHOTOSENSITIZERS FOR PHOTODYNAMIC THERAPY IN THE THERAPEUTIC BIOLOGIC WINDOW

by

Tuğba Muhlise Okyay

B.S., Chemistry, Boğaziçi University, 2012

Submitted to the Institute for Graduate Studies in
Science and Engineering in partial fulfillment of
the requirements for the degree of
Master of Science

Graduate Program in Chemistry
Bogazici University
2016

Dedicated to my venerable spiritual pathfinder and my dear family.

ACKNOWLEDGEMENTS

First and foremost, I thank my academic co-advisor Assist. Prof. Fabienne Dumoulin, for accepting me into her group. During my tenure, she contributed to a rewarding graduate lab experience by giving me intellectual freedom in my work, supporting my attendance at various conferences, engaging me in new ideas, and demanding a high quality of work in all my endeavors. I am so grateful for her contribution to my chemistry and experimental knowledge. I gained a lot from her scientific knowledge and bench chemistry. Additionally, I would like to thank my thesis advisor Assist. Prof. Mehmet Fırat İlker. Throughout the thesis, his positive attitude has been the most encouraging force for me to pursue my thesis with an ambition. He was the one who always stands behind me and trusts in me. His mentorship always encouraged me to follow my dreams and his recommendations were consistent with my long-term career goals.

I would like to express my special thanks to Prof. Selim Küsefoğlu for his recommendations and support since my undergraduate years.

I wish to extend my thanks to Fabienne's group members; Tuğba Küçük, Songül Yaşar, Gülçin Kara Ekineker, Ufuk Kumru, Osman Cahit Demirci, Muzaffer Köç, Serkan Alpugan and Zeynel Şahin for their assistance and sharing their experience with me throughout the course of this work.

In particular, I would also like to thank Yunus Zorlu for introducing me to Assist. Prof. Fabienne Dumoulin.

I am grateful for the funding source TUBİTAK (The Scientific and Technological Research Council of Turkey) that supports me financially during my graduate school studies. This work is a part of the French-Turkish bilateral project 113Z595. Also, I would like to thank Kübra Avrupalı Pusat, Sultan Adanır, Büşra Erdem, Zeynep Erçetin, Zehra Uçurum, Semiha Muhterem Ataman, Özge Gençer, Zehra Kural, Saliha İlhan Karagöz for their friendship, support and motivation. Also, I would like to thank to my Bostanian friends

Rabbya RZ, Romeissa Selmane, Amna Khan, Asma Oulbecha, Sadhana Mohammed, Ahlem Assali, Amina Abdussamed, Neima Mohammed, Cassandra Villarael, Asma Soltani and Romeissa Selmane. I am lucky to have met all in Boston.

Lastly, I sincerely thank to my family, my dear father Mesut Okyay, my lovely mother Asiye Okyay and my precious brother Hüseyin Hüsamettin Okyay for their constant love, their faith in me and allowing me to be as ambitious as I wanted. Thank you all.

ABSTRACT

NEAR-INFRARED ABSORBING PHTHALOCYANINES: SECOND-GENERATION OF PHOTOSENSITIZERS FOR PHOTODYNAMIC THERAPY IN THE THERAPEUTIC BIOLOGIC WINDOW

Photodynamic therapy (PDT) is an alternate cancer therapy and it emphasizes the key role of the light and the photosensitizer as well. A photosensitizer is a chemical compound and has special photophysical properties, which can be suitable for the photodynamic therapy process itself. As a kind of promising second-generation photosensitizer, phthalocyanines have been investigated for a long time in photodynamic therapy field. Many novel phthalocyanines are obtained by various structural modifications on them. Recently, attempts to optimize phthalocyanines for PDT focused on the development of near- infrared (NIR) absorbing phthalocyanines. The most important reason for this is the ability of phthalocyanines absorbing in NIR region allows phthalocyanines to penetrate deeper in the tissue and in the therapeutic window as well.

For this reason, in this thesis thiol substituted phthalonitriles and their related derivatives nonperipheral octa -SR phthalocyanines have been designed and synthesized. These molecules were characterized with MALDI, ATR-IR, UV-Vis and NMR spectroscopy.

Additionally, while aiming a new substitution pattern for phthalocyanines a novel asymmetric AB_3 type -diSO_2 substituted phthalocyanine was investigated.

ÖZET

YAKIN KIZILÖTESİ BÖLGESİNDE ABSORPSİYON YAPAN FTALOSİYANİNLER: BİYOLOJİK TEDAVİ PENCERESİNDE FOTODİNAMİK TERAPİ İÇİN İKİNCİ NESİL IŞIĞA DUYARLI MADDELER

Fotodinamik terapi alternatif kanser tedavisi olup aynı zamanda ışığın ve fotosensitizerin önemli rolünü vurgulamaktadır. Fotosensitizer fotodinamik terapi işleminde tanımlanabilecek kendine özgü fotofiziksel özelliklere sahip kimyasal bileşiğe denmektedir. İkinci jenerasyon fotosensitizer olan ftalosiyaninler fotodinamk terapi alanında uzun süredir araştırılmaktadırlar. Pek çok yeni ftalosiyaninler çeşitli yapısal değiştirmeler sonucunda elde edilmektedir. Son dönemlerde fotodinamik tedavi için optimize edilmiş ftalosiyaninler elde etmeye yönelik girişimler yakın kızılötesi bölgede absorpsiyon yapan ftalosiyaninler üzerinde odaklanmıştır. Bunun en önemli sebebi yakın kızıl ötesinde absorpsiyon yapan ftalosiyaninlerin doku içinde daha derine nüfuz edebilmesidir.

Bu sebeple bu tezde tiyol sübstitüe ftalonitriller ve onların nonperiferal okta -SR türevleri dizayn edilmiş ve sentezlenmiştir. Bu moleküller MALDI, ATR-IR, UV-Vis and NMR spektroskopileriyle karakterize edilmişlerdir.

Ek olarak yeni bir sübstitüe arayışı içerisindeyken yeni asimetrik AB_3 tipi -diSO_2 sübstitüe ftalosiyanin incelenmiştir.

TABLE OF CONTENTS

LIST OF FIGURES

LIST OF TABLES

LIST OF SYMBOLS

cm	Centimeter
d	Doublet
eV	Electron volt
g	Gram
mL	Milliliter
mmol	Millimole
MW	Molecular Weight
m.p.	Melting point
nm	Nanometer
ppm	Parts per million
s	Singlet
t	Triplet
µM	Micromolar
ε	Molar absorptivity
°C	Celcius Degrees

LIST OF ACRONYMS/ABBREVIATIONS

ATR-IR	Attenuated total reflection Infrared Spectroscopy
DCB	Dichlorobenzene
DMF	Dimethyl formamide
DCM	Dicholoromethane
EtOH	Ethanol
FDA	US Food and Drug Administration
IUPAC	International Union of Pure and Applied Chemistry
LED	Light emitting diode
MALDI	Matrix assisted laser desorption ionization
NIR	Near-infrared
PDT	Photodynamic therapy
Pc	Phthalocyanine
ROS	Reactive oxygen species
TLC	Thin layer chromatography
UV-Vis	Ultra violet- visible

1. INTRODUCTION

1.1. Photodynamic Therapy

Photodynamic therapy (PDT) is a clinically approved, non-invasive cancer treatment that utilizes the generation of toxic species to eradicate cancer cells. Toxic species, here called as singlet oxygen which is a type of reactive oxygen species (ROS), is a result of activation of photosensitizing agents in the presence of oxygen [1,2]. It is known that PDT as a non-invasive medical technique has a wide range usage mainly developed to treat several types of cancers involving neck, skin, breast, bladder cancer; however, its use is not limited to only oncology. It is also used to treat cardiovascular, dermatological, gynecological and ophthalmic diseases [3,4].

PDT needs three essential components: photosensitizer (PS), light and oxygen. The administered PS becomes active in the patient's body upon irradiation with light of an appropriate wavelength and is singlet produces highly reactive oxygen species which oxygen ($^1O_2$) in PDT case that can act against tumor cells (Figure 1.1) [5,6].

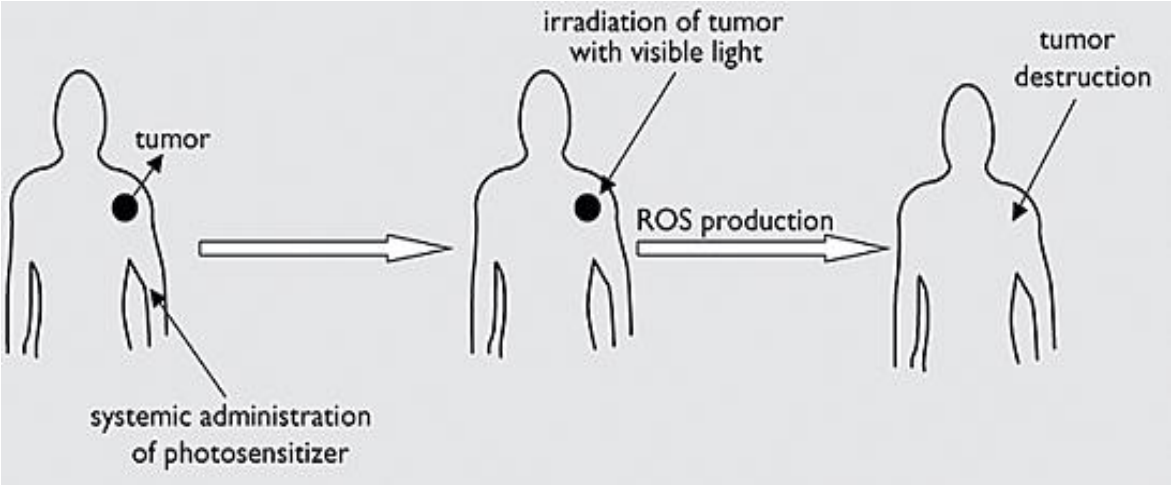

Figure 1.1. Schematic description of the treatment procedure for PDT.

Although PDT has been used for many thousands years, it has emerged as a promising cancer treatment for about four decades. When we look at back to Ancient times we see that Egypt, India, and China have been using sun light in the treatment of disorders such as vitiligo, rickets, psoriasis, skin cancer, and psychosis. The only light source is the sun at the time and people used the healing power of the sun for many years. Later on it is found that artificial light can be used to treat diseases and PDT emerges.

After about 1900, there are many findings related to PDT has started to occur in scientific world. Now it is known that there are many studies that are easily accessible to the readers performed on PDT. At the present time, PDT has been approved for clinical treatment in the United States, the European Union, Canada, Russia, and Japan [7].

1.1.1. Partners of Photodynamic Therapy

Among the three factors, the type of photosensitizer is the most investigated partner of PDT. A photosensitizer is a light-absorbing chemical that initiates a photochemical or photophysical reaction [8]. The type of the photosensitizer affects the efficiency of the PDT. The photosensitizers bring selectivity in PDT since they are activated by light only in a range of specific wavelength. Photoactivation of PS causes the formation of singlet oxygen, which is extremely toxic and leads to cell damage and death [9].

There are several photosensitizing agents currently being used in PDT. Suitable photosensitizers for PDT are mainly porphyrins, including chlorins, bacteriochlorins, phthalocyanines, and naphthalocyanines. They are being considered as second generation photosensitizers. These compounds have extended conjugation and absorb light in the visible region, which makes them colored compounds or dyes (Figure 1.2) [10,11]. Their photophysical properties make them suitable for PDT so they are mostly studied photosensitizers in PDT field.

However, designing improved photosensitizers needs to be considered in many factors such as amphiphilicity, lipophilicity etc.

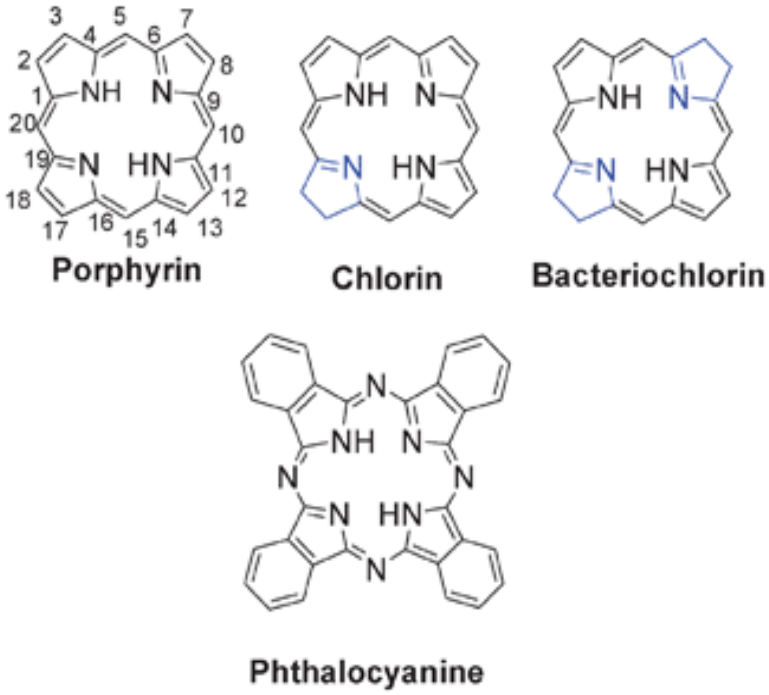

Figure 1.2. Structures of common photosensitizers.

Secondly, light intensity and wavelength are the important factors for PDT efficiency. In the body, photosensitizers accumulates in cancer cells and only become active when light of a certain wavelength is exposed onto the area where the cancer is located.

Main PDT light source includes lasers, light emitting diodes (LEDs) and lamps [12].

1.1.2. Required Properties of a Suitable Photosensitizer for PDT

To facilitate the choice of photosensitizer there are some required properties of a photosensitizer for PDT:

- strong absorption with a high extinction coefficient in the red/near-infrared region of the electromagnetic spectrum (600–850 nm),
- be effective generators of singlet oxygen and other ROS,
- have suitable photophysical characteristics,
- have minimum dark toxicity by itself and negligible cytotoxicity in the absence of

light,

- exhibit greater retention in diseased/target tissue over healthy tissue,
- present rapid excretion from the body,
- be single, well-characterized compounds, with a known and constant composition,
- have a short and high yielding synthetic route (with easy translation into multi-gram scales/reactions),
- have a simple and stable drug formulation,
- be soluble in biological media [13-15].

Depending on the photosensitizing agent, PS can be introduced into body intravenously, orally or topically. After PS was taken, it preferentially accumulates in the tumor region [16].

There are two main reasons for developing PS absorbing near-infrared (NIR) region:

- NIR region is the area where PS achieves the deepest penetration into human tissue, so it facilitates better access to deep tumoral tissues.
- It also minimizes absorption of natural chromophores in therapeutic window.

Since photosensitizer becomes activated upon irradiation, penetration of light into the tissue limits the PDT efficiency. Irradiation with longer wavelengths can penetrate deeper through biological tissue. However water in biological tissues starts to absorb at wavelength longer than 1000 nm and at wavelengths less than 600 nm endogenous chromophores such as hemoglobin have strong absorption. So an ideal PDT photosensitizer should be activated at wavelengths in the range from 600-1000 nm, the so called “therapeutic window”. In this wavelength range, the energy of light is high enough to excite the photosensitizer and yet is low enough so that the light has sufficient penetration into the tissue [17,18].

Figure 1.3 shows the therapeutic window in tissue due to absorption of NIR wavelengths (600-1000 nm) by tissue chromophores [19].

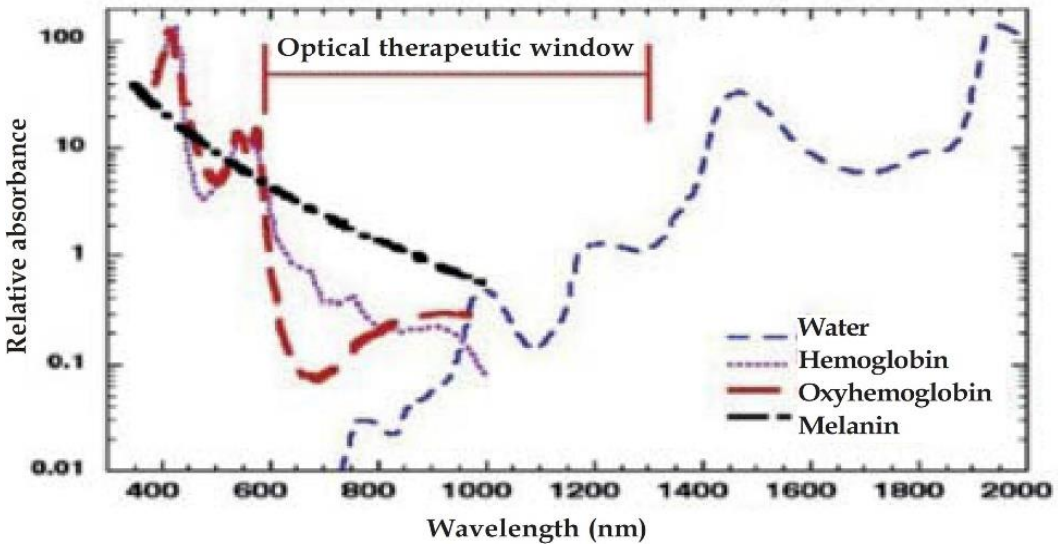

Figure 1.3. Therapeutic window [19].

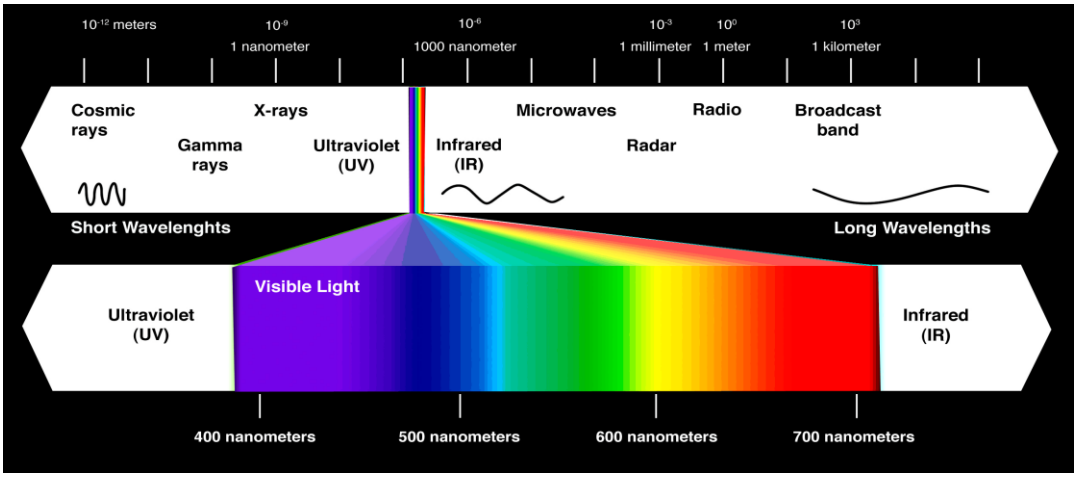

Figure 1.4. Electromagnetic spectrum [20].

One of the primary limitations of photosensitizers which are available now is that their long wavelength absorption is shorter than NIR, which limits their use in treating deep tumors [21].

Hence PDT requires both a selective photosensitizer and a powerful light source.

1.2. Mechanism of Photosensitization

To understand the molecular and cellular mechanisms of PDT one need to look back to the photochemistry processes occurred during PDT. Most available data suggest a common mechanism of action.

Figure 1.5 illustrates the photochemistry of the photosensitizer upon the irradiation with visible light by using Jablonski diagram. A Jablonski diagram, named after the Polish physicist Aleksander Jabłoński, is a diagram that illustrates the electronic states of a molecule and the transitions between them [22].

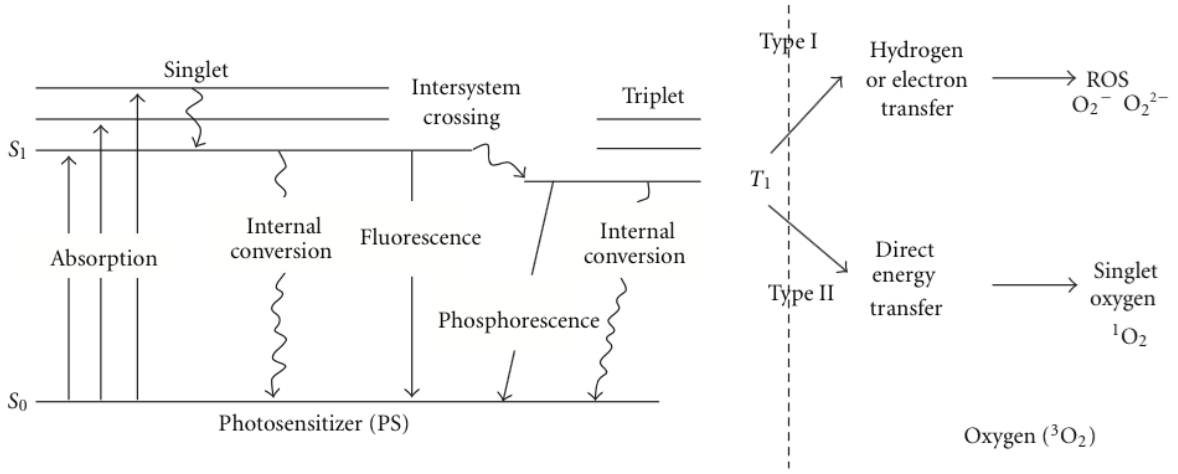

Figure 1.5. Jablonski diagram of the mechanisms of PDT [23].

According to the mechanism of PDT administered photosensitizer in the ground state absorbs the light upon local visible light irradiation and is activated to the single excited state called S_1. During this transition from low energy ground state to the excited singlet state, PS transfer this energy to the oxygen molecules, thereby generates cytotoxic reactive oxygen species (ROS). These ROS are generated during PDT through two types of reactions; type I and type II. Mechanisms (types I and II) of ROS generation by combination of light, photosensitizer (PS) and ground-state oxygen ($^3O_2$) are depicted by Figure 1.5. After the electronic excitation of the molecule, from S_1 it may go down to the ground state S_0, giving

off energy in form of fluorescence or it may undergo an intersystem crossing to the first triplet state, T_1. In type I the triplet PS interacts with a substrate in the surrounding transfers an electron or hydrogen atom producing free radicals. Alternatively in type II triplet PS transfers the energy directly to molecular oxygen to form excited-state singlet oxygen. This highly reactive state of oxygen known as singlet oxygen is the most important reactive specie in PDT. Since the main toxic reagent is the singlet oxygen in PDT, Type II reaction pathway is expected to be the main pathway [24-32].

The combination of these series of events starting with uptake of the photosensitizer gives the therapeutic value. Finally they lead to direct tumor cell death.

Tumor destruction is quite complex it can be said that there is not a direct way to eradicate tumor. Tumor destruction can be achieved not only direct cell kill by necrosis or apoptosis, but also may be indirect such as induction of immunological effects and initiation of tumor anoxia resulting from destruction of the tumor vasculature [33].

1.3. Advantages of Photodynamic Therapy over Other Cancer Therapies

It is well known that PDT offers distinct advantages over other cancer treatments such as chemotherapy, surgery and radiotherapy. The main advantages of PDT are given below:

- PDT is selective,
- It has minimum side effects,
- PDT is less invasive than surgery,
- It is repeatable treatment if needed,
- Finally PDT costs less than other cancer treatments.

PDT offers these advantages whereas chemotherapy has some side effects such as hair loss and vomiting. PDT is selective meaning that minimal damage to surrounding tissue. Since only the area that the light is exposed is cured it can be targeted very precisely. In PDT scalpels are not needed to use as in surgery so less invasive. Lastly PDT can be applied to the same area without the total-dose limitations associated with radiotherapy [34,35].

1.4. Approved Drugs and Their Limitations

Several photosensitizing agents are currently approved by the US Food and Drug Administration (FDA) to treat certain cancers, Table 1.1 gives only some of them.

Table 1.1. Some approved drugs in PDT [36].

Name of the drug	Structure	Name of the drug	Structure
Photofirin	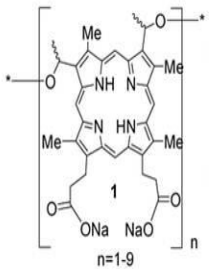	Laserphyrin	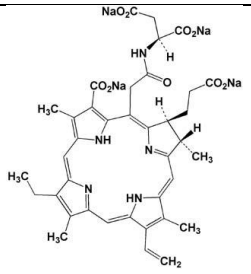
Foscan	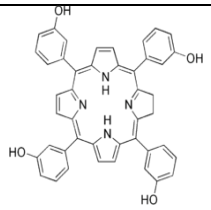	Visudyne	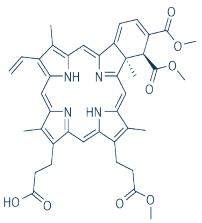
Levulan or ALA	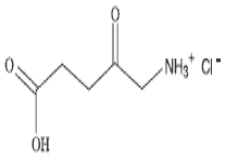	Metvix	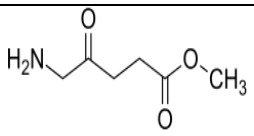

However most of them are far from being ideal photosensitizers. They do not have complete selectivity and localization in tumors. Moreover patients are affected by side effects of these drugs and they are capable of being activated only 1-2 cm under the tissue so it makes difficult to treat reach tumors which are located deeper in the tissue. To improve selectivity and penetration deepness of the photosensitizers, new photosensitizers with different moieties are designed. A class of photosensitizer phthalocyanines are very promising in this manner [37].

Photosensitizers with different structure, charge and hydrophobicity give different interactions with the biological surroundings and in turn determines cytotoxicity. As mentioned before some studied photosensitizers are porphyrins, chlorins, bacteriochlorins, phthalocyanines, and naphthalocyanines. Among them phthalocyanines are really promising so that this thesis will focus on phthalocyanines and their behaviors.

1.5. Phthalocyanines as Suitable Photosensitizers

1.5.1. Structure and Application of Phthalocyanines

Phthalocyanines which are also known as tetrabenzoporphyrazins are kind of porphyrinoids derivatives with 18 π electron and comprise four benzene rings which make them macrocyclic and aromatic compounds. Phthalocyanines are particularly attractive PDT agents; mainly because of their high absorption coefficient at 650–680 nm where penetration of light into tissue is optimal [38-41].

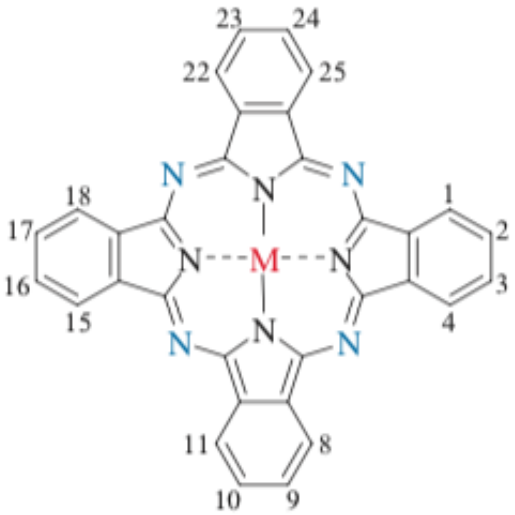

Figure 1.6. Pc ring and numbering the core according to IUPAC [42].

Phthalocyanine had been discovered in 1907 accidentally. The earliest studies about phthalocyanines belongs to Lindstead and his colleagues in 1930. Phthalocyanines were

proposed as a second generation PDT sensitizer in 1985. Since its discovery they have attracted much attention due to their unique physical and chemical properties [43].

Although phthalocyanines are known with their promising photodynamic activity, it is firstly emerged in the textile and dye industry. Applications of phthalocyanines also include optical, semiconductors, electronic and photo-electronic devices. They are used as color agents. For example, copper Pc has a brilliant blue color so it is used for printing materials such as inks, paints etc [44].

Photosensitizer of different chemical structures have widely varying cellular uptake, subcellular localization and cytotoxicity and their varying parameters directly determines PDT activity. For years phthalocyanines have been investigated to tune their photophysical and chemical properties in accordance with its usage. For example phthalocyanines often suffer from low water solubility and aggregation which make phthalocyanines photodynamically less active. Because the planar structure of phthalocyanines make them strongly susceptible to aggregation and the four phenyl groups on Pc ring causes solubility and aggregation problems too [45-47].

In order to penetrate cells phthalocyanine needs to be hydrophilic so their solubility is very crucial. Aggregation of phthalocyanines prevents the energy transfer in Jablonski diagram and in turn stops production of singlet oxygen which is cytotoxic to tumor cells. Besides there is still a need to have an ideal phthalocyanine which has two important properties;

- Absorbing in near-infrared region,
- Enhanced singlet oxygen production.

To address these issues, several modification strategies on Pc rings have been developed. Strategies for the modification of Pc rings include axial coordination of metal atoms, peripheral-nonperipheral substitution of Pc rings and, changing the meso atom [48, 49].

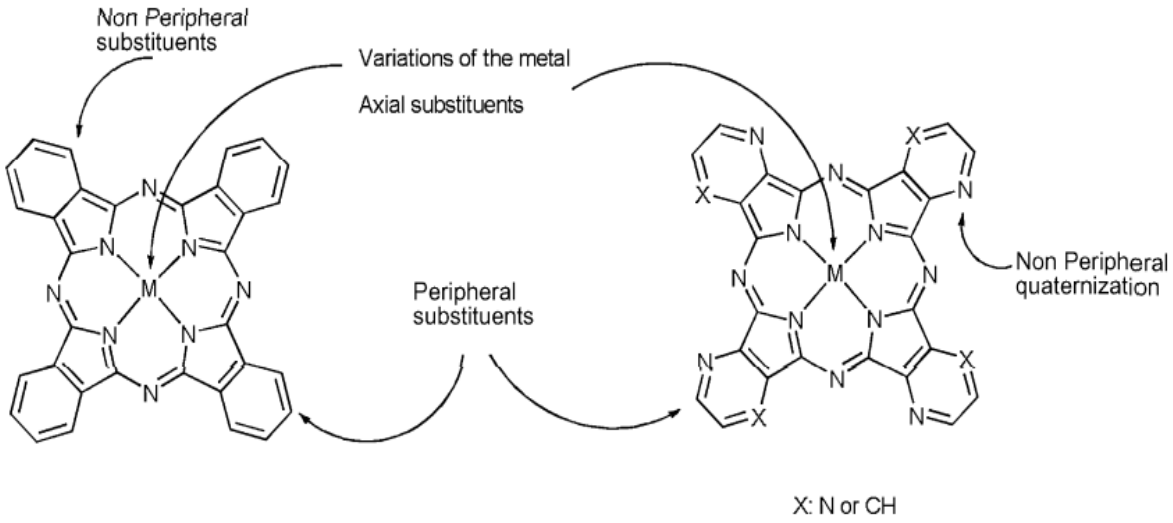

Figure 1.7. Possible modifications of phthalocyanine structure [50].

1.5.2 Photophysical Properties of Phthalocyanines

Phthalocyanines present two main absorption peaks; one belongs to a strong absorption in the region between 650-690 nm of the spectrum called as Q band and the other one is between 320 and 370 nm at shorter wavelengths, called the Soret band in the UV-Vis spectra. The Soret and the Q bands both arise from π–π* transitions and can be explained by considering the four frontier orbitals (HOMO and LUMO orbitals). However, the Soret band is not used for PDT.

The extinction coefficient of the Q band is around logε 4-5 and follows Beer-Lambert law for both the Q-band and Soret-band. The position of the Q band can be tuned by introduction of different substituents such as metals [51]. For this reason, in recent years, phthalocyanines have become of major interest for applications in PDT.

Free phthalocyanines have splitted Q bands compare to their metallated derivatives (Figure 1.8).

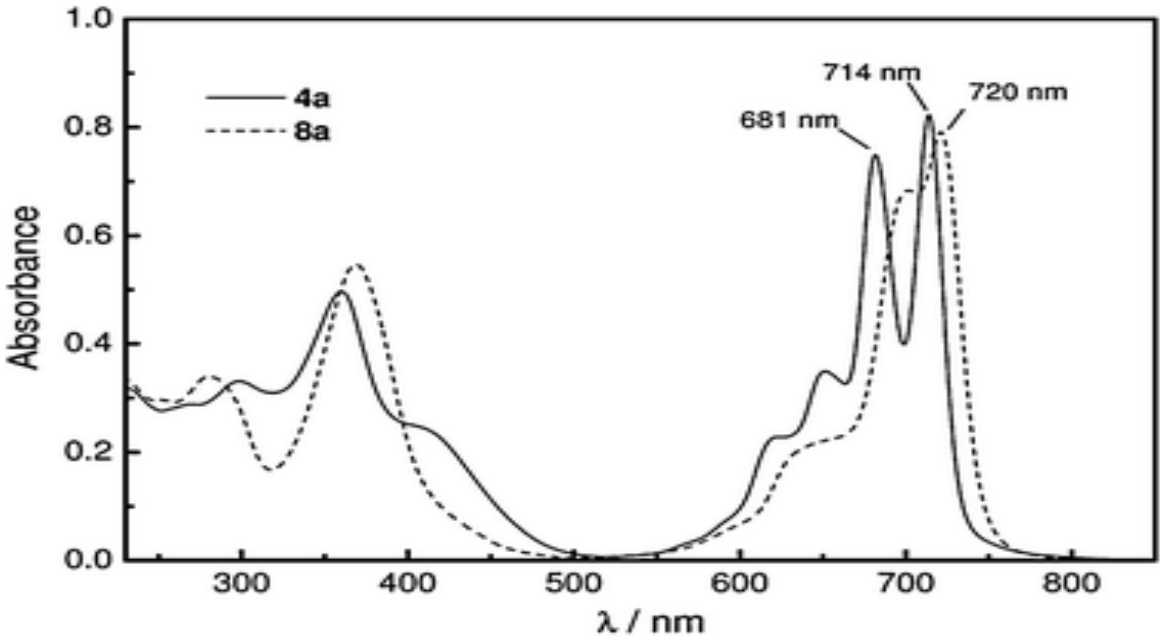

Figure 1.9. UV-Vis spectra of H_2Pc and zincPc (dashed line) in CH_2Cl_2 [44].

1.5.3. Octa -SR Phthalocyanines

Since there are only few promising photosensitizers that are approved by FDA, there has been a systematic search for different new photosensitizers which are designed to increase PDT efficacy.

While the literature on photosensitizers has been growing, there is this need appears to study on Octa -SR substitution pattern for the reasons given below:

- It is known that preferring octasubstituted phthalocyanines over tetrasubstituted phthalocyanines avoids isomeric mixtures in other words purer compounds can be gained [52],
- As an electron donating group alkly thio groups causing red shift in the spectrum of phthalocyanines and other donating groups such as amino, aryl thio groups as well [53].

Moreover, octathiol sulfonyl (OctaSR-) substituted phthalocyanines exhibit approximately a significant red-shift of their Q-bands. This was firstly evidenced by Cook and his coworkers [54, 55]. So that the combination of octa, non-peripheral and thiol substitution factors induce a red-shifted maximum electronic absorption in phthalocyanine structures [56].

These three aspects are crucial issues to be taken into account in the design of new phthalocyanines.

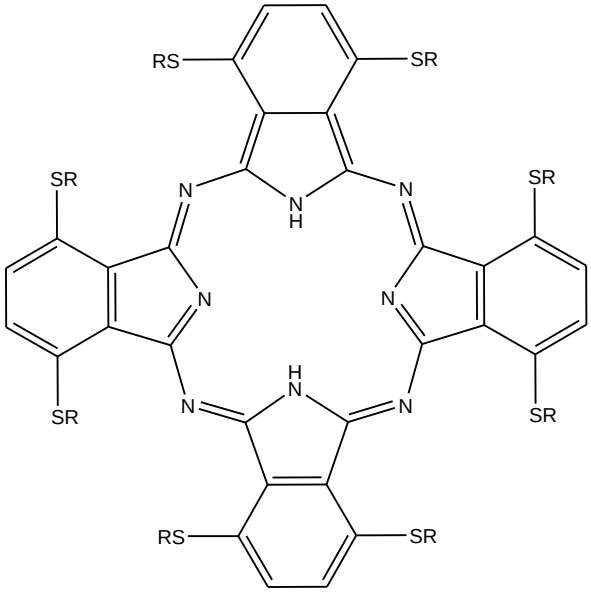

Figure 1.10. Octa -SR phthalocyanine structure.

In the literature Dumoulin *et al*. have compared Zn(II) phthalocyanines with different substitution pattern, Figure 1.10 shows four different phthalocyanines that are selected on purpose [57].

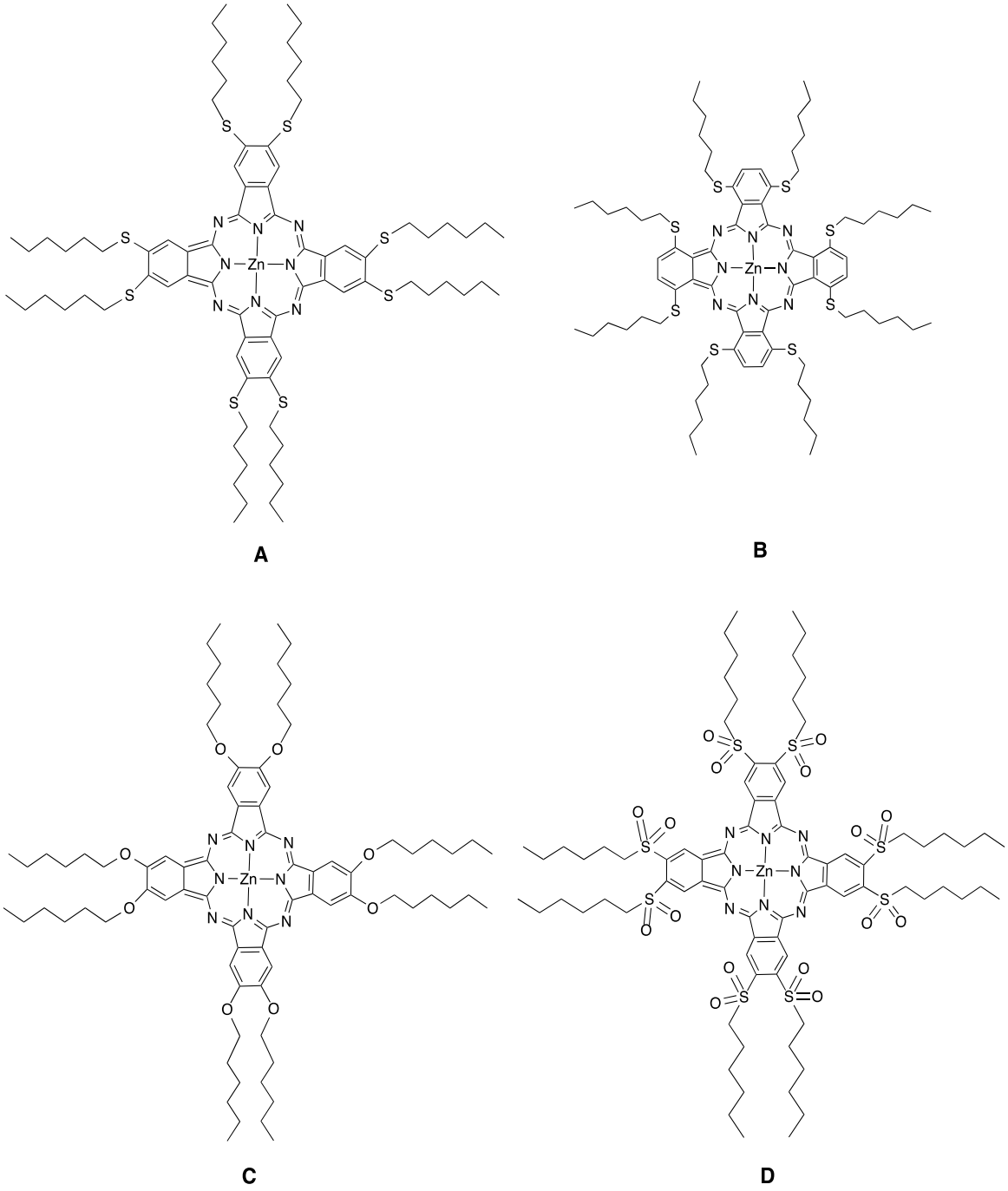

Figure 1.11. Zn(II) phthalocyanine derivatives with different substitution patterns [57].

From the Figure 1.10 it is obvious that the octa nonperipheral hexylsulfanyl substitution pattern of **B** resulted in a remarkably red-shifted absorption appropriate for NIR absorption based applications [57].

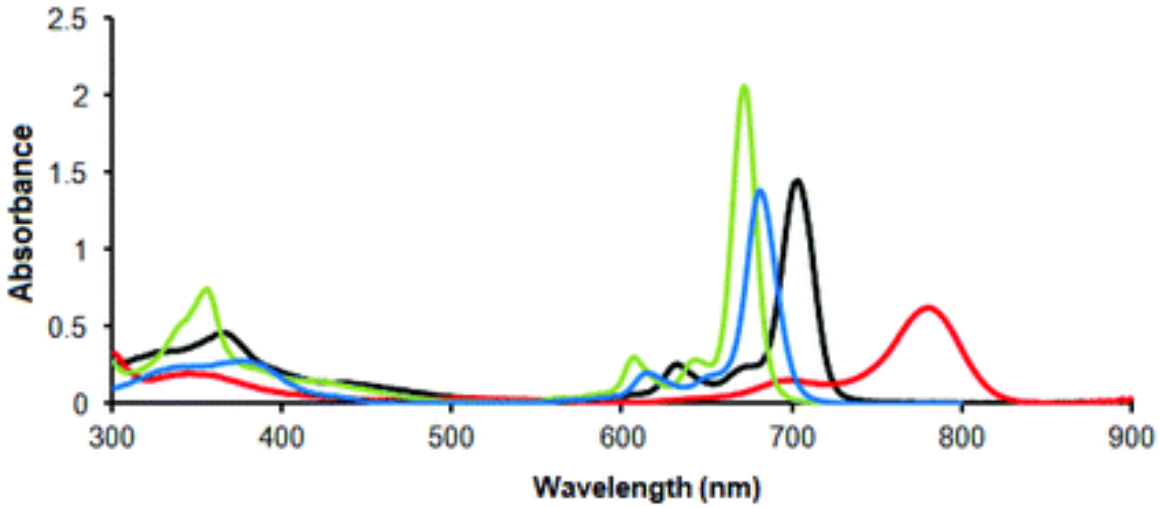

Figure 1.12. UV-Vis spectra of **A** (black), **B** (red), **C** (green) and **D** (blue) in THF (~4.5 × 10−6 M) [57].

In the other study which is done by the same group has proved that non-peripherally octasulfanyl-substituted Zn phthalocyanine numbered as **E** is promising as a NIR photosensitizer because of its maximum absorption at 800 nm [52].

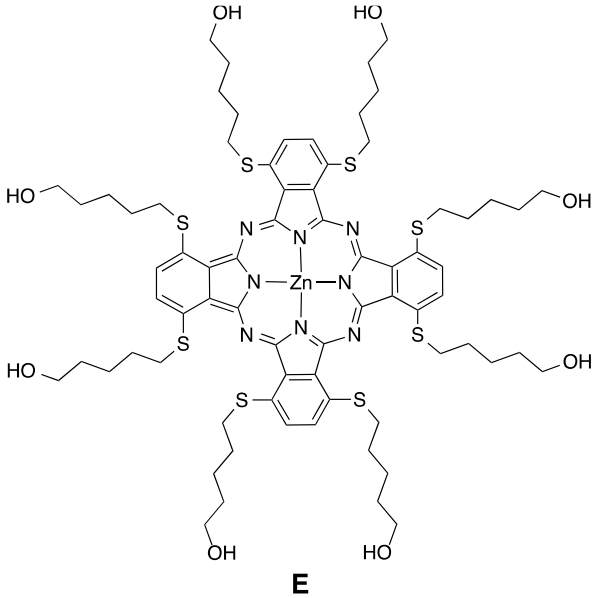

E

Figure 1.13. Molecular design of phthalocyanine **E** [52].

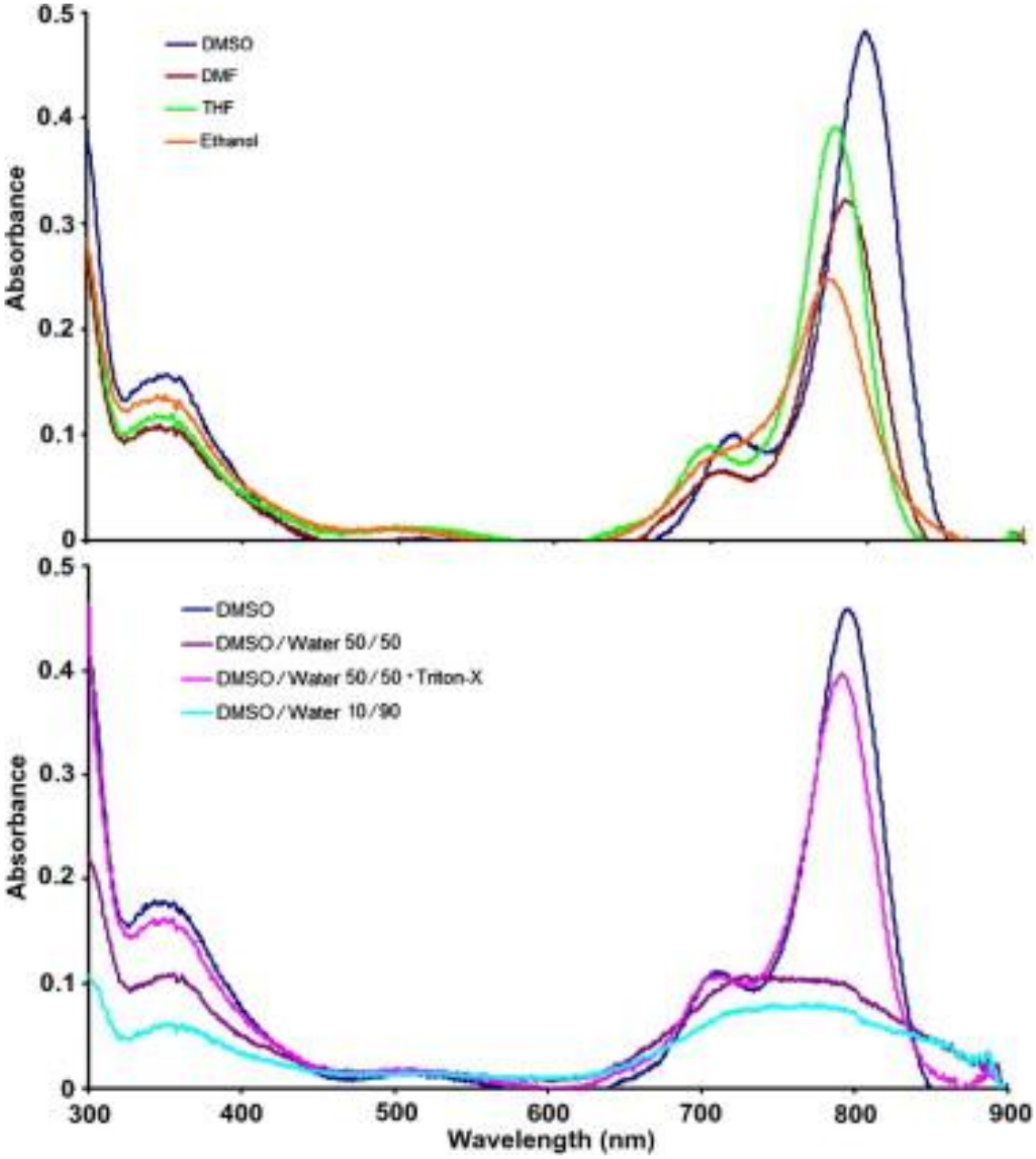

Figure 1.14. UV–Vis spectra of **E** (10 μM) in different organic solvents [52].

Next, Dumoulin and her team have made a comparison between a planar and a distorted phthalocyanine derivative with alkylsulfanyl substituents to see the effect of substituent bulkiness. The planar structure **F** with *n*-hexyl moieties and the distorted structure **G** with *tert*-butylsulfanyl moieties are shown in Figure 1.14. [58].

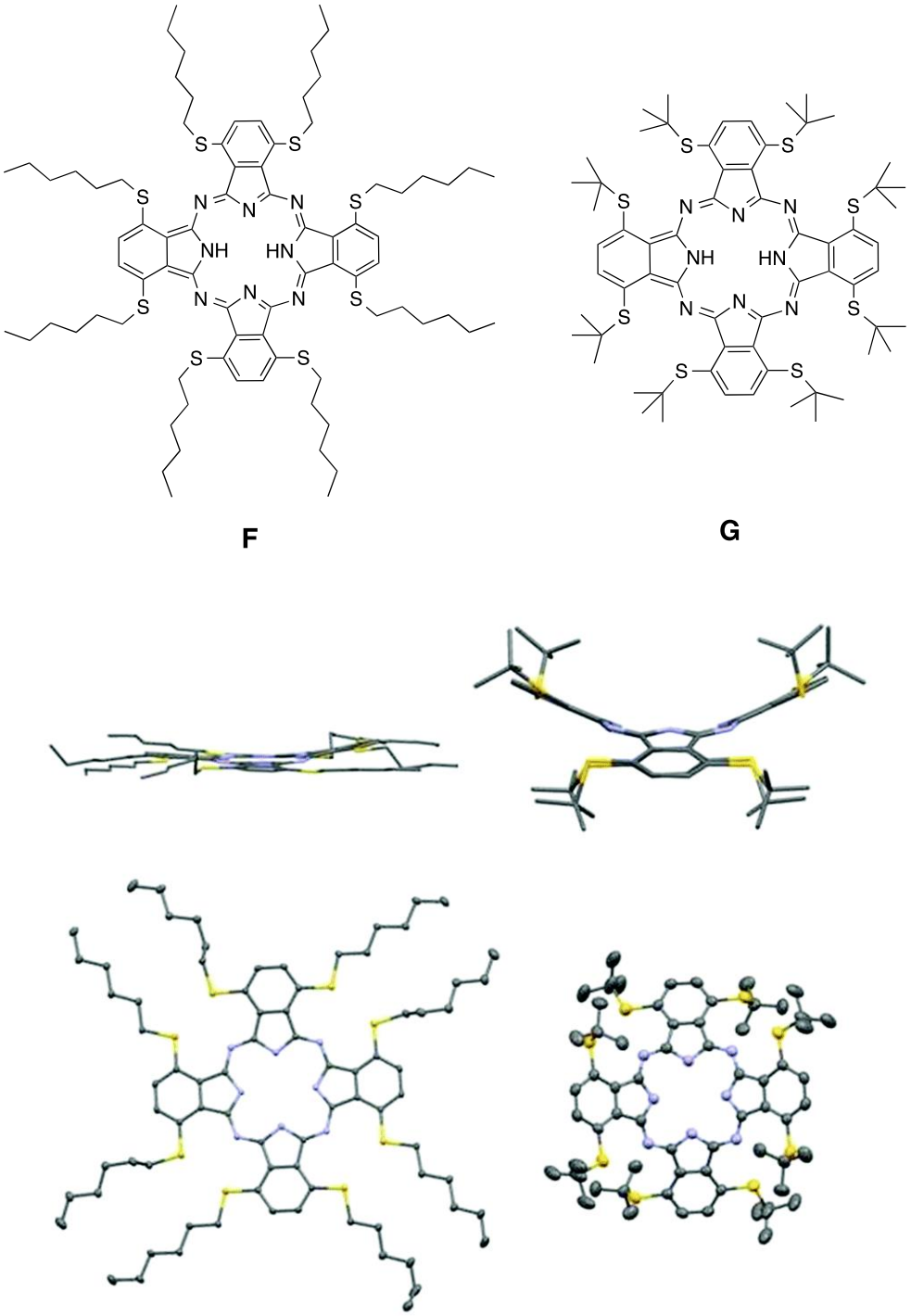

Figure 1.15. Molecular design of phthalocyanines **F** and **G** [58].

In Figure 1.15 there is a huge difference in maximum absorption point of the curves. Phthalocyanine **G** with *tert*-butyl moieties shows blue shift due to its bulkiness.

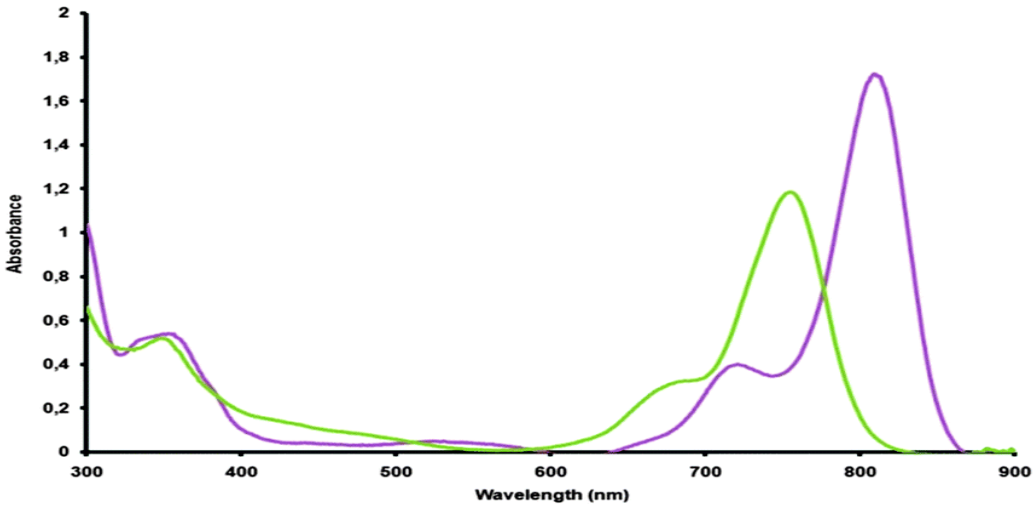

Figure 1.16. UV-Vis spectra of **F** (violet) and **G** (green) in THF (10 μM) [58].

However this blueshift of **G** was unexpected and contradicts with previous studies. To elucidate this contradiction the frontier orbitals were investigated (Figure 1.16). DFT calculations showed that their LUMOs were energetically very close whereas there was a significant difference in the energies of HOMOs. Hence the increased HOMO-LUMO gap resulted in blueshift of maximum absorbance wavelength of **G**.

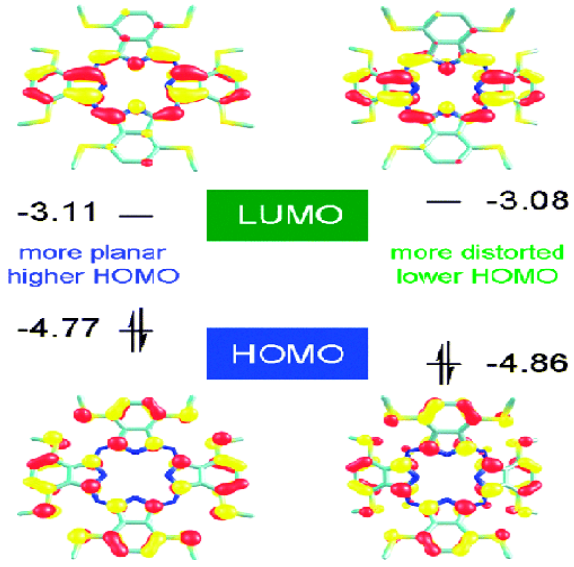

Figure 1.17. Frontier orbital energies (eV) of **F** (left) and **G** (right) in THF [58].

2. AIM OF THE STUDY

The purpose of this thesis is to prepare novel phthalocyanines designed accordingly to the optimal desired properties of PDT photosensitizer, especially NIR absorption.

In 2003, Cook and his team have shown that octa alkyl thiol substituted phthalocyanines have strong absorption in near-infrared region. In this regard the photophysical properties of octa alkyl thiol phthalocyanines with different metallation trials needs to be investigated. We expect to see shift of the maximum absorption of octa -SR substituted phthalocyanines to the near-infrared. All of the phthalocyanines were synthesized from substituted phthalonitriles.

Metallation is very crucial for the singlet oxygen generation and thus the cyto-toxicity. So in course of the project, we report on different phthalocyanines with various central atoms to obtain sufficient water solubility. The metals Zn, Pt, Pd, Al are selected for the metallation of octaalkyl thiol substituted phthalocyanines to study of metal affect regarding PDT.

3. EXPERIMENTAL

3.1. Reagents

The chemicals and materials, used for synthesis, are listed in the Table 3.1.

Table 3.1. Chemicals and materials used in this work.

Name	Suppliers	No	Purity
2,3-dicyano-hydroquonine	Merck	8.14409	Pure
Dichloromethane	Technic		
Ethyl acetate	Technic		
THF	Merck	1.08114	Extra Pure
DMF	Merck	1.03053	Pure
TosCl	Merck	S244438	
Hexane-1-thiol	Merck	8.22063	Pure
n-Hexane	Technic		
n-butanethiol	Merck	32648104	
Ethanol	Technic		
DBU	Fluka	421374/1	Pure
Acetone	Technic	8.04393	
2-methyl-propane-thiol	Merck	34748806	
Pentanol	Fluka	76930	

Table 3.1. Chemicals and materials used in this work. (cont.)

Zn acetate	Sigma Aldrich	1001752364	
Hydrogen Peroxide	Riedel-de Haen	7722-84-1	
Acetic acid	Sigma Aldrich	320099	Pure
Li	Strem Chemicals	B6480040	Pure
DCB	Sigma Aldrich	6971-97-7	

3.2. Instruments

The instruments used to analyze structures synthesized in this work are represented in Table 3.2 below.

Table 3.2. Instruments used in this work.

Name of the Instrument	**Model of the Instrument**	**Location of the Instrument**
Melting Point Apparatus	Büchi 535	Gebze Technical University
ATR-IR Spectrometry	Perkin Elmer Spectrum 100	Gebze Technical University
NMR Spectrometry	Varian 500 MHz	Gebze Technical University
Mass Spectrometry	Bruker Microflex LT MALDI-TOF MS	Gebze Technical University
UV-Vis Spectrometry	Schimadzu 2101 UVPc	Gebze Technical University
X-ray	Bruker APEX II QUAZAR	Gebze Technical University

3.3. General Overview of the Compounds Targeted

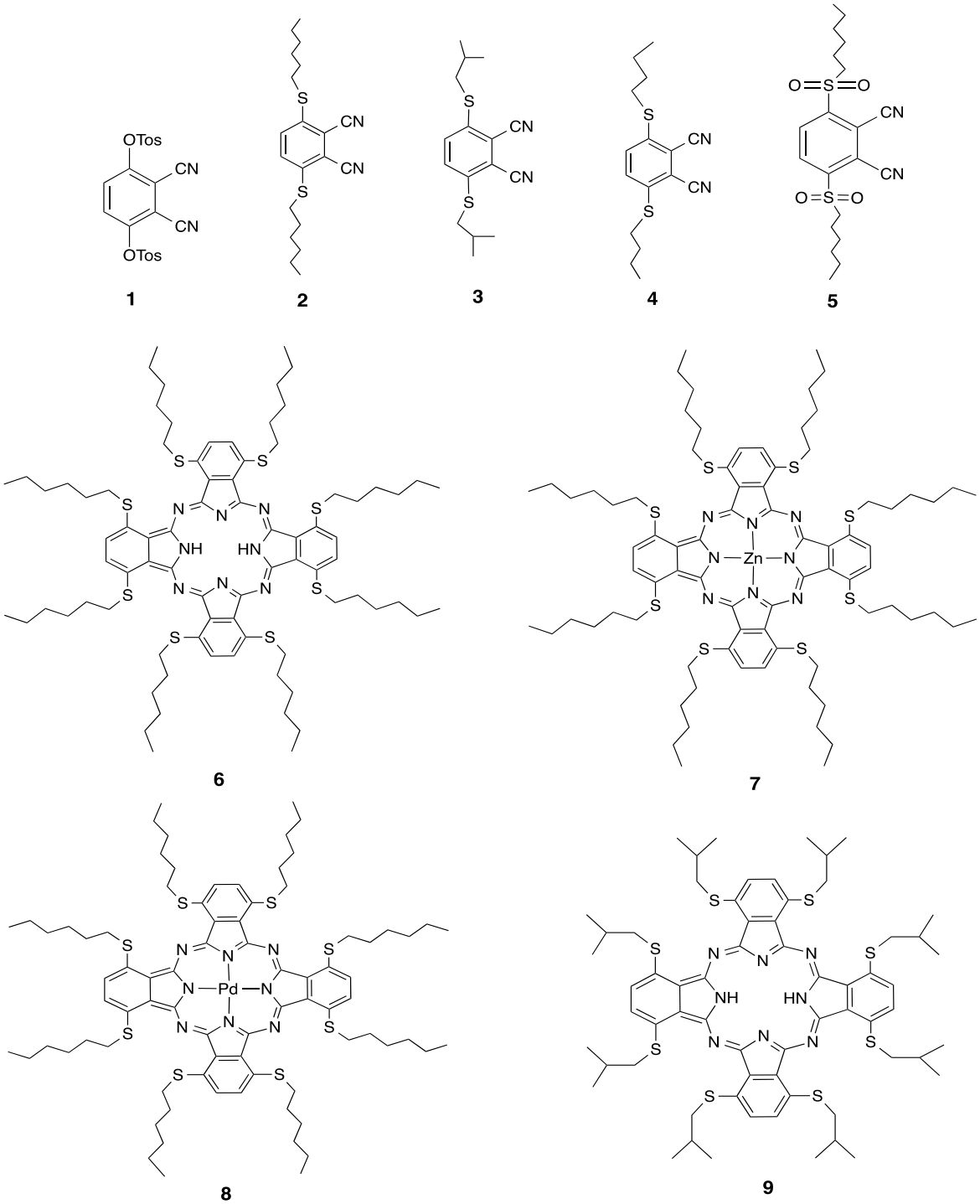

Figure 3.1. Targeted compounds in this work.

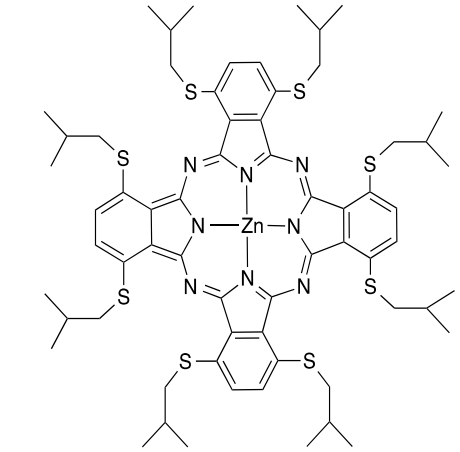

10

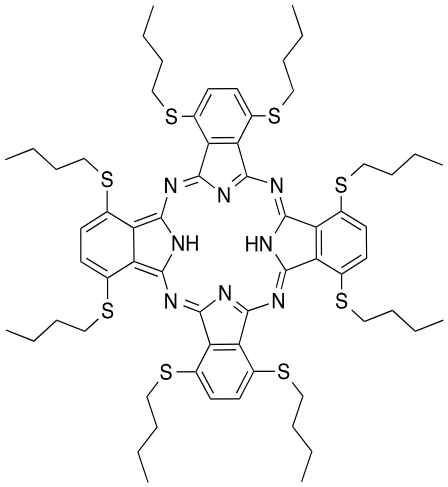

11

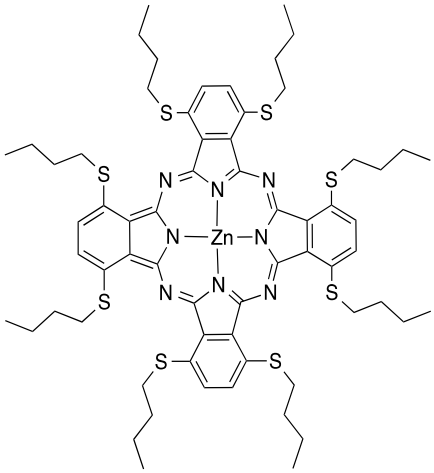

12

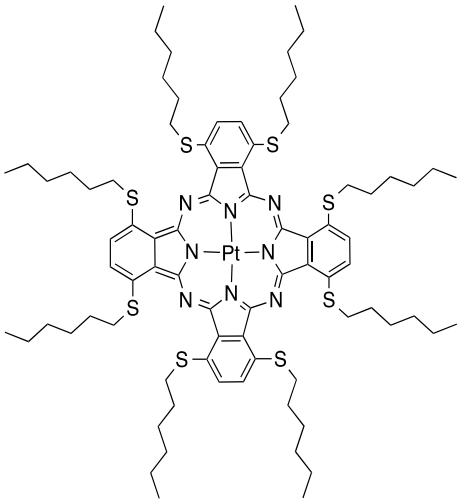

13

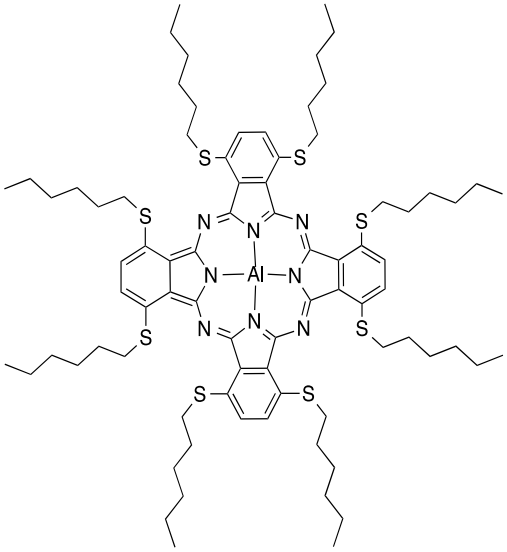

14

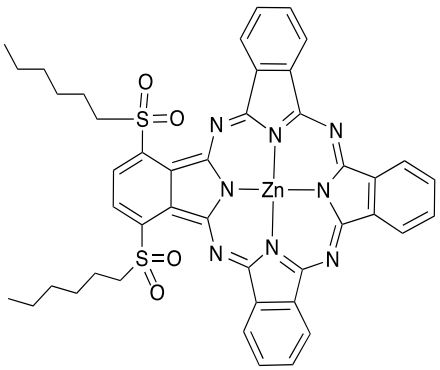

15

Figure 3.1. Targeted compounds in this work. (cont.)

3.4. Synthesis and Spectra of Phthalonitriles

3.4.1. Synthesis of 2,3-dicyano-1,4-phenylene bis(4-methylbenzenesulfonate) (1)

2,3-dicyanohydroquinone (5 g, 31.2 mmol) was refluxed with 4-Toluenesulfonyl chloride (12 g, 62.4 mmol), K_2CO_3 (6.5 g, 46.8 mmol) in pure acetone (50 mL) for 2 hours. Thin layer chromatography was performed to determine the consumption of starting material. The TLC solvent system was Hexane/Ethyl Acetate (3:1). Water was added to reaction mixture and stirred for 15 minutes. Then the light brown product was filtered and dried [59]. Yield: 14 g (97%). $C_{22}H_{16}N_2O_6S_2$, MW: 468.50 g/mol.

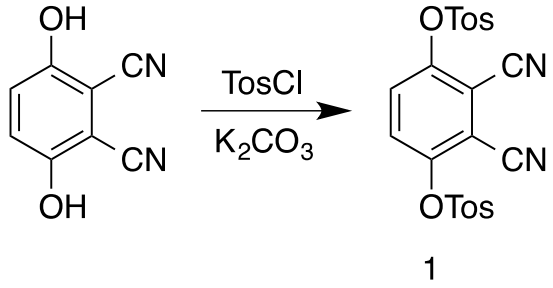

Figure 3.2. Synthesis of compound **1**.

3.4.2. Synthesis of 3,6-bis(hexylthio)phthalonitrile (2)

2,3-dicyano-1,4-phenylene bis(4-methylbenzenesulfonate) (10 g, 21 mmol) and K_2CO_3 (14.5 g, 105 mmol) was stirred with DMF (67 mL) at room temperature. 1-hexanethiol (8.2 mL, 63 mmol) was added to the reaction mixture. After addition, reaction mixture was stirred for a day and reaction completion was checked by TLC (eluent, Hexane/Ethyl Acetate (3:1)). Water was added and resulting precipitate was filtered. Solid dissolved in DCM, dried over Na_2SO_4 and crystallized in ethanol [58]. Yield: 3.7 g (47 %). $C_{20}H_{28}N_2S_2$, MW: 360.58, m.p. 85 °C. ^{1}H NMR ($CDCl_3$) δ (ppm) 7.50 (t, 8H), 3.02 (m, 16H), 1.67 (s, 16H), 1.45 (s, 16H), 1.31 (d, 16H), 0.89 (d, 23H). ATR-IR (cm^{-1}) 3081, 2951, 2939, 2924, 2850, 2226, 1449, 1422, 1207, 1145, 834, 727.

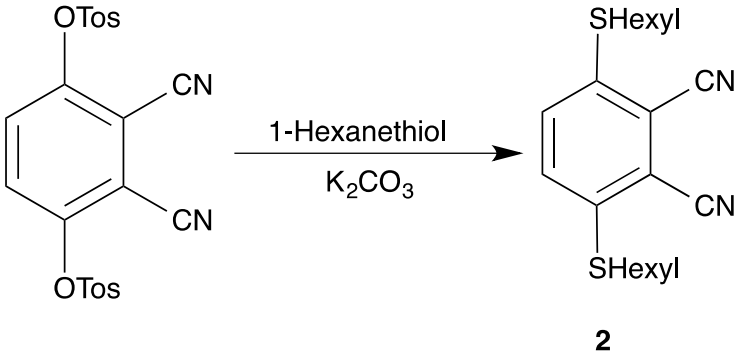

2

Figure 3.3. Synthesis of compound **2**.

3.4.3. Synthesis of 3,6-bis(isobutylthio)phthalonitrile (3)

2,3-dicyano-1,4-phenylene bis(4-methylbenzenesulfonate) (5 g, 11 mmol) and K_2CO_3 (7.6 g, 55 mmol) was stirred with DMF (40 mL). 2-methyl-1-propanethiol (3.6 mL, 33 mmol) was added to the solution. After addition, reaction was stirred for a day and reaction completion was checked by TLC (eluent, Hexane/Ethyl Acetate (3:1)). Water was added to the mixture, the resulting yellow precipitate was filtered and the yellow solid product was purified by silica gel chromatography (eluent DCM) [58]. Yield: 2.75 g (55 %). $C_{16}H_{20}N_2S_2$, MW: 304.47, m.p. 116 °C. ^{1}H NMR ($CDCl_3$) δ (ppm) 7.49 (d, 8H), 2.91 (d, 16H), 1.90 (m, 8H), 1.08 (t, 48H). ^{13}C NMR ($CDCl_3$) δ (ppm) 141.94, 132.32, 117.11, 113.73, 42.68, 28.17, 21.93. ATR-IR (cm^{-1}) 3081,2957, 2928, 2898, 2870, 2221, 1467, 1446, 1427, 1383, 1367, 1340, 1289, 1259, 1208, 1186, 1169, 1144, 1074, 1024, 960, 879, 847, 832, 817, 660.

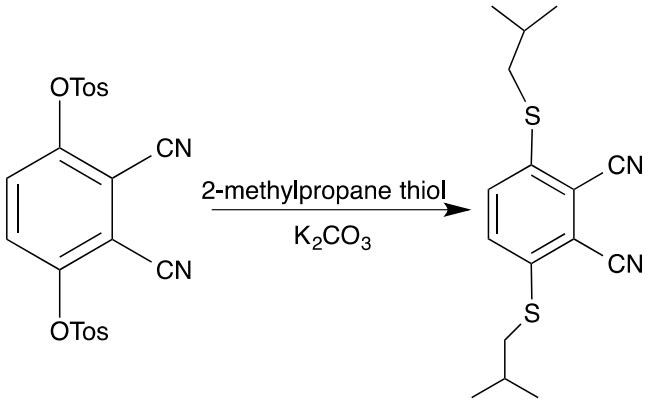

3

Figure 3.4. Synthesis of compound **3**.

3.4.4. Synthesis of 3,6-bis(butylthio)phthalonitrile (4)

2,3-dicyano-1,4-phenylene bis(sulfurochloridate) (10 g, 21 mmol) was dissolved in DMF (69 mL). K_2CO_3 (14.5 g, 105 mmol) and *n*-butanethiol (6.4 mL, 60 mmol) were added. The reaction mixture were stirred for a day at room temperature, the reaction was checked for completion with TLC using Hexane/Ethyl Acetate (3:1) for elution. Water was added to the mixture, the reaction mixture was dried over Na_2SO_4 and filtered. The yellow residue was taken with DCM and the solvent evaporated off [58]. Yield: 10 g (10%). $C_{16}H_{20}N_2S_2$, MW: 304.47, m.p. 102°C. ^{1}H NMR ($CDCl_3$) δ (ppm) 7.50 (d, 8H), 2.66 (d, 16H), 1.66 (d, 16H), 1.48 (d, 16H), 0.94 (d, 24H). ATR-IR (cm^{-1}) 2960, 2926, 2910, 2874, 2862, 2221, 1467, 1443, 1435, 1424, 1410, 1280, 1204, 1196, 1188, 1172, 1155, 1143, 915, 845, 824, 796, 738, 665. MS (MALDI-TOF): *m/z* 343.144 $[M]^+$.

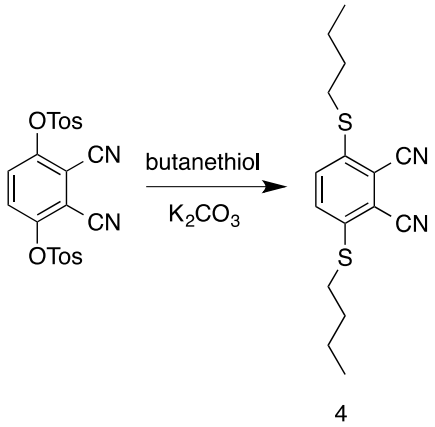

Figure 3.5. Synthesis of compound **4**.

3.4.5. Synthesis of 3,6-dihexylsulfonylphthalonitrile (5)

Phthalonitrile **2** (2.16 g, 6 mmol) was refluxed in acetic acid (40 mL), then hydrogen peroxide (20 mL) was added to the mixture in equal portions every half hour within four hours. Reflux was continued for a further 3 hours, then reaction mixture was cooled down still stirring. Cold water was added and the resulting white precipitate was filtered and purified by silica gel chromatography, eluted first by dichloromethane, then with dichloromethane/ethanol mixtures of increased polarity (up to a 50/1 ratio), yielding 892 mg

of a white crystalline solid (35%) [60]. $C_{20}H_{28}N_2O_4S_2$, MW: 424.57, m.p. 176 °C. ^{1}H NMR ($CDCl_3$) δ (ppm) 8.55 (s, 2H), 3.41 (t, 4H), 1.77 (m, 4H), 1.45 (m, 4H), 1.30 (m, 8H), 0.88 (t, 6H). ^{13}C NMR δ (ppm) 146.90, 134.69, 118.15, 111.90, 55.13, 27.92, 31.02, 27.92, 22.22, 13.99. ATR-IR (cm^{-1}) 3074, 2956, 2927, 2858, 2237, 1558, 1462, 1393, 1330, 1283, 1178, 1014, 854, 833, 725, 675. MS (MALDI-TOF): *m/z* 346.396 $[M]^+$.

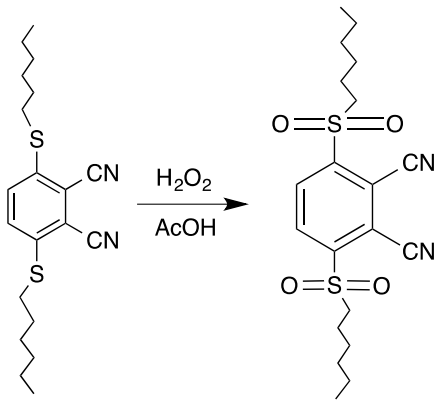

5

Figure 3.6. Synthesis of compound **5**.

3.5. Synthesis and Spectra of Phthalocyanines

3.5.1. Synthesis of Compound 6

Phthalonitrile **2** (1.85 g, 5 mmol) was stirred in pentanol (5 mL) and a portion of lithium granules was added to the mixture under argon. The reaction mixture was refluxed for a day under argon gas atmosphere and then was cooled to room temperature. Ethanol (15 mL) and water (15 mL) mixture was added to the reaction and the suspension was allowed to stand overnight. The resulting precipitate was filtered and columned through a silica gel column using DCM for elution, yielding 1 g (50%) [58]. $C_{80}H_{114}N_8S_8$, MW: 1444.33, m.p. 162 °C. UV-Vis ($CDCl_3$): λ_{max} (nm) (logε): 811 (5.05), UV-Vis (THF): λ_{max} (nm) (logε): 805 (4.16). ^{1}H NMR ($CDCl_3$) δ (ppm) 8.04 (s, 8H), 3.34 (s, 16H), 2.01 (s, 16H), 1.67 (s, 16H), 1.40 (s, 16H), 1.24 (s, 16H), 0.93 (s, 24H). ATR-IR (cm^{-1}) 2953, 2921, 1566, 1461, 1434, 1311, 1278, 1225, 1204, 1183, 1159, 1143, 1113, 1091, 1030, 916, 908, 868, 788, 753, 724, 709. MS (MALDI-TOF): *m/z* 1444.646 $[M]^+$.

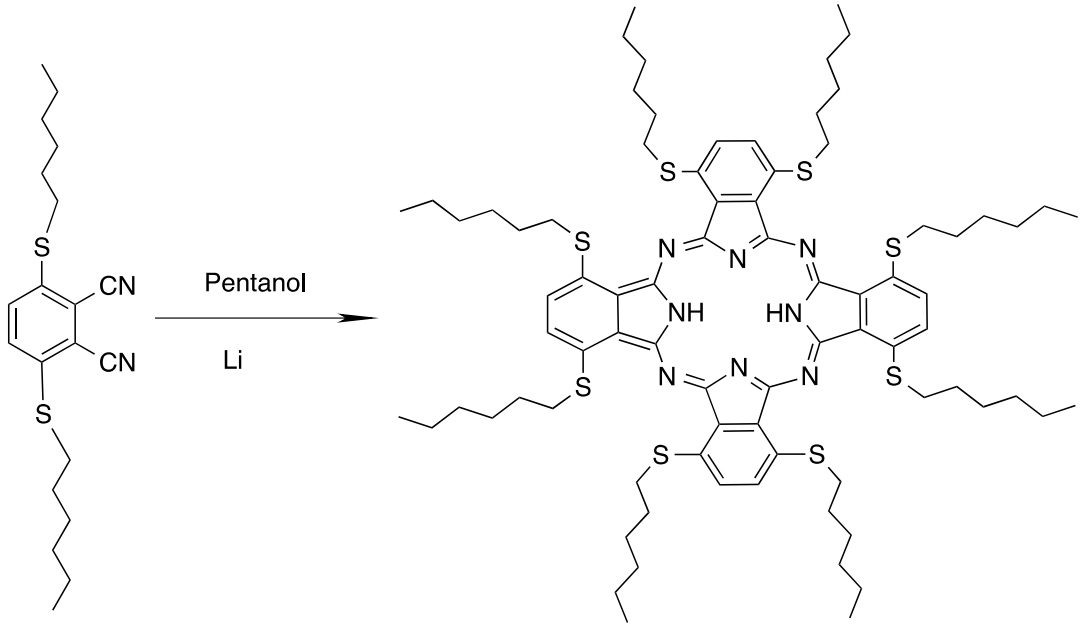

6

Figure 3.7. Synthesis of compound **6**.

3.5.2. Synthesis of Compound 7

1,4,8,11,15,18,22,25-octakis(hexylthio)phthalocyanine **6** (500 mg, 0.35 mmol) was dissolved in DMF (5 mL). $Zn(OAc)_2$ (269.9 mg, 1.23 mmol) was added to the mixture [54]. The reaction mixture was heated to 80 °C and water was added to the reaction. After 8 hours, reaction was left to cool and was checked with TLC using DCM for elution . The resulting black precipitate was filtered and concentrated, yielding 480 mg (96%). $C_{80}H_{112}N_8S_8Zn$, MW: 1507.69, m.p. 176 °C. UV-Vis ($CDCl_3$): λ_{max} (nm) (logε): 799 (4.74), UV-Vis (THF): λ_{max} (nm) (logε): 782 (5.14). ^{1}H NMR ($CDCl_3$) δ (ppm) 7.41 (s, 8H), 2.90 (s, 16H), 1.67 (s, 16H), 1.55 (s, 16H), 1.34 (s, 16H), 1.26 (s, 16H), 0.95 (d, 24H). ATR-IR (cm^{-1}) 2953, 2921, 1566, 1461, 1434, 1311, 1278, 1225, 1204, 1183, 1159, 1143, 1113, 1091, 1030, 916, 908, 868, 788, 753, 724, 709. MS (MALDI-TOF): *m/z* 1507.710 $[M]^+$.

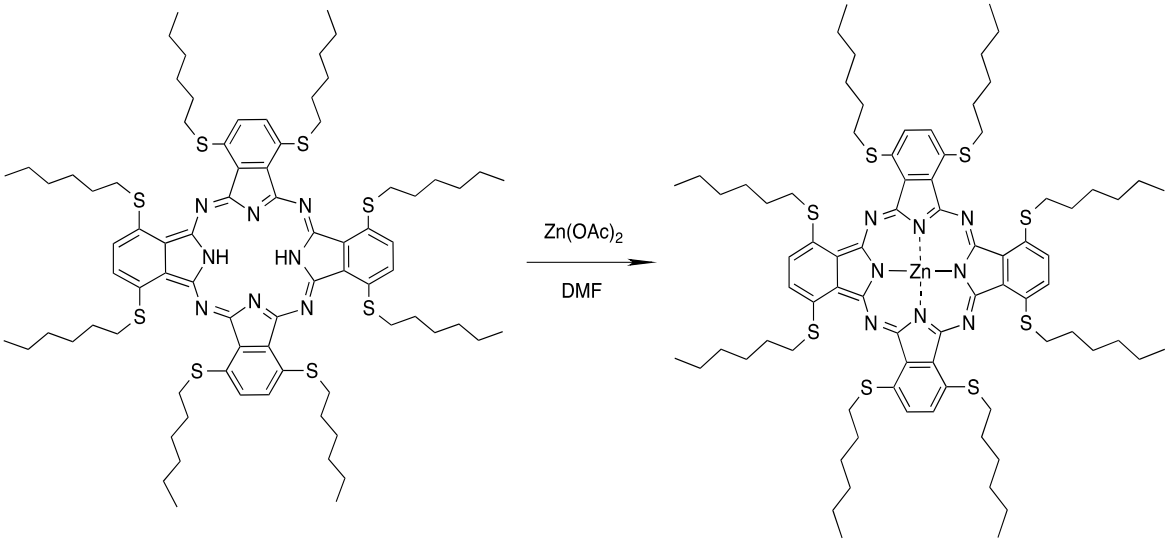

Figure 3.8. Synthesis of compound **7**.

3.5.3. Synthesis of Compound 8

A 50 mL flask was charged with compound **6** (100 mg, 0.069mmol), $Pd(acac)_2$ (63.3 mg, 2.07 mmol), 5 mL and a magnetic stirring bar. Once the mixture was homogeneous, it was stirred for 5 min at room temperature, and then the mixture was subjected to microwave irradiation (800 W) under ambient pressure for 30 min. The reaction was monitored by TLC and the TLC solvent system was DCM/EtOH (10:1). After completion, the mixture was cooled to room temperature and then diluted with 25 mL solution of Hexane and the resulting green precipitate was filtered, yielding 97 mg (61%). $C_{80}H_{112}N_8PdS_8$, MW: 1548.73. ^{13}C NMR ($CDCl_3$) δ (ppm) 131.55, 128.20, 127.29, 125.36, 47.41, 30.28, 29.37, 28.49, 22.47, 13.98. ATR-IR (cm^{-1}) 2926, 2926, 2856, 2358, 2343, 2326, 2317, 2309, 2300, 1725, 1672, 1463, 1378, 1276, 1261, 1156, 1038, 764, 750.

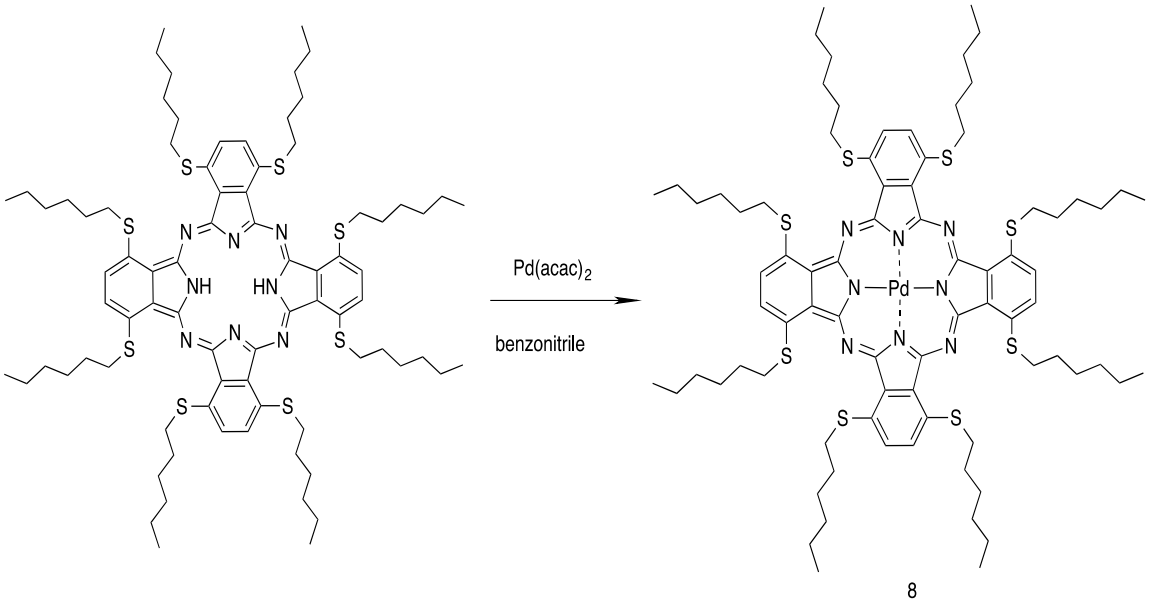

Figure 3.9. Synthesis of compound **8**.

3.5.4. Synthesis of Compound 9

3,6-bis(isobutylthio)phthalonitrile **3** (500 mg, 1.67 mmol) was dissolved in pentanol (5 mL) and the reaction mixture was refluxed at 110 °C for a day, after adding lithium granules under argon gas [58]. Then completion of the reaction was checked by TLC (eluent DCM/Hexane (9:1)). The reaction mixture was cooled and water was added. The resulting precipitate was filtered and purified via silica column chromatography using DCM/Hexane (9:1) for elution yielding 105 mg (21%). $C_{64}H_{82}N_8S_8$, MW: 1219.90, m.p. 88 °C. UV-Vis ($CDCl_3$): λ_{max} (nm) (logε): 803 (4.04), UV-Vis (THF): λ_{max} (nm) (logε): 802 (5.11).^{1}H NMR ($CDCl_3$) δ (ppm) 7.84 (s, 8H), 3.25 (s, 16H), 2.27 (m, 8H), 1.29 (d, 48H). ATR-IR (cm^{-1}) 3081, 2960, 2926, 2910, 2874, 2862, 2221, 1467, 1443, 1435, 1424, 1410, 1280, 1204, 1196, 1172, 1143, 915, 845, 824, 738, 665. MS (MALDI-TOF): *m/z* 1219.711 $[M]^+$.

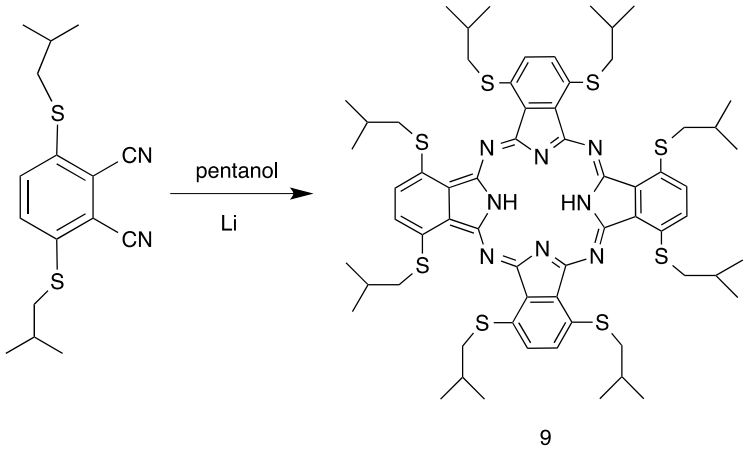

Figure 3.10. Synthesis of compound **9**.

3.5.5. Synthesis of Compound 10

1,4,8,11,15,18,22,25-octakis(isobutylthio)phthalocyanine **9** (100 mg, 0.82 mmol) was dissolved in DMF (5 mL) and $Zn(OAc)_2$ (269.9 mg, 1.23 mmol) was added to the mixture [54]. The reaction mixture was heated to 80 °C and water was added to the reaction. The resulting precipitate was filtered and purified with preparative TLC using DCM/Hexane (1:1) for elution. $C_{64}H_{80}N_8S_8Zn$, MW: 1283.26. UV-Vis ($CDCl_3$): λ_{max} (nm) (logε): 785 (4.38), UV-Vis (THF): λ_{max} (nm) (logε): 774 (4.53). ^{13}C NMR ($CDCl_3$) δ (ppm) 152.74, 134.29, 132.37, 124.74, 28.14, 22.78, 22.10. ATR-IR (cm^{-1}) 3006, 2957, 2926, 2869, 1727, 1658, 1560, 1464, 1431, 1366, 1276, 1261, 1212, 1144, 1108, 1035, 919, 792, 764, 750, 725. MS (MALDI-TOF): *m/z* 1283.109 $[M]^+$.

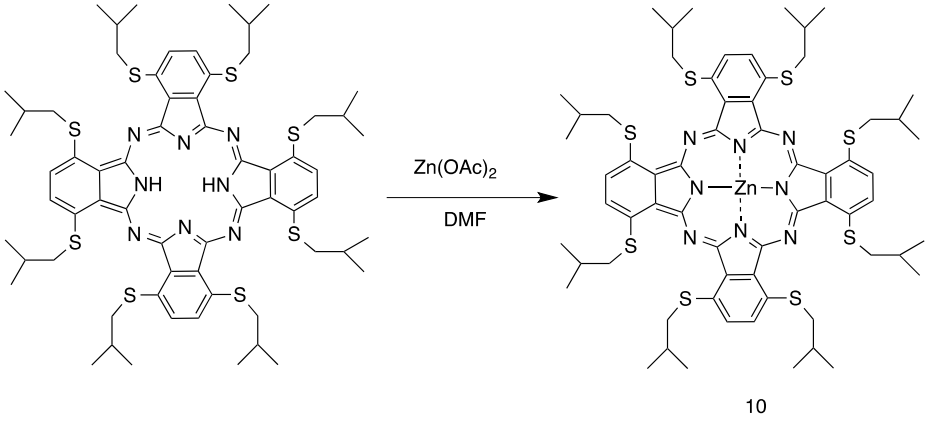

Figure 3.11. Synthesis of compound **10**.

3.5.6. Synthesis of Compound 11

3,6-bis(butylthio)phthalonitrile **4** (400 mg, 1.31 mmol) was dissolved in pentanol (5 mL) and lithium granules was added to the mixture [58]. The reaction mixture was refluxed for a day under argon and was cooled to room temperature. Ethanol (15 mL) and water (15 mL) mixture was added to the reaction. The resulting black precipitate was filtered and dissolved in DCM. Then the solvent was removed and the black product columned through a silica gel column using DCM for elution yielding 120 mg (30%). $C_{64}H_{82}N_8S_8$, MW: 1219.90, m.p. 210 °C. UV-Vis ($CDCl_3$): λ_{max} (nm) (logε): 810 (5.01), UV-Vis (THF): λ_{max} (nm) (logε): 804 (5.06). ^{13}C NMR ($CDCl_3$) δ (ppm) 135.72, 130.58, 128.71, 125.41, 30.16, 29.42, 22.88, 13.81. ATR-IR (cm^{-1}) 2960, 2931, 2874, 1738, 1464, 1434, 1369, 1277, 1180, 1141, 1062, 1041, 1020, 964, 868, 801, 754, 750, 722. MS (MALDI-TOF): *m/z* 1220.820 $[M]^+$.

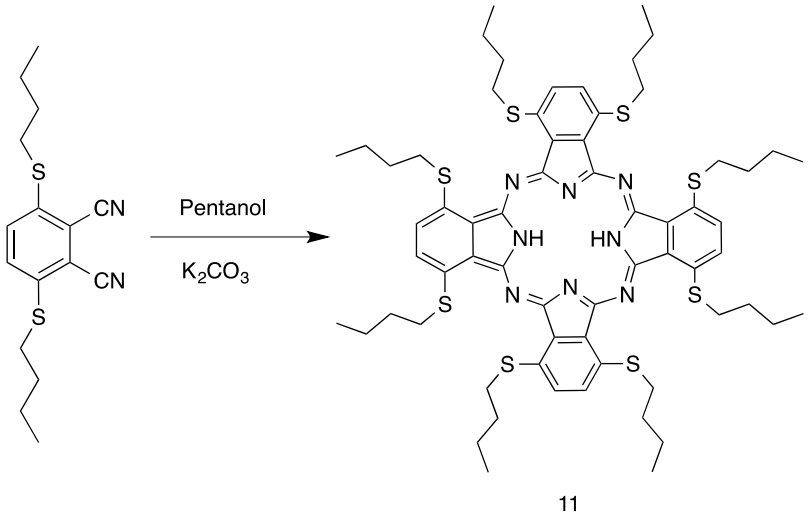

Figure 3.12. Synthesis of compound **11**.

3.5.7. Synthesis of Compound 12

1,4,8,11,15,18,22,25-octakis(butylthio)phthalocyanine **11** (100 mg, 0.078 mmol) was dissolved in DMF (5 mL) and then Zn acetate (171.1 mg, 7.79 mmol) was added to the mixture and was heated to 80 °C [54]. After stirring the reaction for a day at 80 °C, check it with TLC using DCM solvent system. Water was added to the reaction mixture and the

resulting precipitate was filtered, dissolved in DCM. Then the solvent was removed and product purified with preparative TLC using DCM/Ethanol (100:1) for elution yielding 90 mg (90%). $C_{64}H_{80}N_8S_8Zn$, MW: 1283.96, m.p. >250 °C. UV-Vis ($CDCl_3$): λ_{max} (nm) (logε): 792(4.86), UV-Vis (THF): λ_{max} (nm) (logε): 781 (5.26), UV-Vis (DMSO): λ_{max} (nm) (logε): 798(5.30). ATR-IR (cm^{-1}) 2955, 2927, 2870, 2857, 1558, 1461, 1435, 1316, 1286, 1209, 1145, 1109, 1037, 924, 884, 801, 788, 750.

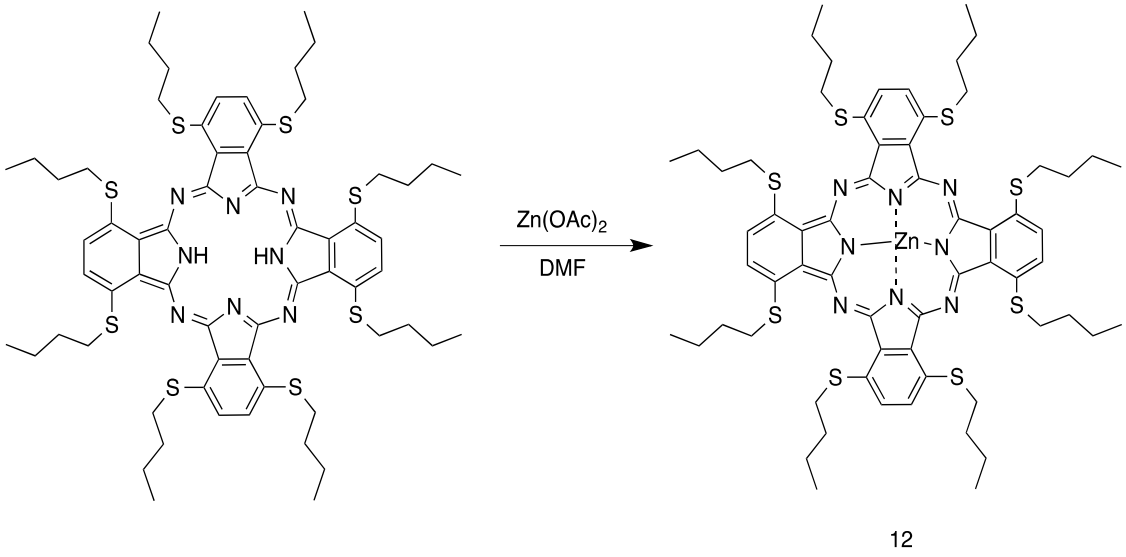

Figure 3.13. Synthesis of compound **12**.

3.5.8. Synthesis of Compound 15

A 100 mL round bottom flask was charged with compound **6** (430 mg, 1 mmol), phthalonitrile (1.3 g, 10 mmol), DCB (3 mL) and DMF (1 mL). Then Zn acetate (1.3 mg, 6 mmol) was added to the reaction and the mixture was stirred for a day at 150 °C [61-61]. After cooling down, ethanol-water mixture in equal amount was added to the mixture and the precipitate was filtered, dissolved in DCM. The solvent was removed and the product was purified with preparative TLC using DCM/Ethanol, 40:1 for elution. $C_{44}H_{40}N_8O_4S_2Zn$, MW: 874.36. ATR-IR (cm^{-1}) 2954, 2925, 2855, 1482, 1467, 1411, 1329, 1307, 1281, 1217, 1166, 1138, 1125, 1058, 921, 886, 808, 770, 757, 739, 705. MS (MALDI-TOF): *m/z* 875.354 $[M]^+$.

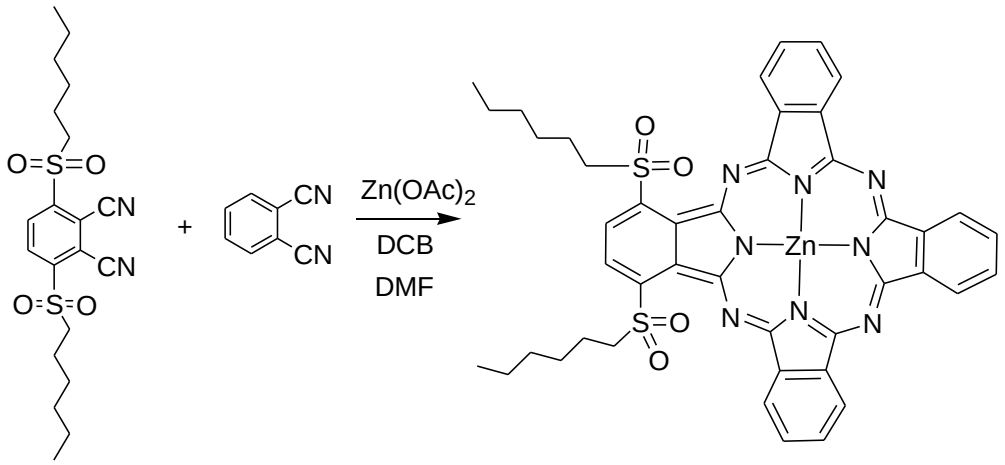

15

Figure 3.14. Synthesis of compound **15**.

4. RESULTS AND DISCUSSION

4.1. Phthalonitriles: Comparative Synthesis and Characterization

4.1.1. -SR Phthalonitriles

In this work all of the phthalonitriles either novel for the literature or not, were characterized by ATR-IR, mass, ^{1}H NMR and ^{13}C NMR spectroscopy. We also obtained crystal data for **3** and **4.**

The starting material was 2,3-dicyano hydroquinone which is a commercially available product for all of the phthalonitriles. After tosylation of the alcohol groups in 2,3-dicyano hydroquinone, the product **1** undergoes nucleophilic substitution reactions in basic condition with different thiol groups which were chosen on purpose.

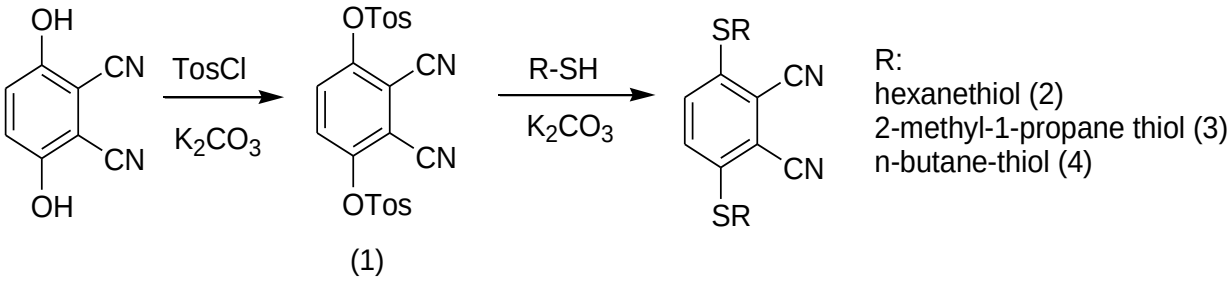

Figure 4.1. General overview of the synthesis of phthalonitriles; **2**, **3**, **4**.

From Table 4.1 it is seen that the first two phthalonitriles have good yields compare to phthalonitrile **4**. Compound **3** which is the branched form of **4** has higher m.p. due to the fact that branching gives it a more compact structure, which packs more easily into a solid structure thereby increasing melting point.

Table 4.1. M.p. and yield values of non-peripheral phthalonitriles.

		Compound Number	Yield (%)	Melting Point (°C)
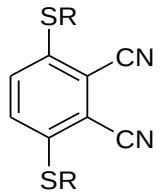	R: hexyl	**2**	47	85
	R: isobutyl	**3**	55	116
	R: *n*-butyl	**4**	10	102

Figure 4.2 shows the ATR-IR superimposed spectra of the compounds **2**, **3**, **4** respectively and their common peaks at around 2226 cm^{-1} imply to -C≡N bonds of the phthalonitriles. The other peaks belong to phthalonitriles can also be detected from the spectra below (Figure 4.2): aliphatic C-H bonds (2950-2860 cm^{-1}), aromatic -C-H bonds (3000-3100 cm^{-1}) and -C=C- bonds (1400-1560 cm^{-1}).

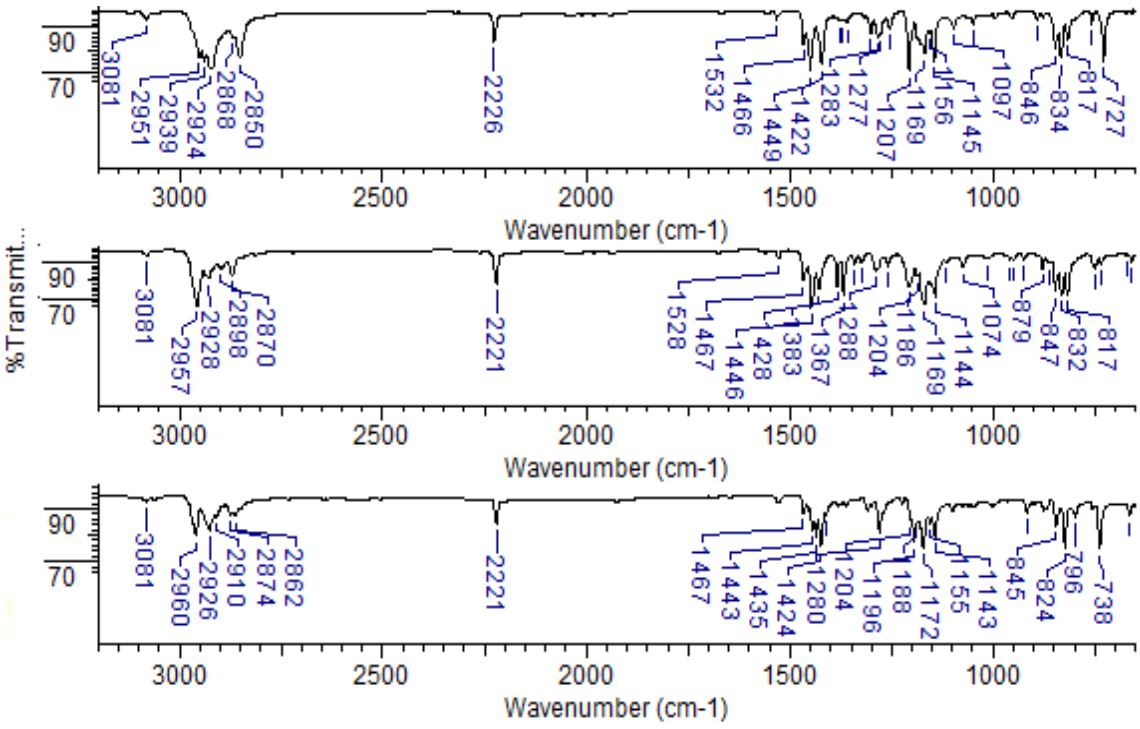

Figure 4.2. ATR-IR spectra of the compounds **2** (up), **3**, **4** (down) respectively.

Phthalonitriles **2**, **3**, **4** have similar ATR-IR spectra because of their alike structures. The presence of nitrile peaks around 2230 cm^{-1} in the spectra were the biggest evidence for

existence of phthalonitriles. The weak peak around 3081 cm^{-1} refers to Ar-H in phthalonitriles.

Due to unavailability of the mass spectrum, only mass spectra of compound **4** could be obtained. The main peak has the value 343.144 which has confirmed with theoretical mass value 304.47, when the mass of potassium ion 39 was added to theoretical mass. This additional mass stems from KBr pellet of the instrument itself.

^{1}H NMR of phthalonitriles truly confirm the molecules with the expected. Figure 4.3 shows ^{1}H NMR spectra of the compounds **2, 3, 4** respectively. All of the peaks come after the solvent chloroform peak around 7.26 ppm belong to benzene proton of phthalonitriles. Aliphatic hydrogen atoms appear on the right side of the spectrums as expected and their intensities are proportional to number of hydrogen atoms they have.

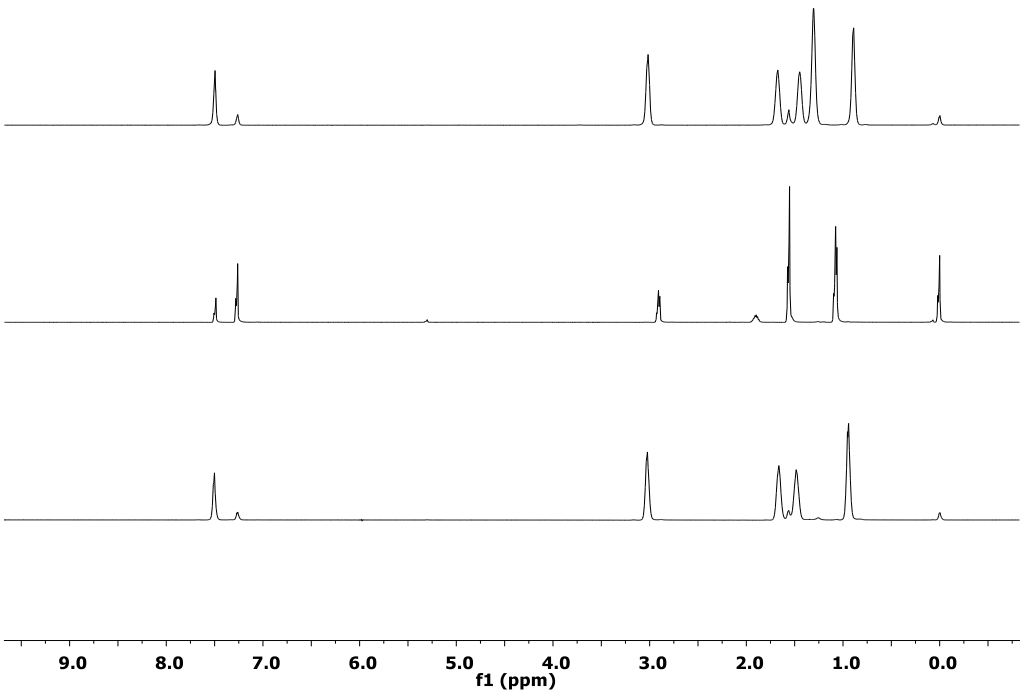

Figure 4.3. ^{1}H NMR spectra of the compounds **2** (up), **3**, **4** (down) respectively.

Phthalonitrile **3** has an intense H_2O peak around 1.54 ppm and apart from that peak there is an intense peak around 1 ppm implying to -CH_3 protons which look each other in the isobutyl-thiol group. Around 2 ppm there is a very weak peak belongs to -CH group.

However phthalonitrile **4** has four aliphatic peaks in its spectrum because of the fact that it is linear and hydrogen dispersion is more homogenous so the intensities of the peaks are similar.

The crystal structures were also obtained for phthalonitriles **3**, **4** depicted below. The crystals were grown in (DCM+Ethanol) solvent mixture.

Figure 4.4. Crystal structure of phthalonitrile **3**.

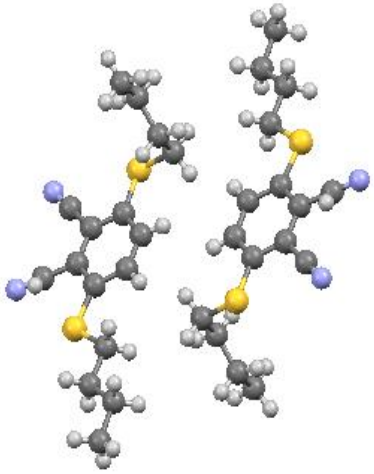

Figure 4.5. Crystal structure of phthalonitrile **4**.

4.1.2. –SO_2R Phthalonitrile

Compound **5** had a second step which was the oxidation of thiol groups of compound **2**.

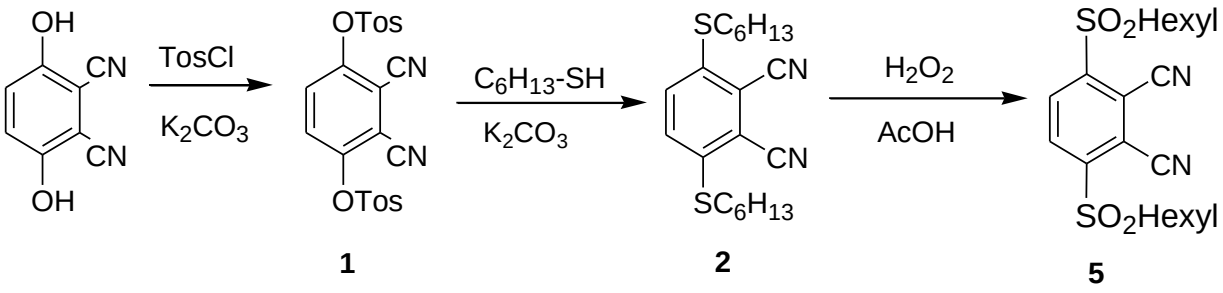

Figure 4.6. Synthesis of phthalonitrile **5**.

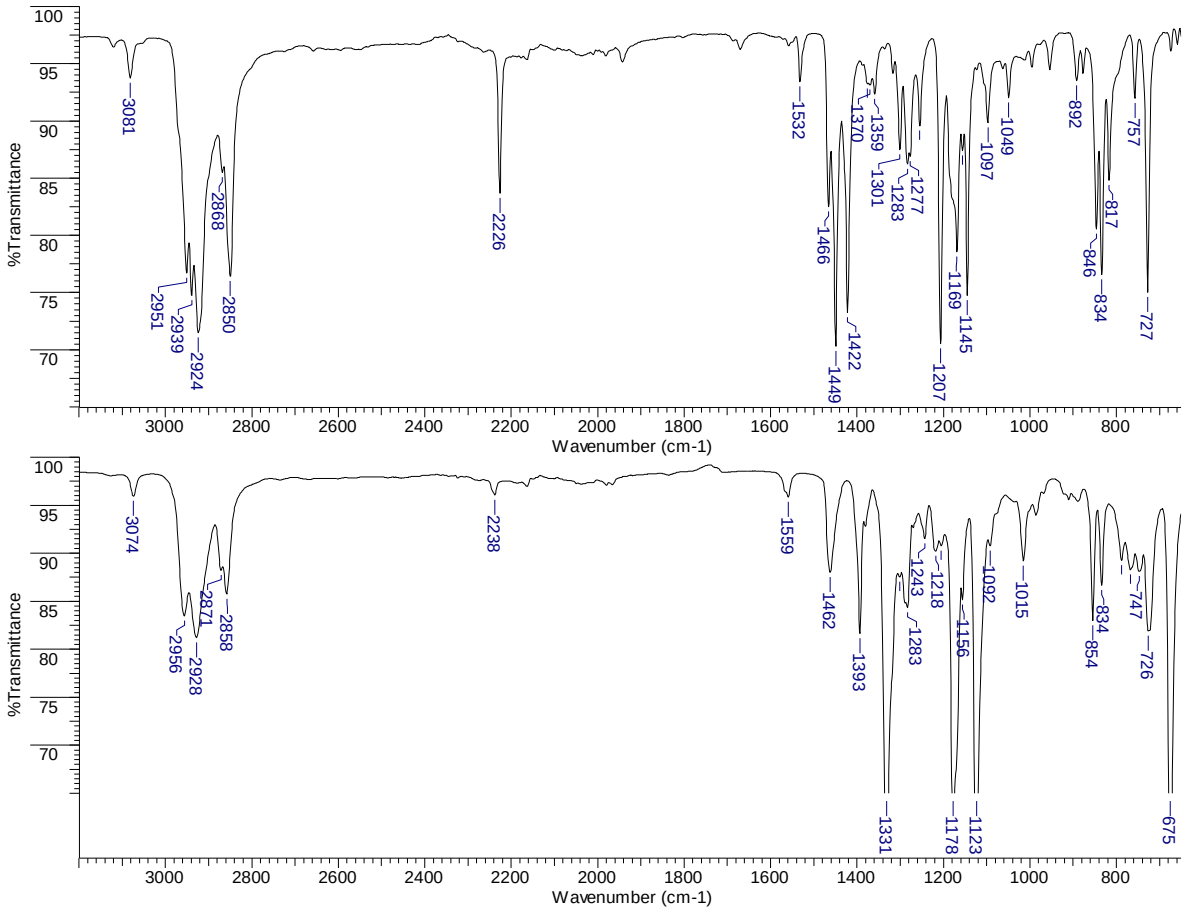

Figure 4.7. ATR-IR spectra of the compounds **2** (up), **5** (down) respectively.

For the compound **5** sulfonyl substitution pattern did not affect ATR-IR spectrum result too much compared to compound **2**. It also shows for the compound **5**, the characteristic peaks of the sulfonyl function at 1178 and 1330 cm^{-1}, and the peaks centered at 2900 cm^{-1} corresponding to the alkyl chains. Unlike for most of phthalonitrile derivatives, peak of the CN function is not intense but appears anyway at 2238 cm^{-1}.

It can easily be seen from the spectra that aromatic proton of phthalonitrile **5** appears at higher ppm because of the oxygen atoms in -SO_2 groups. The greater electron density results in higher ppm. This is also valid for -SCH_2 protons of **5** as well. While -SCH_2 protons of thiol substituted phthalonitriles appear around 3 ppm, -SCH_2 protons of sulfonyl substituted phthalonitrile **5** are shifted to slightly higher ppm.

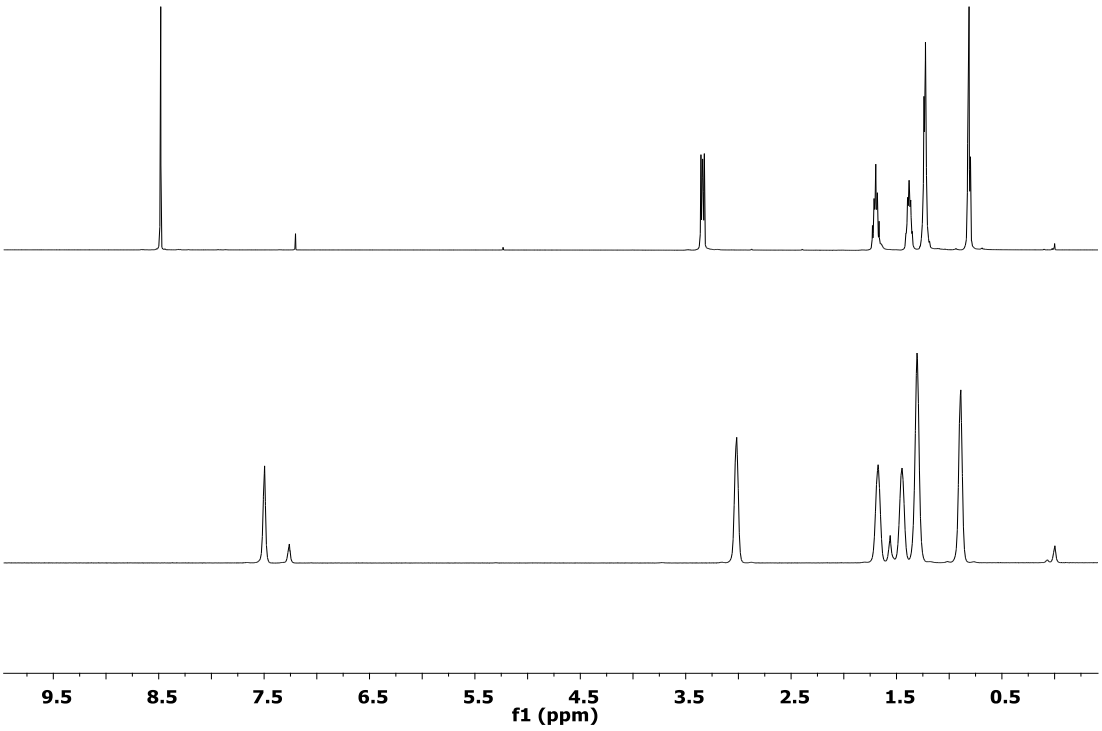

Figure 4.8. ^{1}H NMR spectra of the compounds **2** (down), **5** (up) respectively.

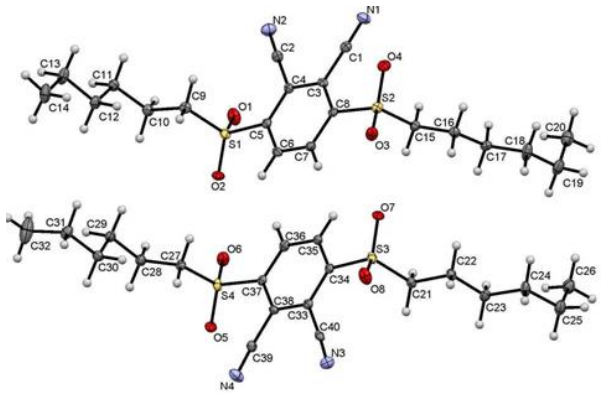

Figure 4.9. Crystal structure of phthalonitrile **5**.

4.2. Synthesis of Octa -SR Free Phthalocyanines

Phthalocyanines synthesized in this work were characterized by ATR-IR, Mass, UV-Vis, ^{1}H NMR and ^{13}C NMR spectroscopy. Firstly, free phthalocyanines were synthesized and their metallation part were done as the second step. The schematic description of the synthesis of free phthalocyanines is given in Figure 4.10.

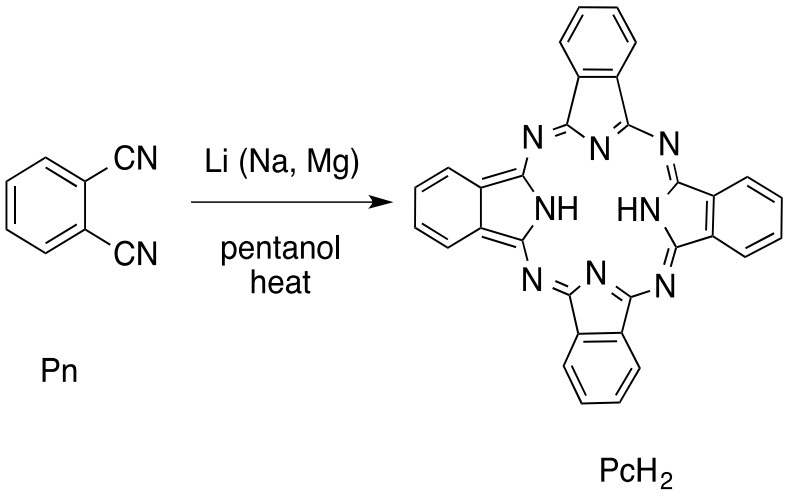

Figure 4.10. Synthesizing method of free phthalocyanines.

During the first step of synthesis of symmetric phthalocyanines pentanol was used as solvent and lithium was added too. By adding water, lithium was extracted from the mixture. Reaction were accomplished under argon gas at high temperatures. Free phthalocyanines were prepared by lithium-assisted templating method from the corresponding phthalonitriles [58].

Table 4.2. Yields and melting points of phthalocyanines **6**, **9**, **11**.

Compound	**Yield (%)**	**Melting Point (°C)**
6	50	162
9	21	88
11	30	210

As it can be seen from Table 4.3, free phthalocyanines have mass peaks in accordance with theoretical masses of them. The whole mass spectra of the compounds were given before.

Table 4.3. MS MALDI spectra of the phthalonitriles **6**, **11** in DHB matrix.

Compound	**6**	**11**
Theoretical Mass (g)	1444.330	1218.44
Mass Peak m/z	1444.646	1220.820

^{13}C and ^{1}H NMR spectra were taken in $CDCl_3$, the results support the expected structures. All of the ^{13}C NMR spectra show a multiplet solvent peak of $CDCl_3$ between 75-80 ppm. Other intense peak at 110 ppm and a weak peak at around 196 ppm have no meaning in terms of our structures and they are resulted from the instrument itself.

Figure 4.11 shows ^{1}H NMR of phthalocyanine **9** with its structure. Due to electronegativity of the sulphur atom -SCH_2 protons are shifted to the left apart from other aliphatic hydrogen atoms. The aromatic hydrogen appears around 7.84 ppm. The integrals of the peaks are in accordance with the numbers of the hydrogen atoms that phthalocyanine has. There is also an inset structure with numbered hydrogen atoms assigned to peaks.

^{1}H NMR spectra of phthalocyanine **9** and **11** were compared in Figure 4.12 below. They both have aromatic protons further 7.5 ppm. The closest protons to sulphur atom appear a little bit far from other alkyl protons at around 3.5 ppm. Linear carbon chain of phthalocyanine **11** results in addition of one more peak to the spectra.

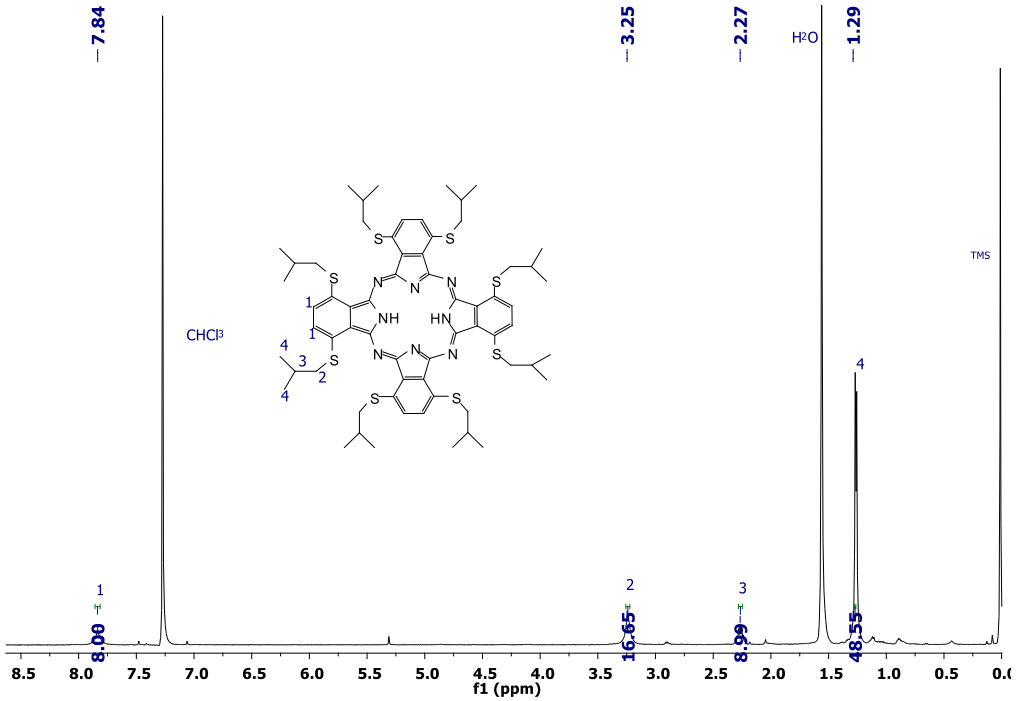

Figure 4.11. ^{1}H NMR of phthalocyanine **9** with its structure.

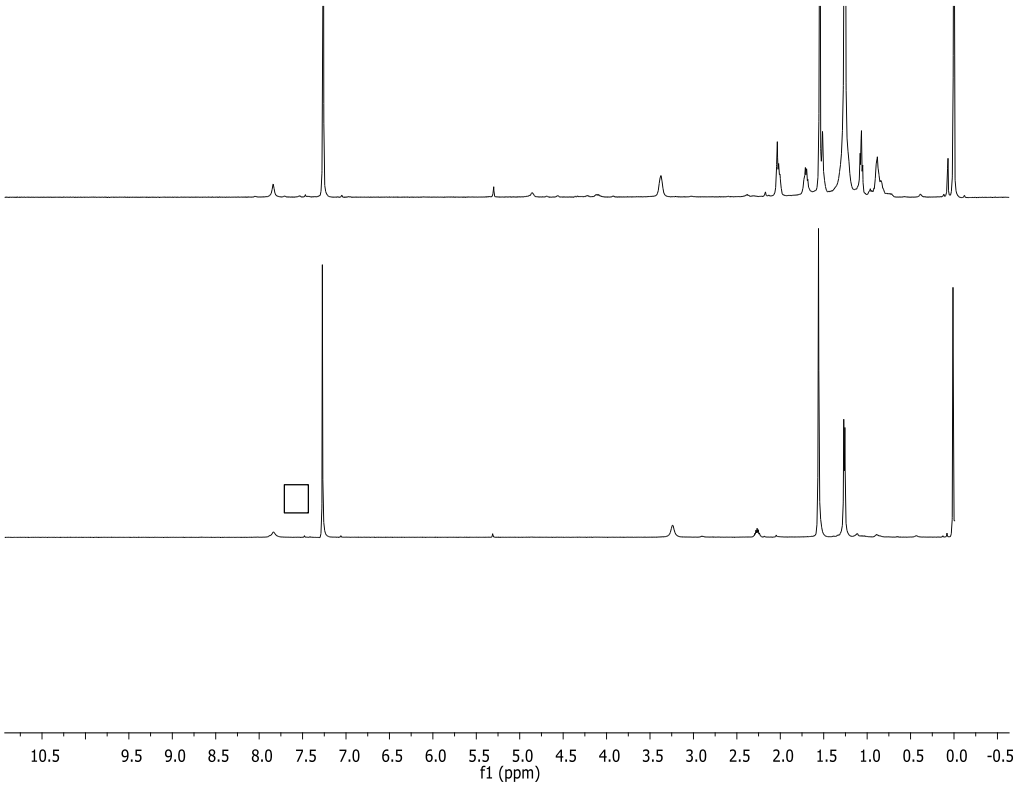

Figure 4.12. ^{1}H NMR spectra of phthalocyanine **9** (up) and **11** (down) respectively.

UV-Vis spectra of the compounds made it possible to have an idea about photophysical properties of the compounds synthesized. Figure 4.13 shows UV-Vis spectra of the compound **11** in THF with increasing molarity 2 µM (up to 10 µM). The linear increasing trend of absorbance as going up to 10 µM demonstrates that the spectra follows the Beer-Lambert Law.

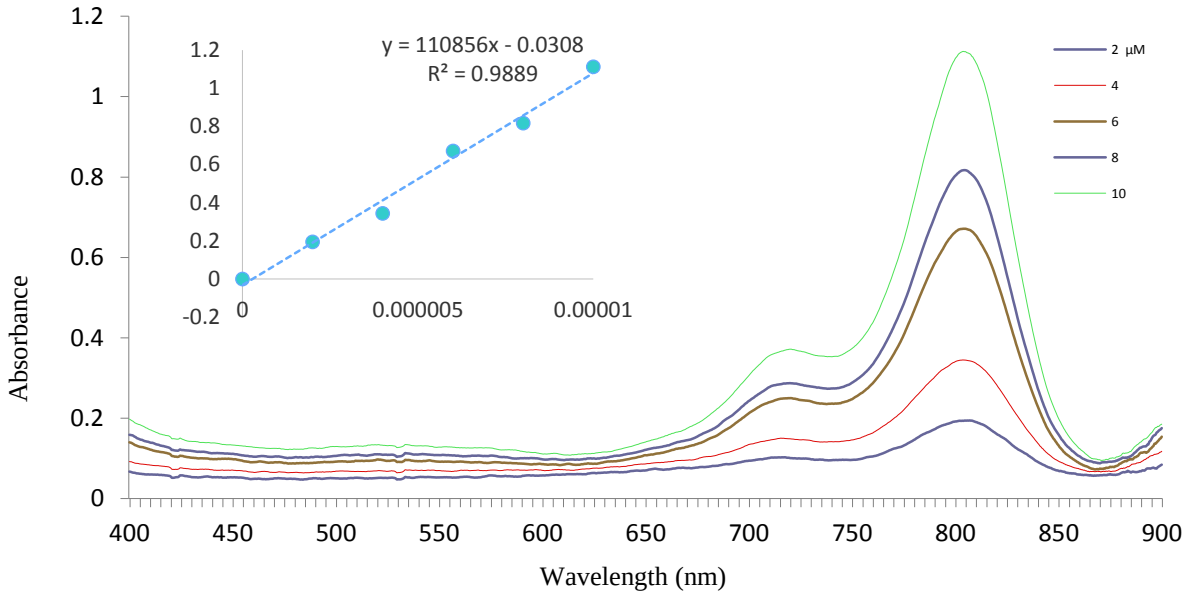

Figure 4.13. UV-Vis spectra of compound **11** in THF at different concentrations.

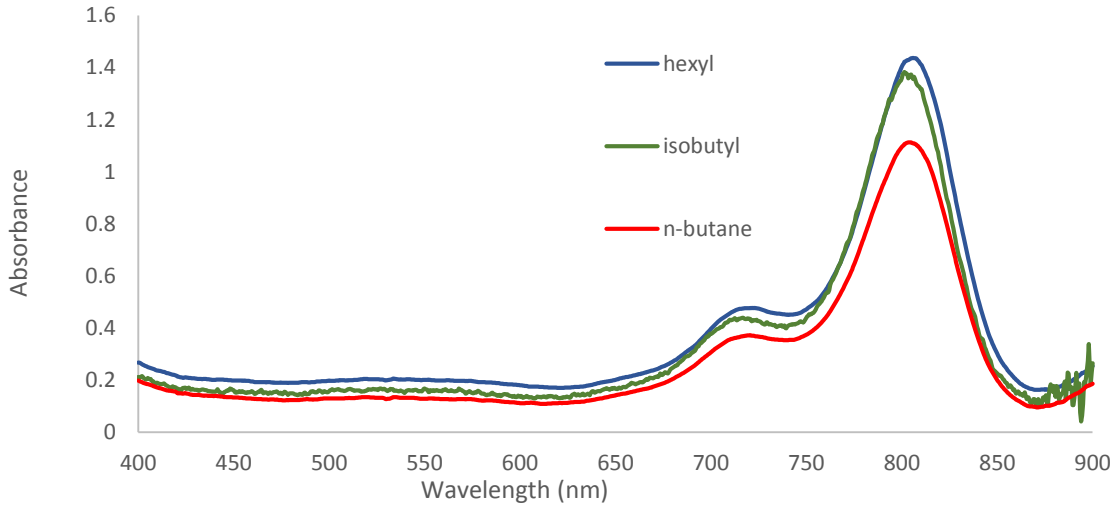

Figure 4.14. UV-Vis spectra of the compounds **6**, **9**, **11** (10 µM) in THF.

To see the effect of length of the carbon chains in phthalocyanines, the UV spectra of phthalocyanine **6**, **9** and **11** were overlaid below. While the length of the carbon chain does not affect the maximum absorption wavelength, absorption value shows a decreasing trend as the chain becomes shorter. This decrease becomes very slight when it comes to branched chains.

4.3. Metallation of Phthalocyanines

Metallation of free phthalocyanines **6**, **9** and **11** were done using DMF as solvent at relatively lower temperatures than the first step composing free phthalocyanines. Although metallation of phthalocyanine **6** was successful with zinc and platinum metals, metallation with metals aluminum and platinum failed. Targeted phthalocyanine **13** and **14** could not be obtained. The targeted compound **13** was mixed with Pt(II)2,4-pentane-dionate in benzonitrile at 180 °C in microwave. To obtain phthalocyanine **14,** the reaction was run with Al metal in DMF at 80 °C, $AlCl_3$ was used in the reaction as metal salt.

Phthalocyanine **8** underwent a reaction using benzonitrile in microwave and $Pd(acac)_2$ was used as metal source. Microwave assistance was used to lower the reaction time. Microwave assisted reactions provide a convenient and faster way for the metallation of free phthalocyanines [63]. Table 4.4 gives very high yield values for metallation of phthalocyanines.

Table 4.4. Yields and melting points of phthalocyanines **7**, **8**, **10**, **12**.

Compound	**Yield (%)**	**Melting Point (°C)**
7	90	176
8	95	waxy
10	93	waxy
12	98	>250

Table 4.5. Mass spectra of the phthalocyanines **7**, **10** in DHB matrix.

Compound	**7**	**10**
Theoretical Mass (g)	1507.69	1283.26
Mass Peak m/z	1507.710	1283.109

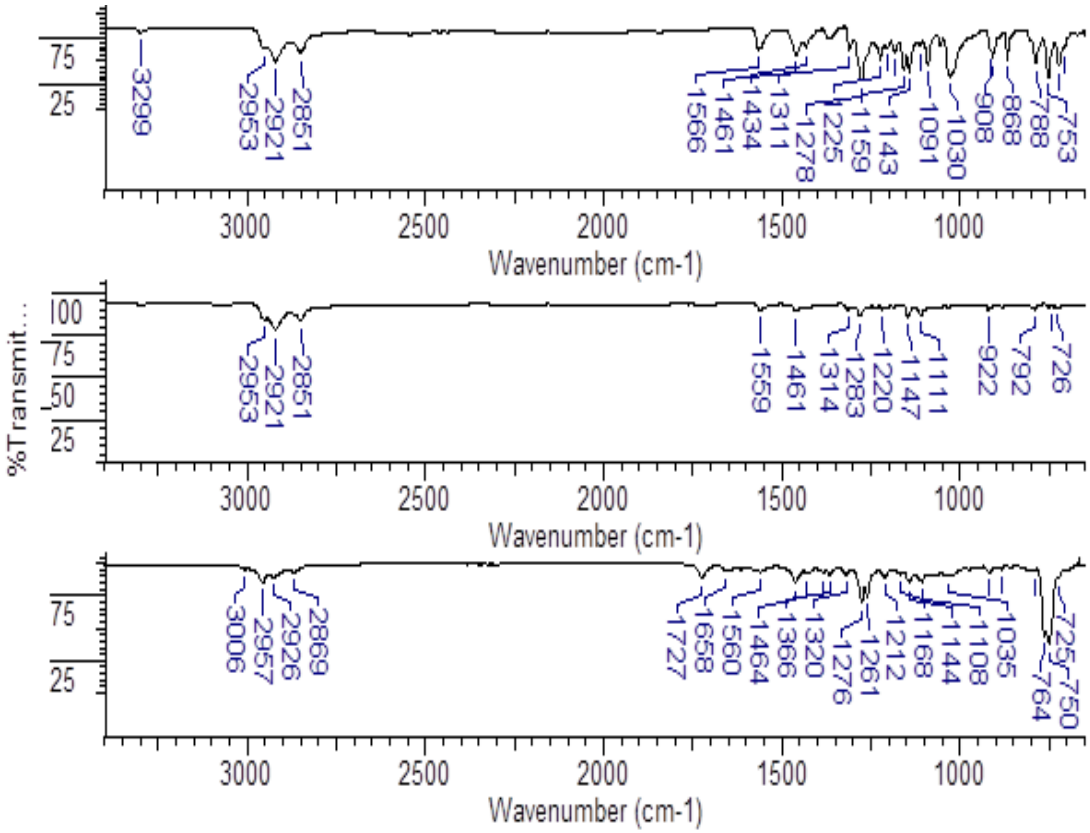

Figure 4.15. Comparative ATR-IR spectra of **6** (up), **7** (middle), **10** (down) respectively.

Figure 4.15 demonstrates disappearance of all the nitrile peaks proving the existence of phthalocyanines and also after metallation of compound **6** the peak at 3299 cm^{-1} which is responsible for N-H stretch has disappeared in compound **7** and **10**. This results from the metal they have in the core. Between 2950-2850 cm^{-1}, spectra have alkyl C-H stretch peaks as expected

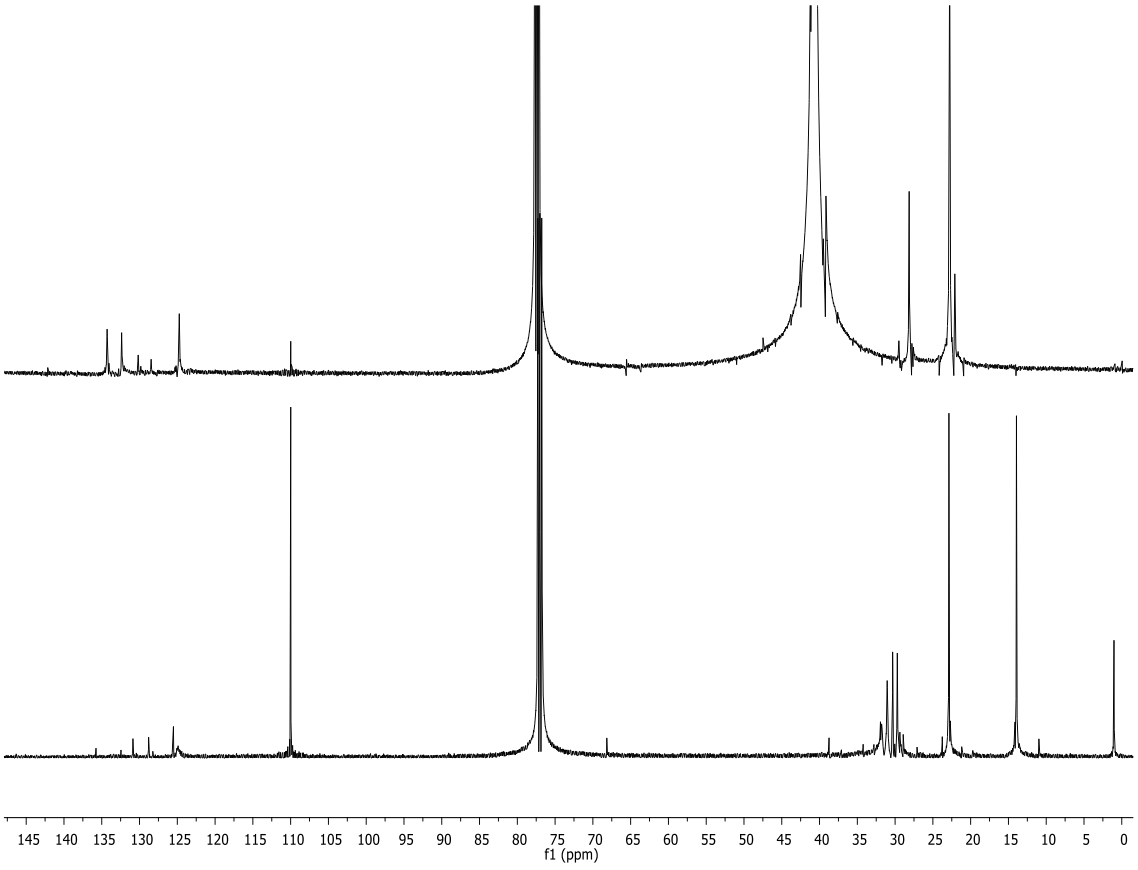

Figure 4.16. ^{13}C NMR of phthalocyanine **10** (up) and **11** (down) respectively.

Both phthalocyanine **10** and **11** ^{13}C NMR spectra are matching with expectations (Figure 4.16). Linear *n*-butane group in phthalocyanine **11** has one more carbon atom to branched isobutyl in phthalocyanine **10**. This difference appears on NMR spectrum as addition of one peak to spectra of phthalocyanine **10**.

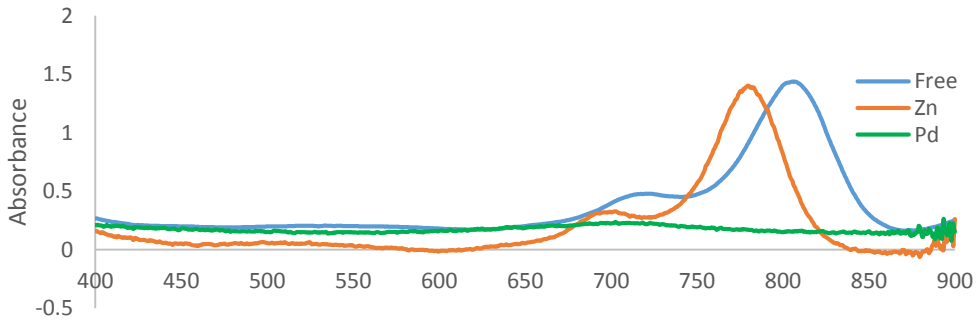

Figure 4.17. UV-Vis spectra of the compounds **6**, **7**, **8** (10 µM) in THF.

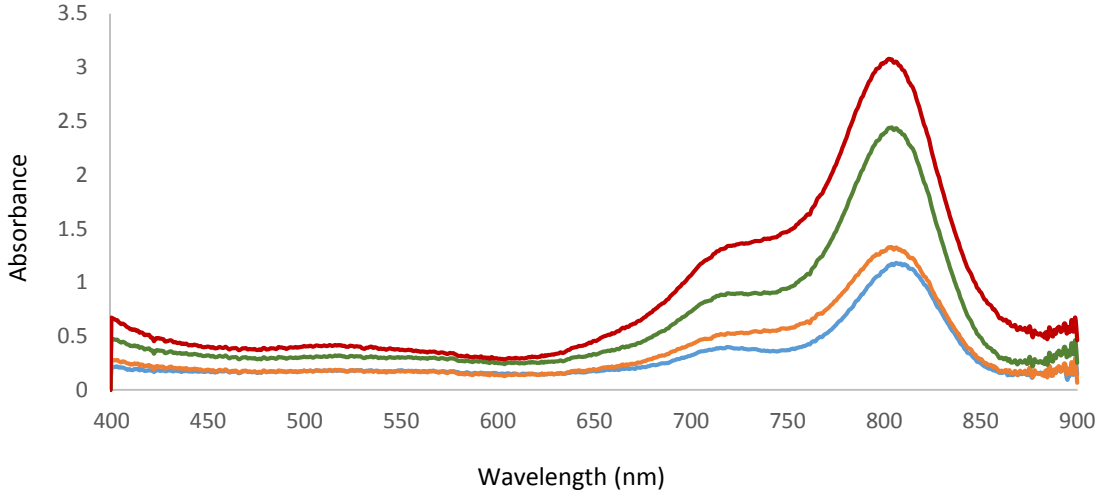

Figure 4.18. UV-Vis spectra of **9** (down), **10**, **11**, **12** (up) (10 µM) respectively in $CHCl_3$.

From the Figure 4.17 it can be observed that ZnPc has blue shifted contrary to the expectations and Pd-phthalocyanine's absorbance intensity is very low compare to the other two phthalocyanines.

Figure 4.18 compares isobutyl Pc, *n*-butane Pc and their metallated Zn derivatives. From the figure, it is very obvious that metallation increases the absorbance and shifts the maximum absorption to the left.

4.4. Octa Alkyl Sulfonyl Substituted A3B Type Phthalocyanine

Seeking for a new substitution pattern resulted in synthesis of phthalonitrile **6** by oxidation of thiol groups in phthalonitrile **2**. In addition to metallation part asymmetrically substituted phthalocyanine **15** with AB_3 type was designed and was synthesized by statistical condensation of appropriate precursors. The use of one of the phthalonitriles in excess is one such modification that may favor the formation A_3B phthalocyanines. After optimization of the reaction conditions six major differently substituted phthalocyanines are expected to be formed (Figure 4.19).

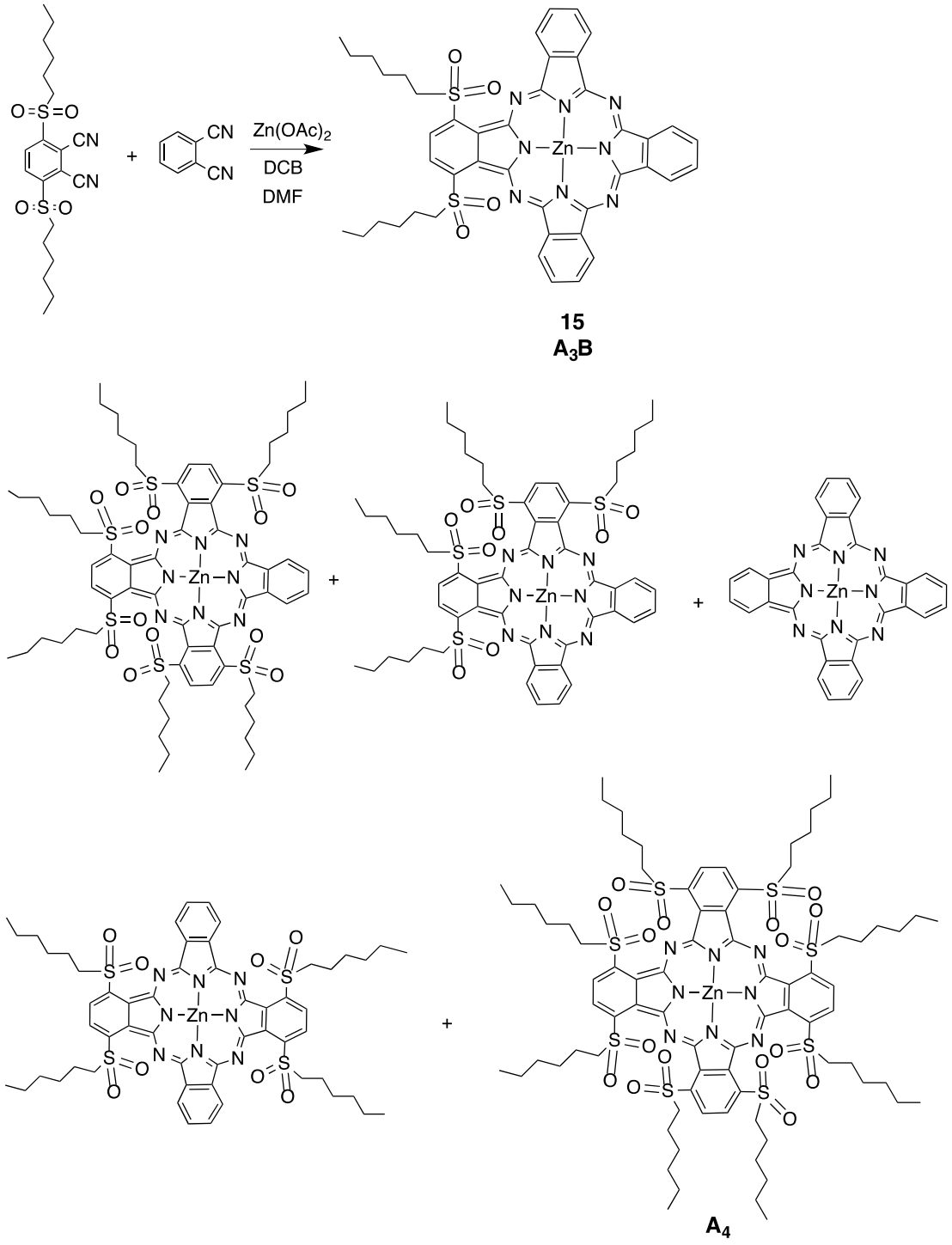

Figure 4.19. A_3B type of phthalocyanine and other isomers.

Based on this fact phthalonitrile **6** was put in reaction with an excess of unsubstituted phthalonitrile, following the statistical conditions routinely used (9:1 ratio), in the presence of zinc acetate. Dimethylformamide/o-dichlorobenzene solvent mixture was used and the

reaction was followed by chromatographic separation of the desired product with A_3B type. After tedious chromatographic procedures, all of the isomers were obtained except phthalocyanine with A_4 type. So symmetric isomer of the reaction could not be obtained.

The desired phthalocyanine **15** with A_3B type which has a molecular ion peak at 875.354 (Figure A.48) is in accordance with theoretical value 874.36 g/mol.

Contrary to metallated phthalocyanines zinc acetate was added to reaction meanwhile forming phthalocyanines. So phthalocyanine **15** was both synthesized and metallated in one step. During the reaction DCB also was used as a solvent.

5. CONCLUSION

In this thesis to tailor required properties of phthalocyanines, modification of the phthalocyanine macrocycle was needed. To do so, metallated octa -SR phthalocyanines have been investigated. Metallation of these phthalocyanines have played a big role. The central metal played a significant role in the red shifting behavior of phthalocyanines. All of them were well characterized.

The new substitution pattern -diSO_2 phthalonitrile was composed additionally and a novel asymmetric AB_3 type -diSO_2 substituted phthalocyanine was investigated.

REFERENCES

1. Dewaele, M., T. Verfaillie, W. Martinet, and P. Agostinis "Death and Survival Signals in Photodynamic Therapy", *Methods in Molecular Biology*, Vol. 635 pp. 7-33, 2010.

2. Biel M. A., "Photodynamic Therapy of Head and Neck Cancers", *Methods in Molecular Biology*, Vol. 635, pp. 281-293, 2010.

3. Shishkova N., O. Kuznetsova, and T. Berezov, "Photodynamic Therapy for Gynecological Diseases and Breast Cancer", *Cancer Biology Med*, Vol. 9, pp. 9-17, 2012.

4. Dolmans D. E. J. G. J., D. Fukumura and R. K. Jain "Photodynamic Therapy for Cancer", *Nature Reviews Cancer*, Vol. 3, pp. 380-387, 2003.

5. Agostinis P., K. Berg, K. A. Cengel, T. H. Foster, A. W. Girotti, S. O. Gollnick, S. M. Hahn, M. R. Hamblin, A. Juzeniene, D. Kessel, M. Koerbelik, J. Moan, P. Mroz, D. Nowis, J. Piette, B. C. Wilson, J. Golab, "Photodynamic Therapy of Cancer: an Update", *CA Cancer Jornal of Clinicians*, Vol. 61(4), pp. 250–281, 2011.

6. Riberio J. N., A. R. Silva, R. A. Jorge, "Involvement of Mitochondria in Apoptosis of Cancer Cells Induced by Photodynamic Therapy", *Journal Of The Brazilian Chemical Soceity*, Vol. 40, pp. 383-390, 2004.

7. Moan J. and Q. Peng, "An outline of the hundred-year history of PDT", *Anticancer Research*, Vol. 23, pp. 3591-600, 2003.

8. Berg K., P. K. Selbo, A. Weyergang, A. Dietze, L. Prashmickaite, A. Bonsted, B. Ø. Engesaeter, E. Angel-Petersen, T. Warloe, N. Frandsen and A. HØgset, "Porphyrin-related Photosensitizers for Cancer Imaging and Therapeutic Applications", *Journal*

of Microscopy, Vol 218, pp. 133-147, 2005.

9. Josefsen L. B. and R W Boyle, "Photodynamic Therapy: Novel Third-Generation Photosensitizers One Step Closer*?", British Journal of Pharmacology*, Vol. 154, pp. 1-3, 2008.

10. Vo-Dinh T., *Biomedical Photonics Handbook, Second Edition: Therapeutics and Advanced* , CRC Press, 2014.

11. Ethirajan M. , Y. Chen , P. Joshi and R. K. Pandey, "The Role of Porphyrin Chemistry in Tumor Imaging and Photodynamic Therapy", *Chemical Society Reviews*, Vol. 40, pp. 340-362, 2011.

12. Ferraz R. , C. R. Fontana, A. P. D. Ribeiro, F. Z. Trindade, F. H. Bartoloni, J. W. Baader, E. C. Lins, V. S. Bagnato and C. Kurachi, "Chemiluminescence as a PDT Light Source for Microbial Control", *Journal of Photochemistry and Photobiology B: Biology*, Vol. 103, pp. 87-92, 2011.

13. Kadish K. M., K. M. Smith, R. Guilard, *The Porphyrin Handbook, Academic Press*, USA,2000.

14. Nyman E. S. and P. H. Hynninen, "Research Advances in the Use of Tetrapyrrolic Photosensitizers for Photodynamic Therapy", *Journal of Photochemistry and Photobiology B : Biology*, Vol. 73, pp. 1-28, 2004.

15. Josefsen L. B. and R. W. Boyle, "Photodynamic Therapy and the Development of Metal-based Photosensitizers", *Metal Based Drugs*, Vol. 2008, pp. 1-24, 2007.

16. Weber R. and B. A. Moore, *"Cutaneous Malignancy of the Head and Neck: A Multidisciplinary Approach",* Plural Publishing, USA, 2011.

17. Branceleon L. and H. Moseley, "Laser and Non-laser Light Sources for Photodynamic Therapy", Lasers in Medical Science, Vol 17, pp. 173-176, 2002.

18. Patrice T., "*Photodynamic Therapy",* The Royal Society of Chemistry, Cambrigde, 2003.

19. Chaves M. E. A., A. R. de Araújo , A. C. C. Piancastelli , M. Pinotti, "Effects of Low-power light Therapy on Wound Healing: LASER x LED", *Anais Brasileiros de Dermatalogia,* Vol. 89(4), pp. 616-623, 2014.

20. Immunolight, *Technology*, 2014, http://www.immunolight.com/technology/, February 2015.

21. Monge-Fuentes V., L. A. Muehlmann and R. B. de Azevedo, "Perspectives on the application of nanotechnology in photodynamic therapy for the treatment of melanoma", *Nano Reviews,* Vol. 5, 2014.

22. Atkins P., J. de Paula, *J. Atkins' Physical Chemistry*, 7th ed., Oxford University Press, USA, 2001.

23. Bae B. and K. Na, "Development of Polymeric Cargo for Delivery of Photosensitizer in Photodynamic Therapy", *International Journal of Photoenergy*, Vol. 2012, 2012.

24. Luksiene Z., "Photodynamic Therapy: Mechanism of Action and Ways to Improve the Efficiency of Treatment", *Medicina*, Vol. 39 (12), pp. 1137-1150, 2003.

25. Dougherty T. J., C. J. Gomer, B. W. Henderson, G. Jori, D. Kessel, M. Korbelik, J. Mohan and Q. Peng, "Photodynamic Therapy", *Journal of the National Cancer Institute*, Vol. 90(12), pp. 889-905, 1998.

26. J. P. Celli, B. Q. Spring, I. Rizvi, C. L. Evans, K.S. Samkoe, S. Verma, B. W. Pogue and T. Hasan, "Imaging and Photodynamic Therapy: Mechanisms, Monitoring, and Optimization", *Chemical Review*, Vol. 110, pp. 2795–2838, 2010.

27. Ochsner M., "Photophysical and Photobiological Progress in the Photodynamic

Therapy of Tumors", *Journal of Photochemistrry and Photobiology B-Biology,* Vol. 39,pp. 1-18, 1997.

28. Schmidt R. L., "Photosensitized Generation of Singlet Oxygen", *Photochemistry and Photobiology,* Vol. 2, pp. 1161-1177, 2006.

29. Huang Y., M. Tanaka, D. Vecchio, M. G. Diaz, J. Chang and M. R. Hamblin, "Photodynamic Therapy Induces an Immune Response Against a Bacterial Pathogen", *Expert Review of Clinical Immunology,* Vol. 8(5), pp. 479-494, 2012.

30. Verhille M., P. Couleaud, R. Vanderesse, D. Brault and M. Barberi-Heyob, C. Frochot, "Modulation of Photosensitization Processes for an Improved Targeted Photodynamic Therapy", *Current Medicinal Chemistry,* Vol. 17(32), pp. 3925-3943, 2010.

31. Ortel B., C. R. Shea and P. Calzavara-Pinton, "Molecular Mechanisms of Photodynamic Therapy", *Frontiers in Bioscience,* Vol. 14, pp. 4157-4172, 2009.

32. Castano A. P., T. D. Demidova and M. R. Hamblin, "Mechanisms in photodynamic therapy: part-one photosensitizers, photochemistry and cellular localization", *Photodiagnosis and Photodynamic Therapy,* Vol. 1, pp. 279-293, 2004.

33. Mroz P., A. Yaroslavsky, G. B. Kharkwal and M. R. Hamblin, "Cell Death Pathways in Photodynamic Therapy of Cancer", *Cancers,* Vol. 3, pp. 2516-2539, 2011.

34. Abdel-Kader M. H., *Photodynamic Therapy: From Theory to Application,* Springer, 2014**.**

35. Wachowska M., A. Muchowicz, M. Firczuk, M. Gabrysiak, M. Winiarska, M. Wańczyk, K. Bojarczuk and J. Golab, "Aminolevulinic Acid (ALA) as a Prodrug in Photodynamic Therapy of Cancer", *Molecules,* Vol. 16, pp. 4140-4164, 2007.

36. Huang Z., H. Xu, A. D. Meyers, A. I. Musani, L. Wang, R. Tagg, A. B. Barqawi and Y. K. Chen, "Photodynamic Therapy for Treatment of Solid Tumors – Potential and Technical", *Technology in Cancer Research and Treatment,* Vol. 7, pp. 309-320, 2008.

37. Samat N., PJ Tan, K. Shaari, HB. Lee, "Prioritization of Natural Extracts by LC-MS-PCA for the Identification of New Photosensitizers for Photodynamic Therapy", *Analytical Chemistry,* Vol. 86(3), pp. 1324-1331, 2014.

38. Ganicz T., T. Makowski, W. A. Stanczyk and A. Tracz, "Side chain polysiloxanes with phthalocyanine moieties", *Express Polymer Letters,* Vol. 6, pp. 373–382, 2012.

39. Hone D. C. , P. I. Walker , R. Evans-Gowing , S. FitzGerald , A. Beeby , I. Chambrier , M. J. Cook , and D. A. Russell , "Generation of Cytotoxic Singlet Oxygen via Phthalocyanine-Stabilized Gold Nanoparticles: A Potential Delivery Vehicle for Photodynamic Therapy", *Langmuir,* Vol. 18 (8), pp. 2985–2987, 2002.

40. Garcia I. A. de C., A. M. Sevim, A. de la Escosura and T. Torres, "Synthesis of Unsymmetrical Carboxyphthalocyanines by Palladium -Catalyzed Hydroxycarbonylation of Iodo-Substituted Precursors", *Organic and Biomolecular Chemistry,* Vol. 11, pp. 2237-2240, 2013.

41. Torre G. D.L., C. G. Claessens and T. Torres, "Phthalocyanines: The Need for Selective Synthetic Approaches", *European Journal of Organic Chemistry,* Volume 2000(16), pp. 2821–2830, 2000.

42. Wöhrle D., G. Schnurpfeil, S. G. Makarov, A. Kazarin and O. N. Suvorova, "Practical Applications of Phthalocyanines _ from Dyes and Pigments to Materials for Optical, Electronic and Photo_electronic Devices", *Macroheterocycle,* Vol. 5, pp. 191-192, 2012.

43. Linstead R. P., "212. Phthalocyanines. Part I. A new type of synthetic colouring matters", *Journal of Chemical Soceity,* pp. 1016-1017, 1934.

44. Dehe D., C. Lothschütz and W. R. Thiel, "Novel pyrazole functionalized phthalocyanines and their first row transition metal complexes", *New Journal of Chemistry*, Vol. 34, pp. 526-532, 2010.

45. Oliveira K. T., F. F. de Assis, A. O. Ribeiro, C. R. Neri, A. U. Fernandes, M. S. Baptista, N. P. Lopes, O. A. Serra and Y. Iamamoto, "Synthesis of Phthalocyanines-ALA Conjugates: Water-Soluble Compounds with Low Aggregation", *Journal of Organic Chemistry*, Vol. 74, pp. 7962-7965, 2009.

46. Makhseed S., M. Machacek, W. Alfadly, A. Tuhl, M. Vinodh, T. Simunek, V. Novakova, P. Kubat, E. Rudolfe and P. Zimcik, "Water-soluble Non-Aggregating Zinc Phthalocyanine and In vitro Studies for Photodynamic Therapy", *Chemical Communications*, Vol. 49, pp. 11149-11151, 2013.

47. Bayrak R., H. T. Akçay, F. Ş. Beriş, E. Şahin, H. Bayrak and Ü. Demirbaş, "Synthesis, Aggregation and Spectroscopic Studies of Novel Water Soluble Metal Free, Zinc, Copper and magnesium Phthalocyanines and Investigation of their Anti-bacterial Properties", *Spectrochimica Acta Part A: Molecular and Biomolecular Spectroscopy*, Vol. 133, pp. 272-280, 2014.

48. Gobo N. R. S., T.J. Brocksom, J. Zukerman-Schpector and K. T. D. Oliveira, "Synthesis of an Octa-tert-butylphthalocynaine: A low-aggregating and Photochemically Stable Photosensitizer", *European Journal of Organic Chemistry*, Vol. 2013, pp. 5028–5031, 2013.

49. Walsh C. J. and B. K. Mandal, "A Novel Method for the Peripheral Modification of Phthalocyanines. Synthesis and Third-Order Nonlinear Optical Absorption of a-Tetrakis(2,3,4,5,6- pentaphenylbenzene)phthalocyanine", *Chemistry of Materials*, Vol. 12, pp. 287-289, 2000.

50. Dumoulin Fabienne, M. Durmuş, V. Ahsen. And T. Nyokong, "Synthetic pathways

to water-soluble phthalocyanines and close analogs", *Coordination Chemistry Reviews*, Vol. 254, pp. 2792-2847, 2010.

51. Sakamoto K. and E. Ohno-Okumura, "Syntheses and Functional Properties of Phthalocyanines", *Materials*, Vol. *2*, pp. 1127-1179, 2009.

52. Tekdas D. A., U. Kumru, A. G. Gürek, M. Durmus, V. Ahsen , F. Dumoulin, "Towards near-infrared photosensitisation: a photosensitising hydrophilic non-peripherally octasulfanyl-substituted Zn phthalocyanine", *Tetrahedron Letters*, Vol. 53, pp. 5227–5230 , 2012.

53. Jiang J. and Ö. Bekaroğlu, 2010, *Functional Phthalocyanine Molecular Materials*, Springer, Berlin.

54. Burnham P. M., M. J. Cook, L. A. Gerrard, M. J. Heeney and D. L. Hughes, "Structural characterisation of a red phthalocyanine", *Chemical Communication*,Vol.21, pp. 2064-2065, 2003.

55. Iqbal Z., N. Masilela, T. Nyokong, A. Lyubimtsev, M. Hanack and T. Ziegler , "Spectral, Photophysical and Photochemical Properties of Tetra- and Octaglycosylated Zinc Phthalocyanines", *Photochemical and Photobiological Science*, Vol. 11, pp. 679, 2012.

56. Kobayashi N., H. Ogata, N. Nonaka and E. A. Luk'yanets, "Effect of Peripheral Substitution on the Electronic Absorption and Fluorescence Spectra of Metal-Free and Zinc Phthalocyanines", *Chemistry a European Journal*, Vol. 9, pp. 5123–5134, 2003.

57. Topal Z. S.,Ü. İşci, U. Kumru, D. Atilla, A. G. Gürek,C. Hirel, M. Durmuş, J. Tommasino , D. Luneau, S. Berber, F. Dumoulin and V. Ahsen, "Modulation of the electronic and spectroscopic properties of Zn(II) phthalocyanines by their substitution pattern", *Dalton Transactions*, Vol. 43, pp. 6897-6908, 2014.

58. Zorlu Y., U. Kumru, Ü. İşçi, B. Divrik, E. Jeanneau, F. Albrieux, Y. Dede, V. Ahsen and F. Dumoulin, "1,4,8,11,15,18,22,25-Alkylsulfanyl phthalocyanines: effect of macrocycle distortion on spectroscopic and packing properties", *Chemical Communication"*, Vol. 51, pp. 6580-6583, 2015.

59. Schmid G., M. Sommerauer and M. Hanack, "Chromatographic Separation of the Four Possible Structural Isomers of a Tetrasubstituted Phthalocyanine: Tetrakis(2-ethylhexyloxy)phthalocyaninatonickel(II)", Vol. 32, pp. 1422-1424, *Angewandte Chemie*, 1993.

60. İşci Ü., F. Dumoulin, V. Ahsen and A.B. Sorokin, "Preparation of N-bridged diiron phthalocyanines bearing bulky or small electron-withdrawing substituents", *Journal of Porphyrins Phthalocyanines*, Vol. 14, pp. 324-334, 2010.

61. Tuncel S., A. Trivella, D. Atilla, K. Bennis, H. Savoie, F. Albrieux, L. Delort, H. Billard, V. Dubois, V. Ahsen, F. Caldefie-Chézet, C. Richard, R.W. Boyle, S. Ducki and F. Dumoulin, "Assessing the Dual Activity of a Chalcone−Phthalocyanine Conjugate: Design, Synthesis, and Antivascular and Photodynamic Properties", *Molecular Pharmaceutics*, Vol. 10, pp. 3706-3716 , 2013.

62. Topkaya D., F. Dumoulin, V. Ahsen and Ü. İşçi, "Axial Binding and Host-guest Interactions of a Phthalocyanine Resorcinarene Cavitand Hybrid", *Dalton Transaction*, Vol. 43, pp. 2032-2037, 2014.

63. Shaabani A., R. Maleki-Moghaddam and A. Maleki, "Microwave assisted synthesis of metal-free phthalocyanine and metallophthalocyanines", *Dyes and Pigments*, Vol. 74, pp. 279-282, 2007.

APPENDIX A: SPECTROSCOPY DATA

^{1}H NMR, ^{13}C NMR, UV-Vis, ATR-IR and Mass spectra of the synthesized compounds are included.

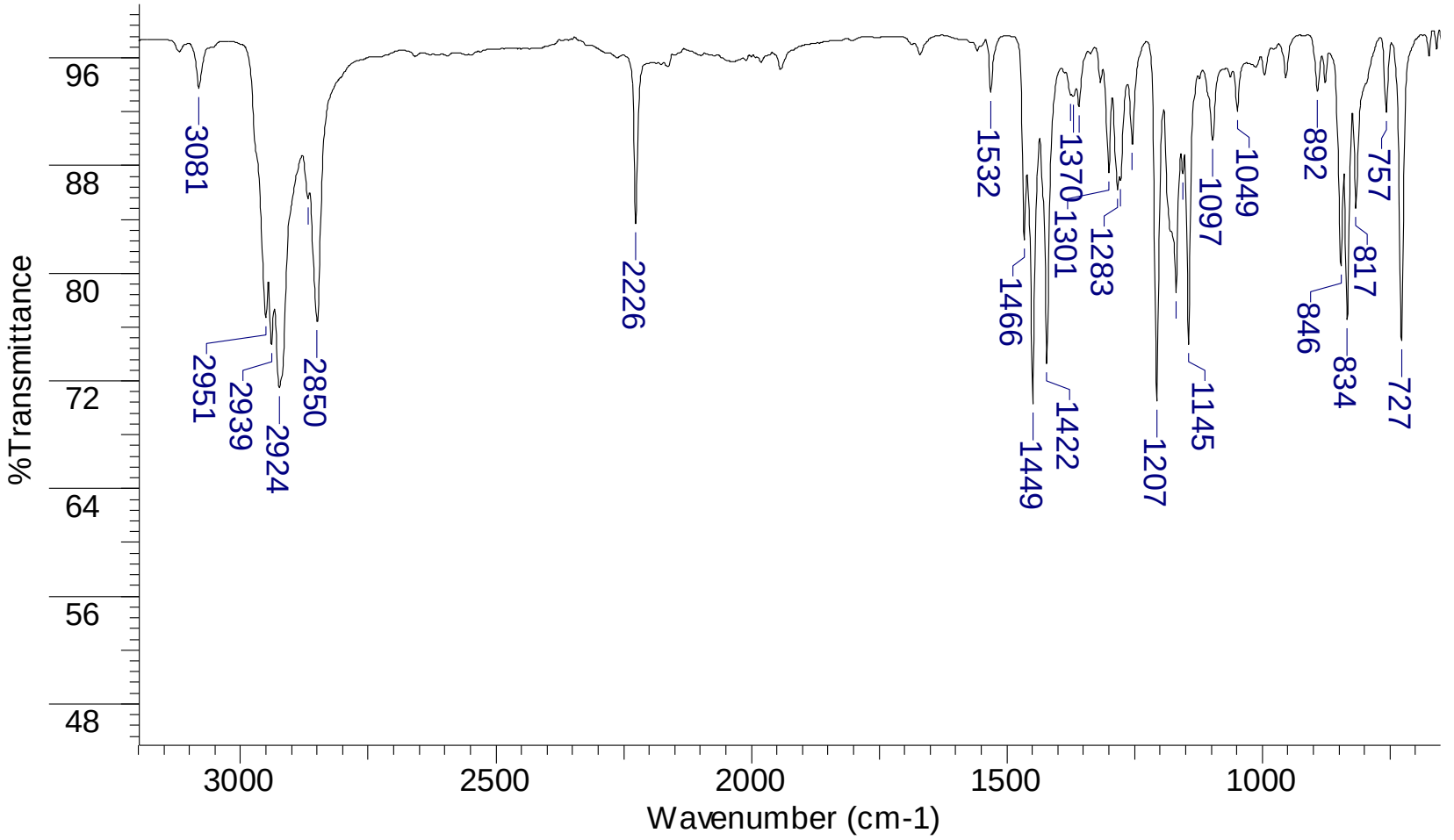

Figure A.1. ATR-IR spectrum of compound **2**.

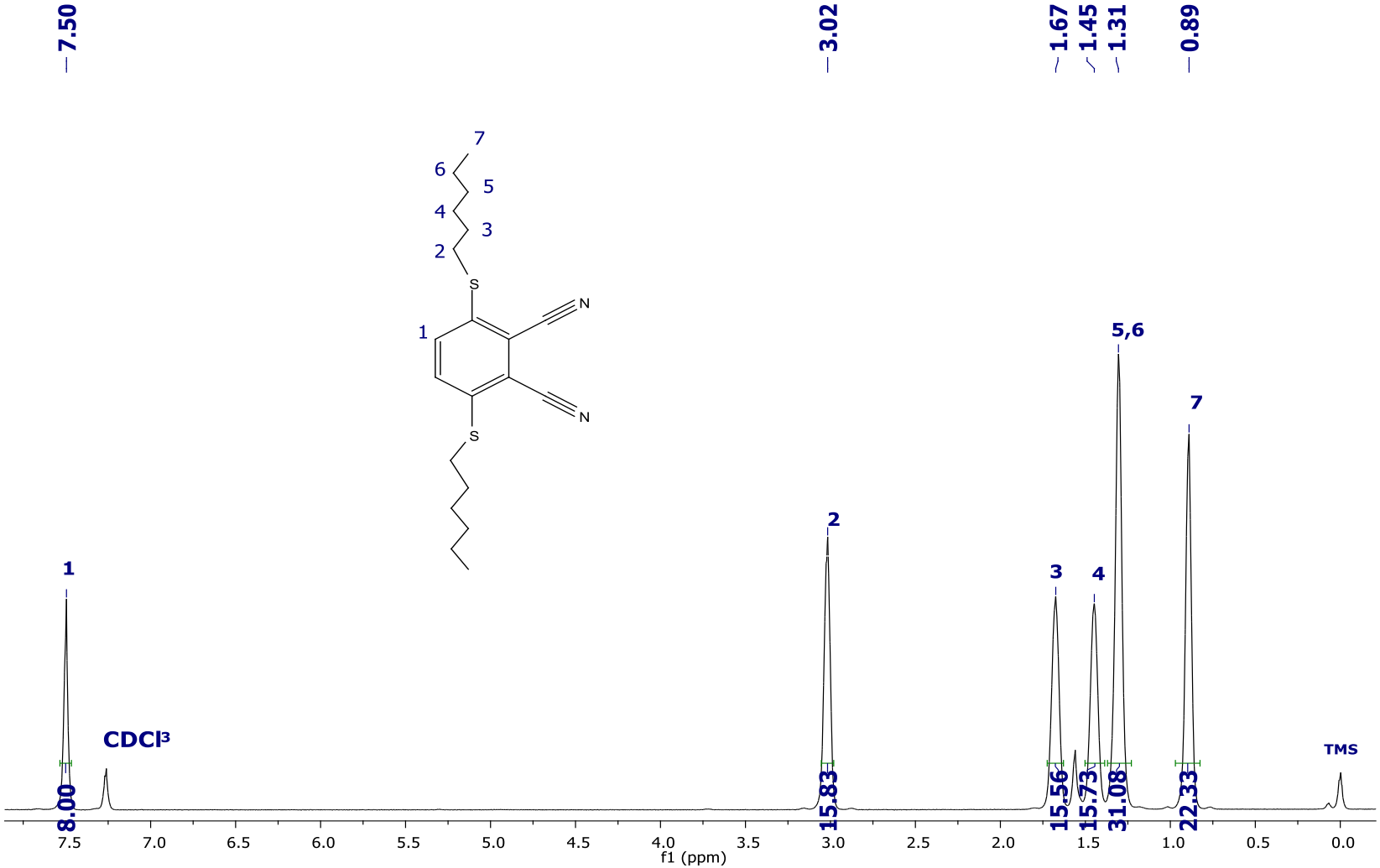

Figure A.2. ^{1}H NMR of the compound **2**.

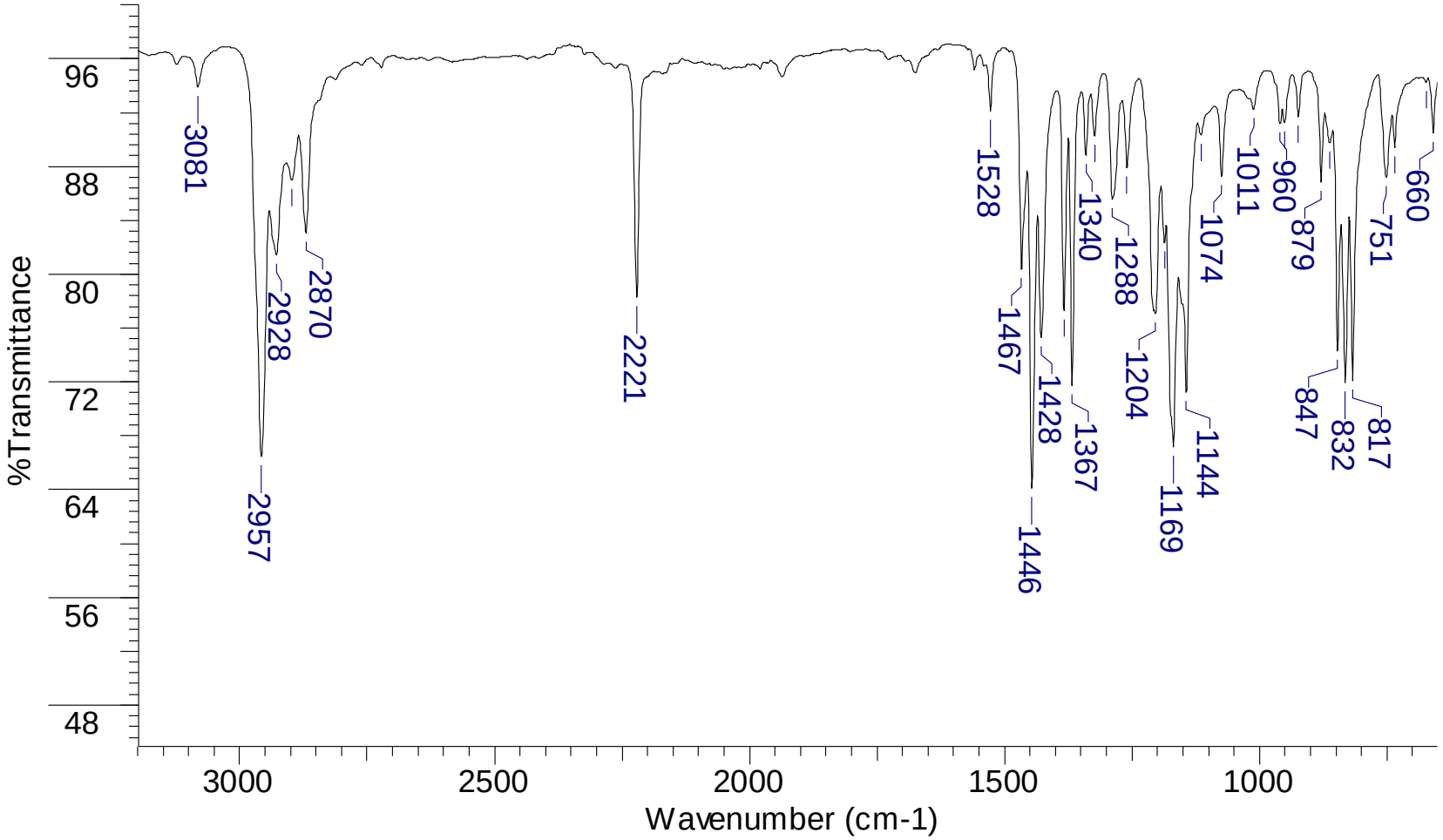

Figure A.3. ATR-IR spectrum of compound **3**.

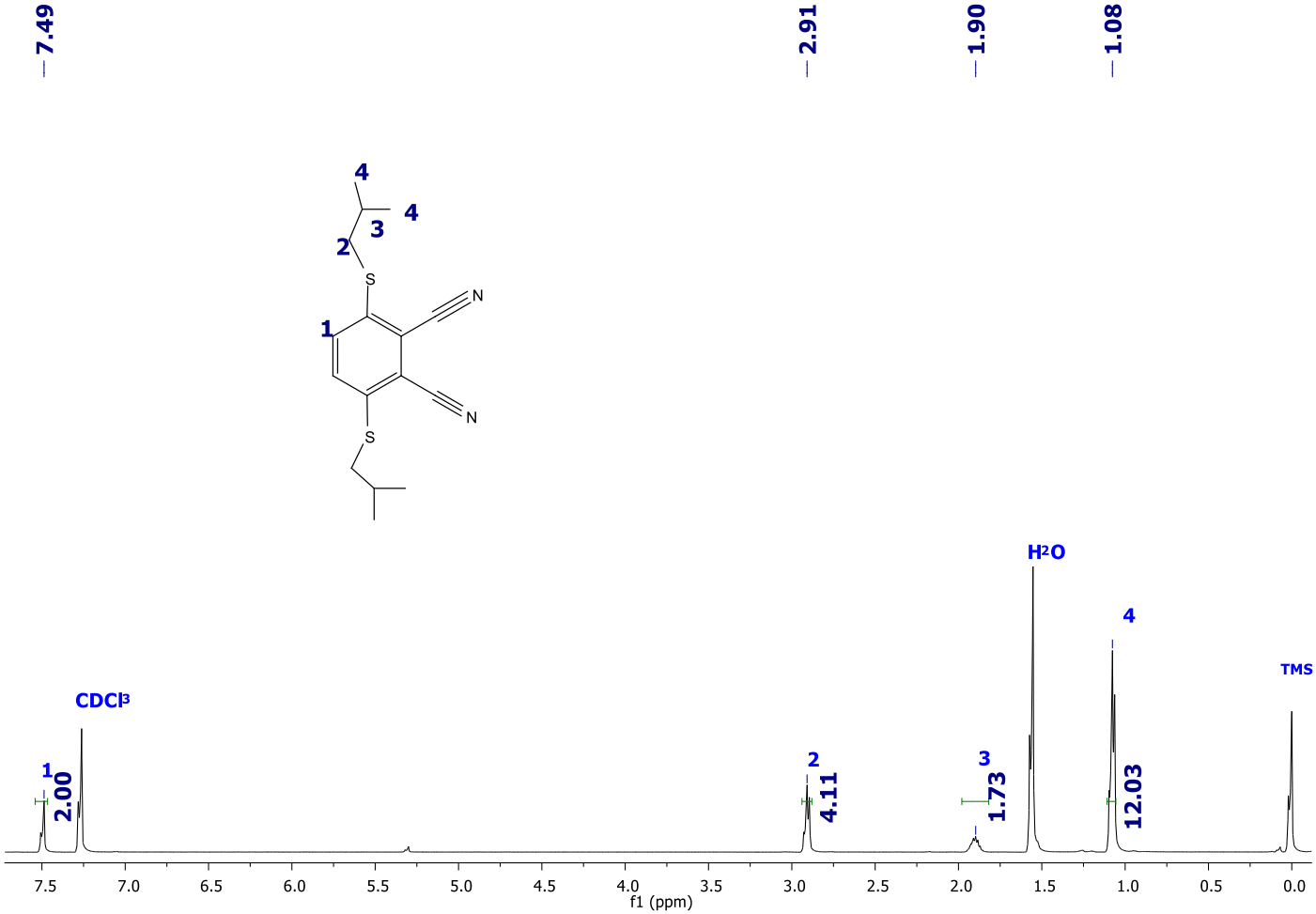

Figure A.4. ^{1}H NMR spectrum of compound **3**.

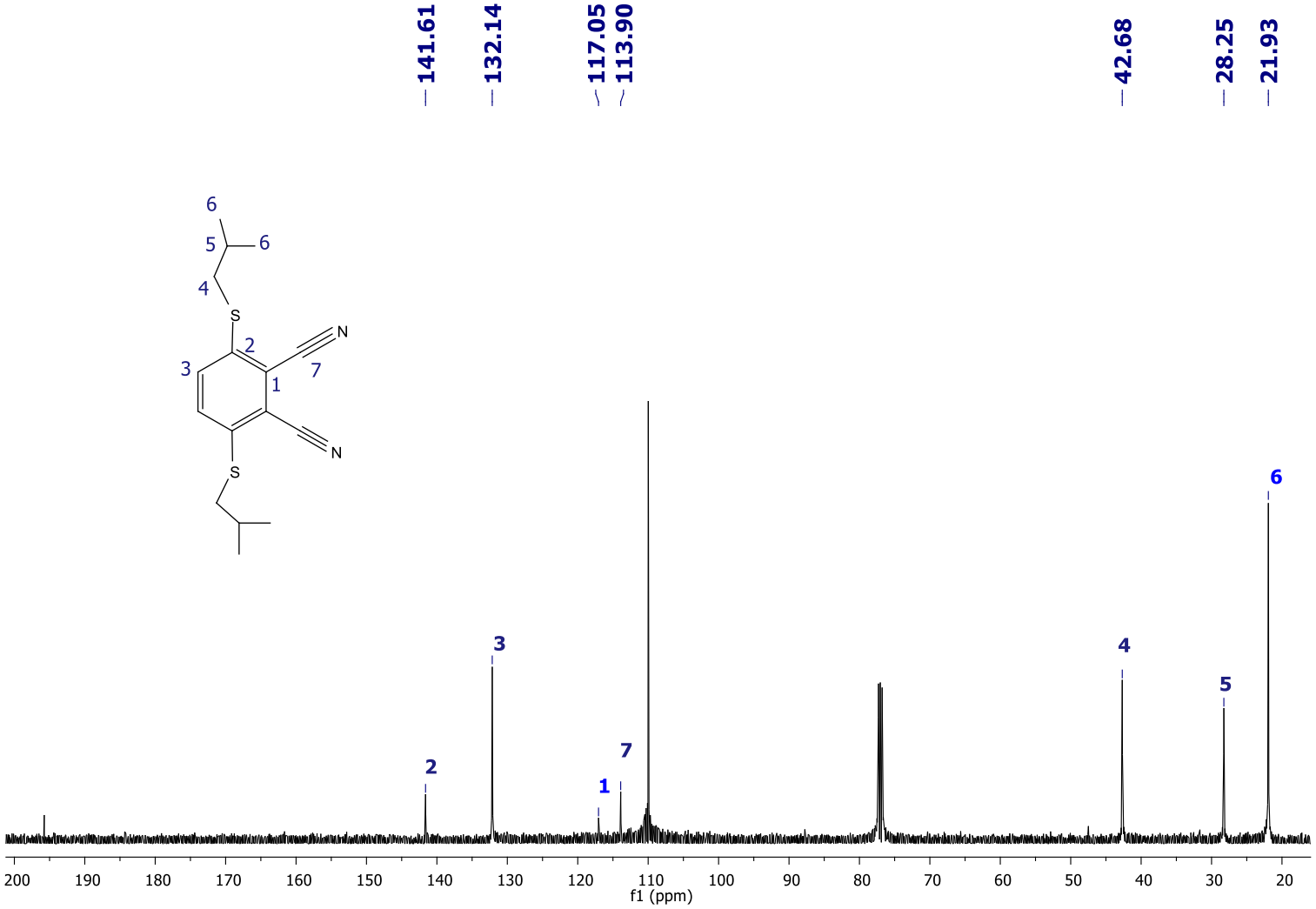

Figure A.5. ^{13}C NMR spectrum of compound **3**.

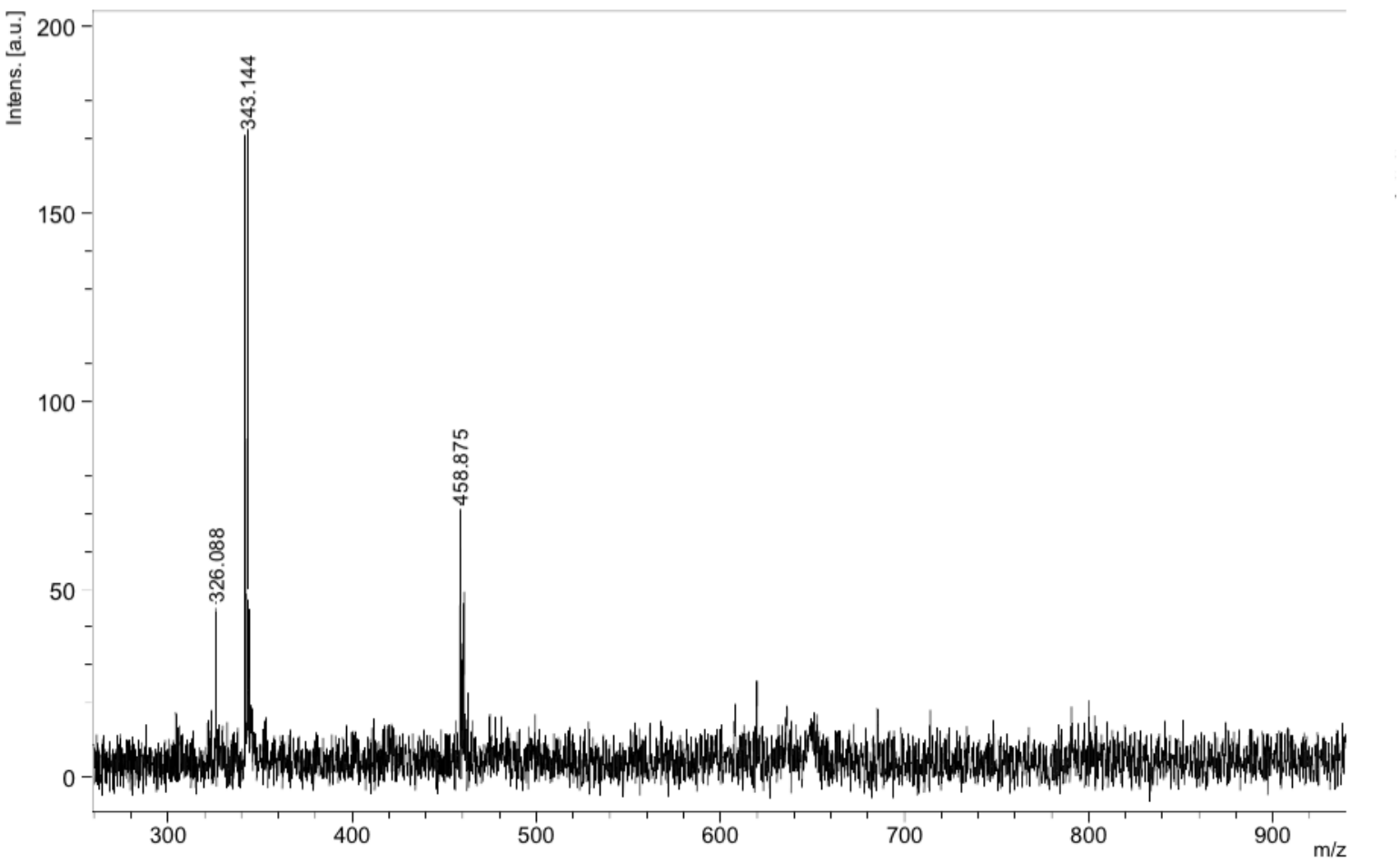

Figure A.6. Mass spectrum of compound **4**.

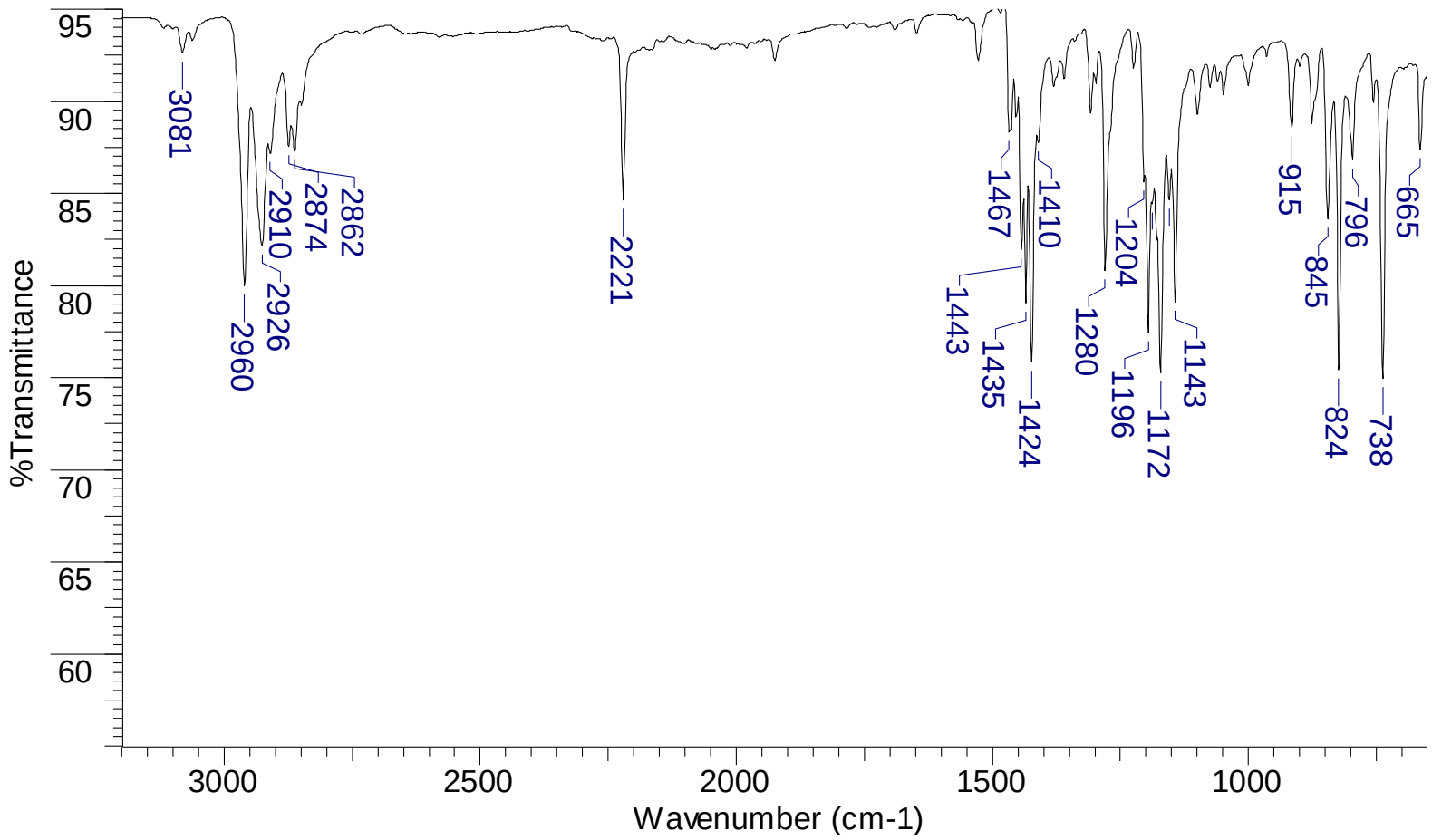

Figure A.7. ATR-IR spectrum of compound **4**.

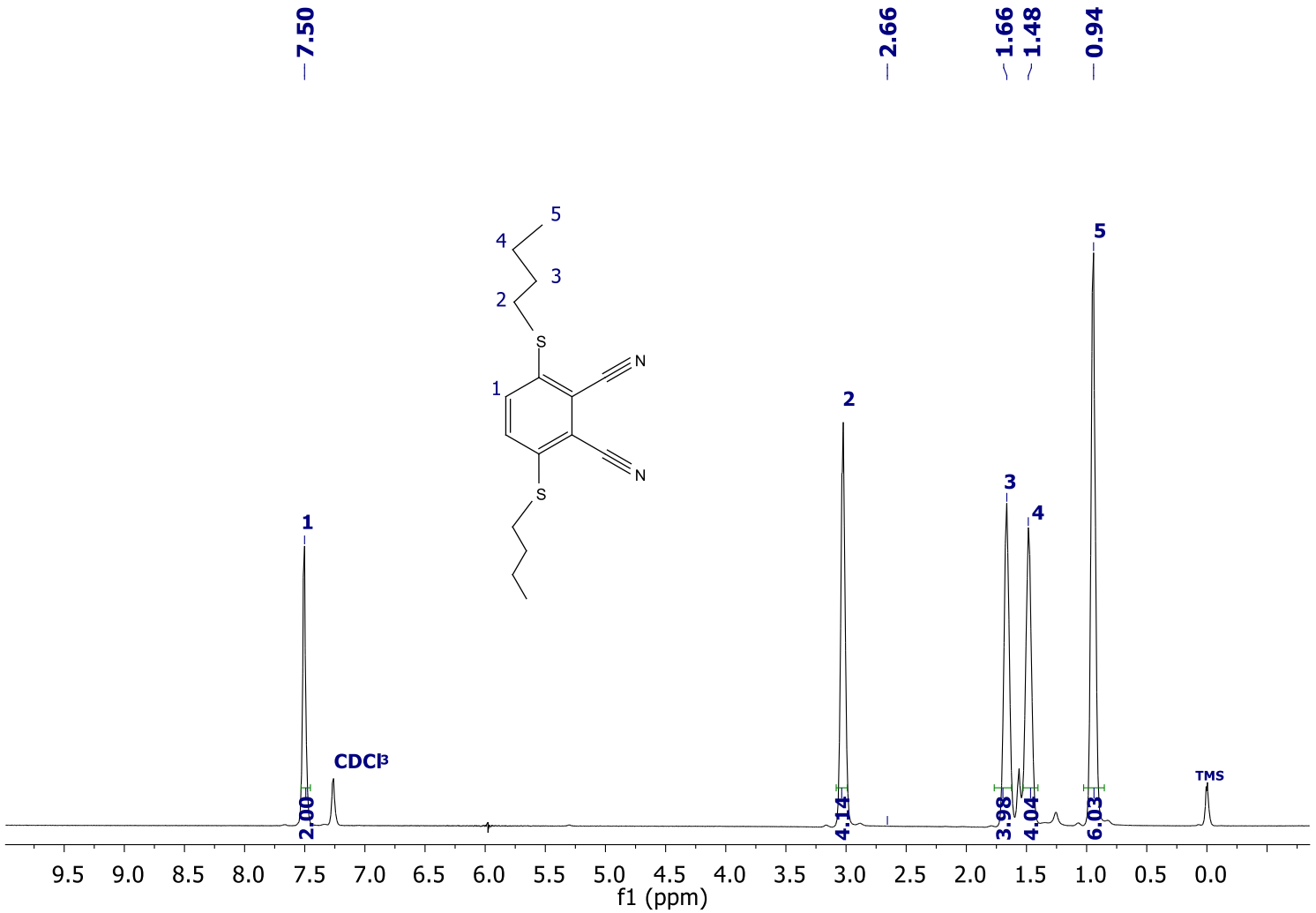

Figure A.8. ^{1}H NMR spectrum of compound **4**.

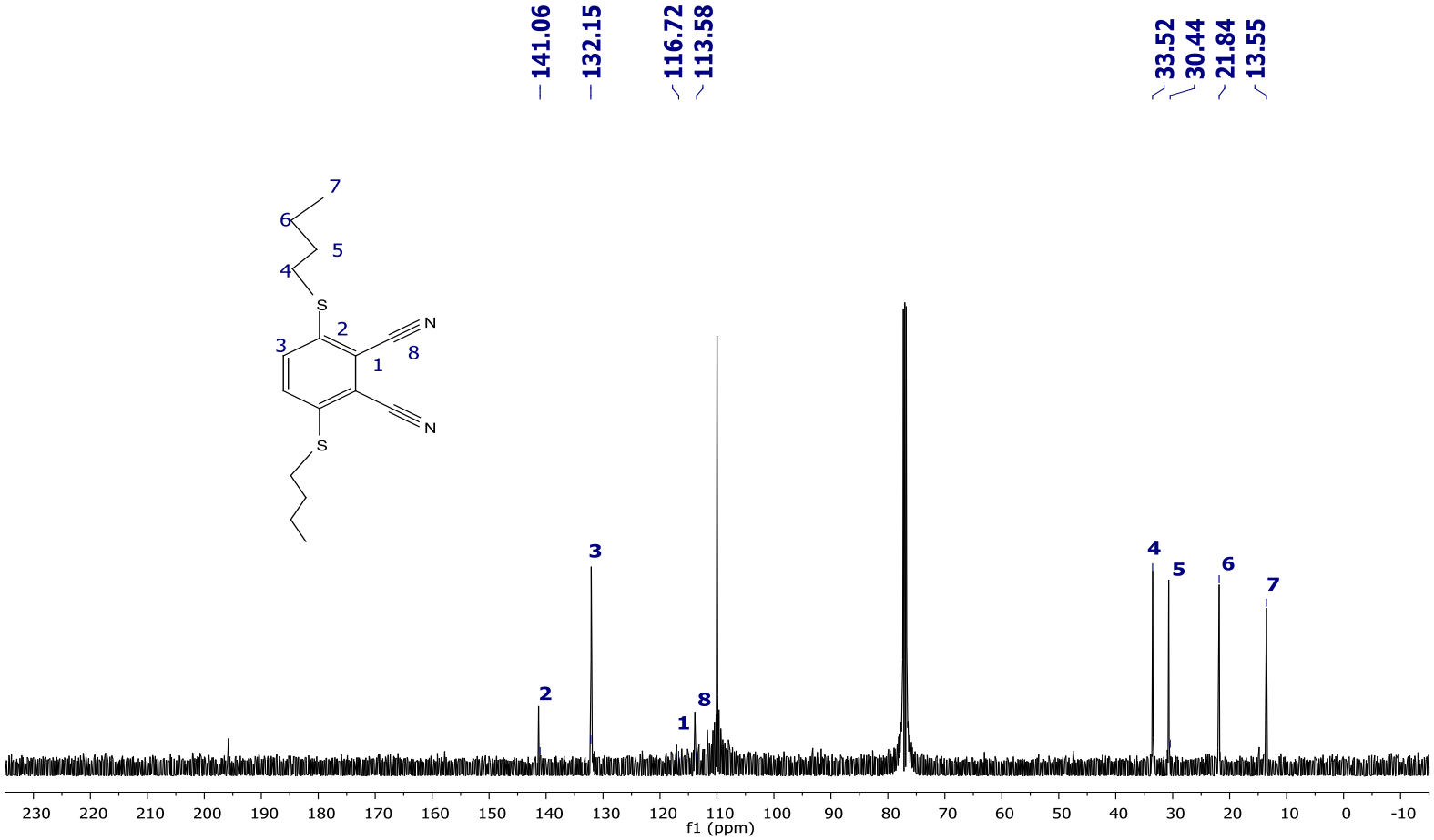

Figure A.9. ^{13}C NMR spectrum of compound **4**

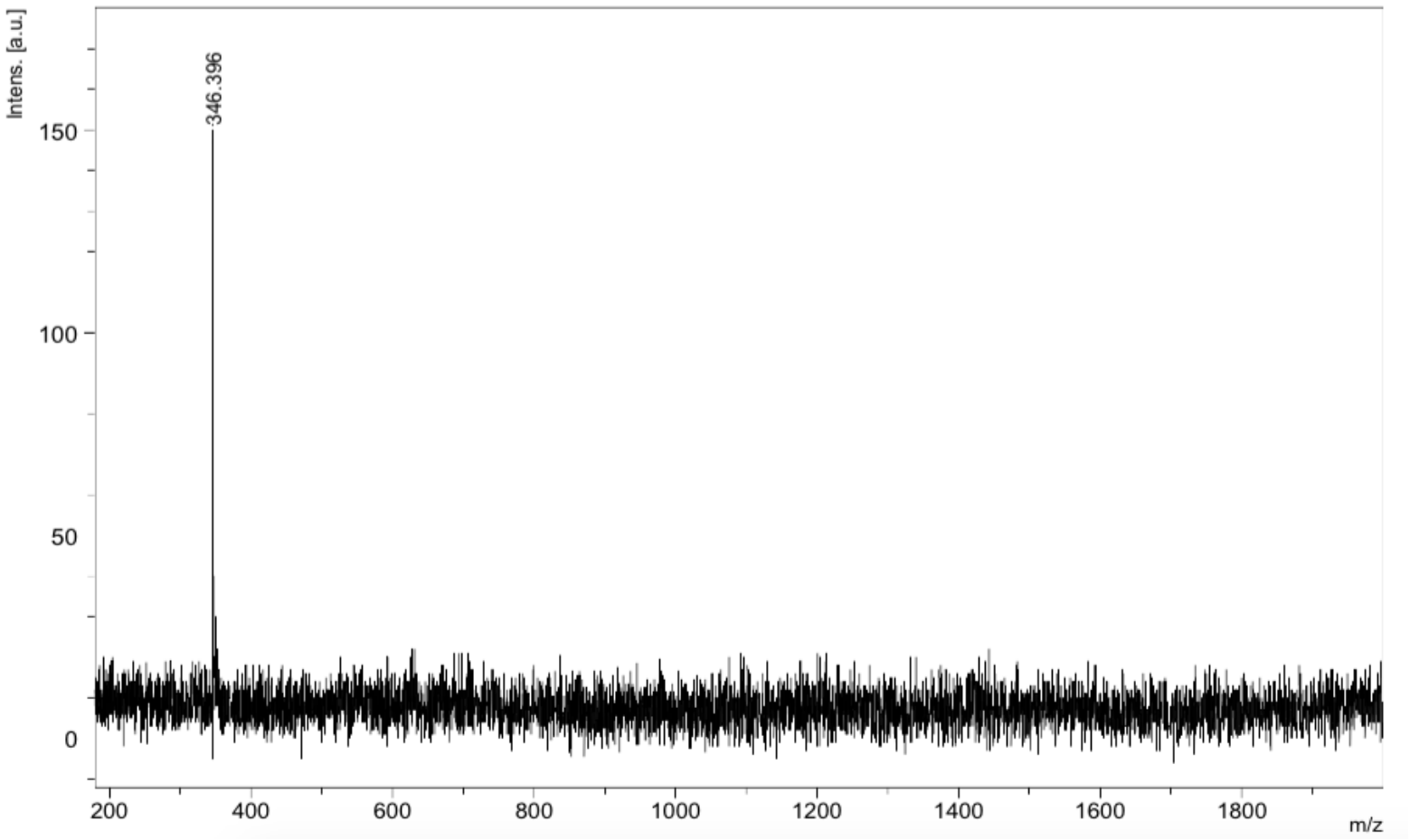

Figure A.10. Mass spectrum of compound **5**.

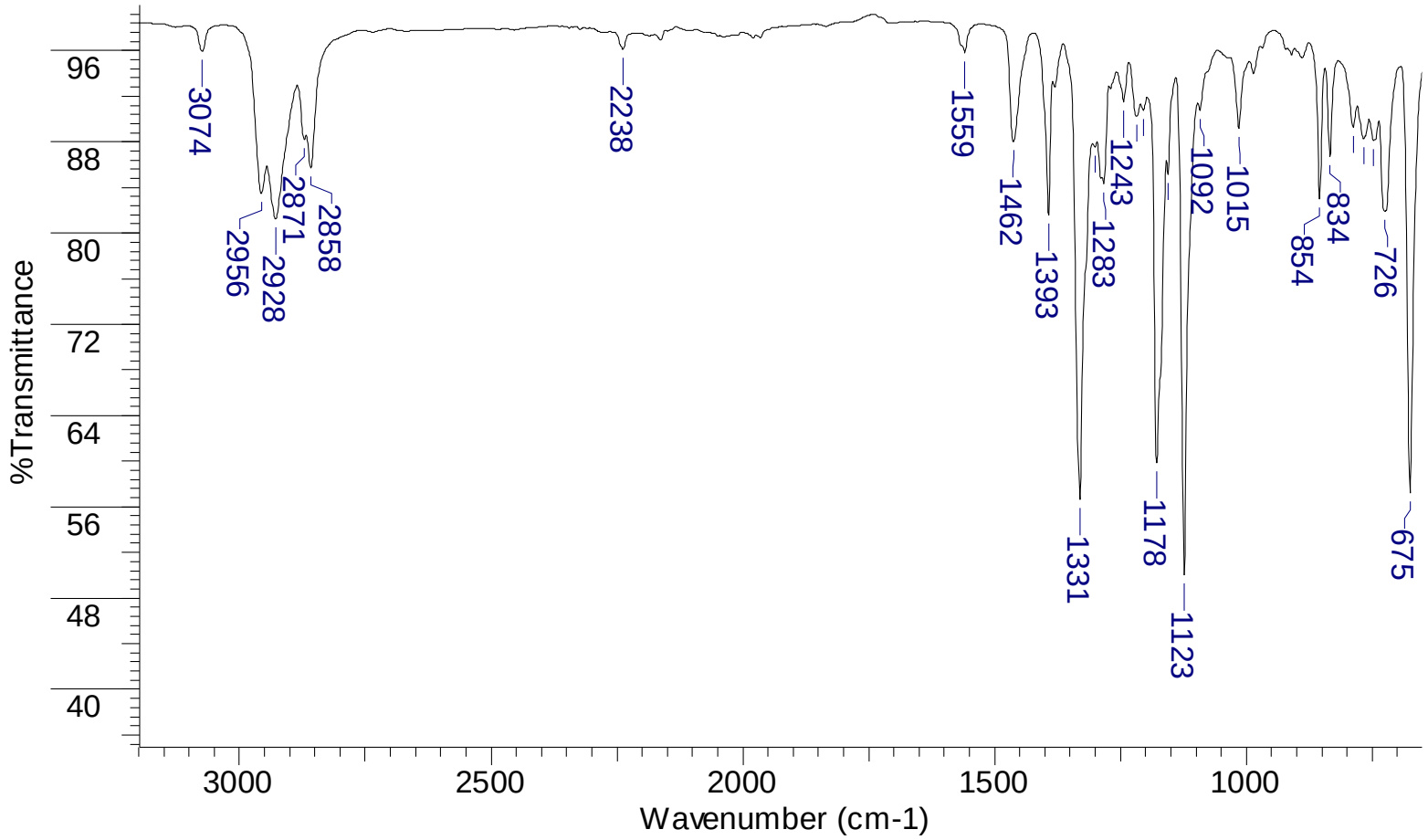

Figure A.11. ATR-IR spectrum of compound **5**.

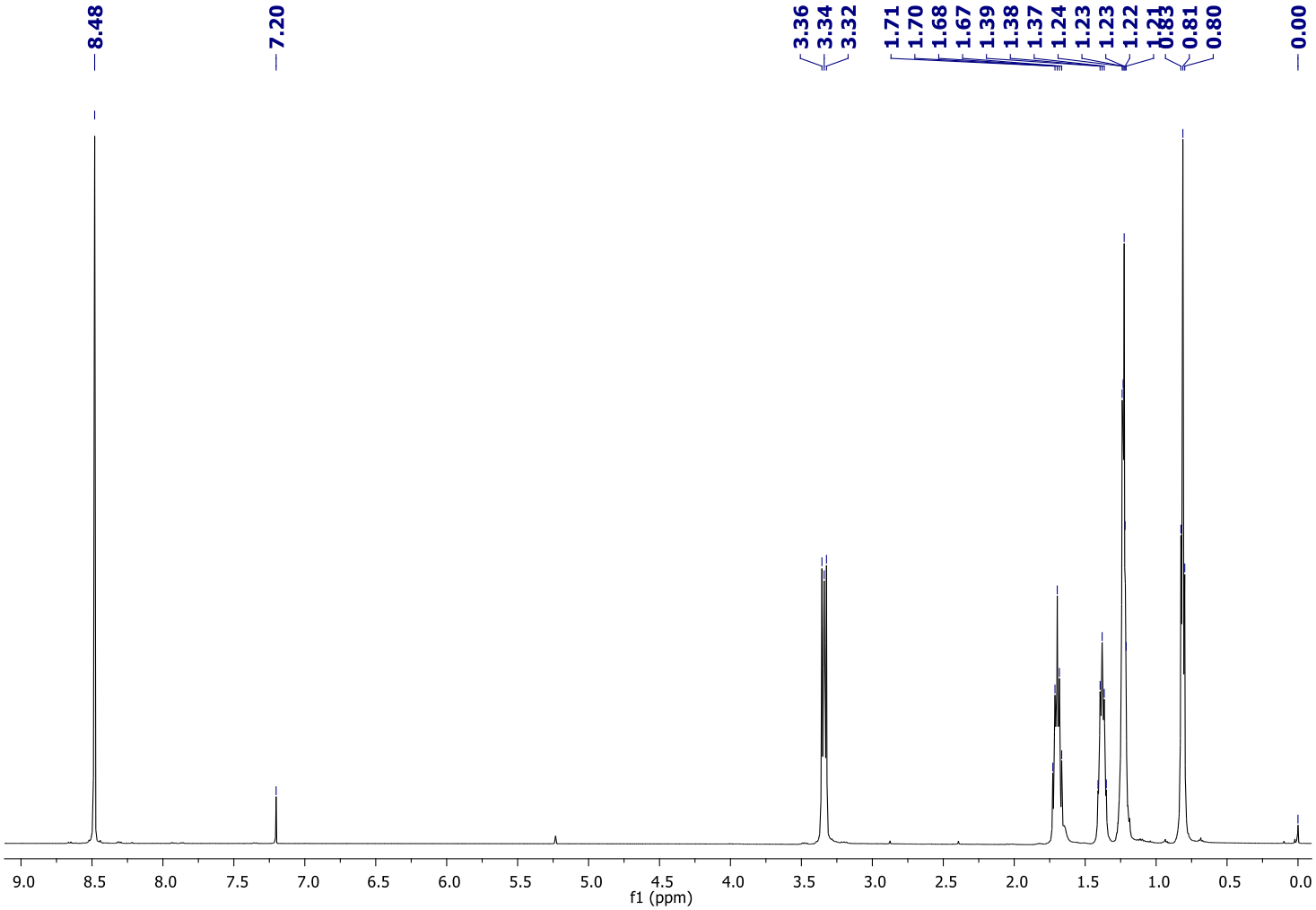

Figure A.12. ^{1}H NMR spectrum of compound **5**.

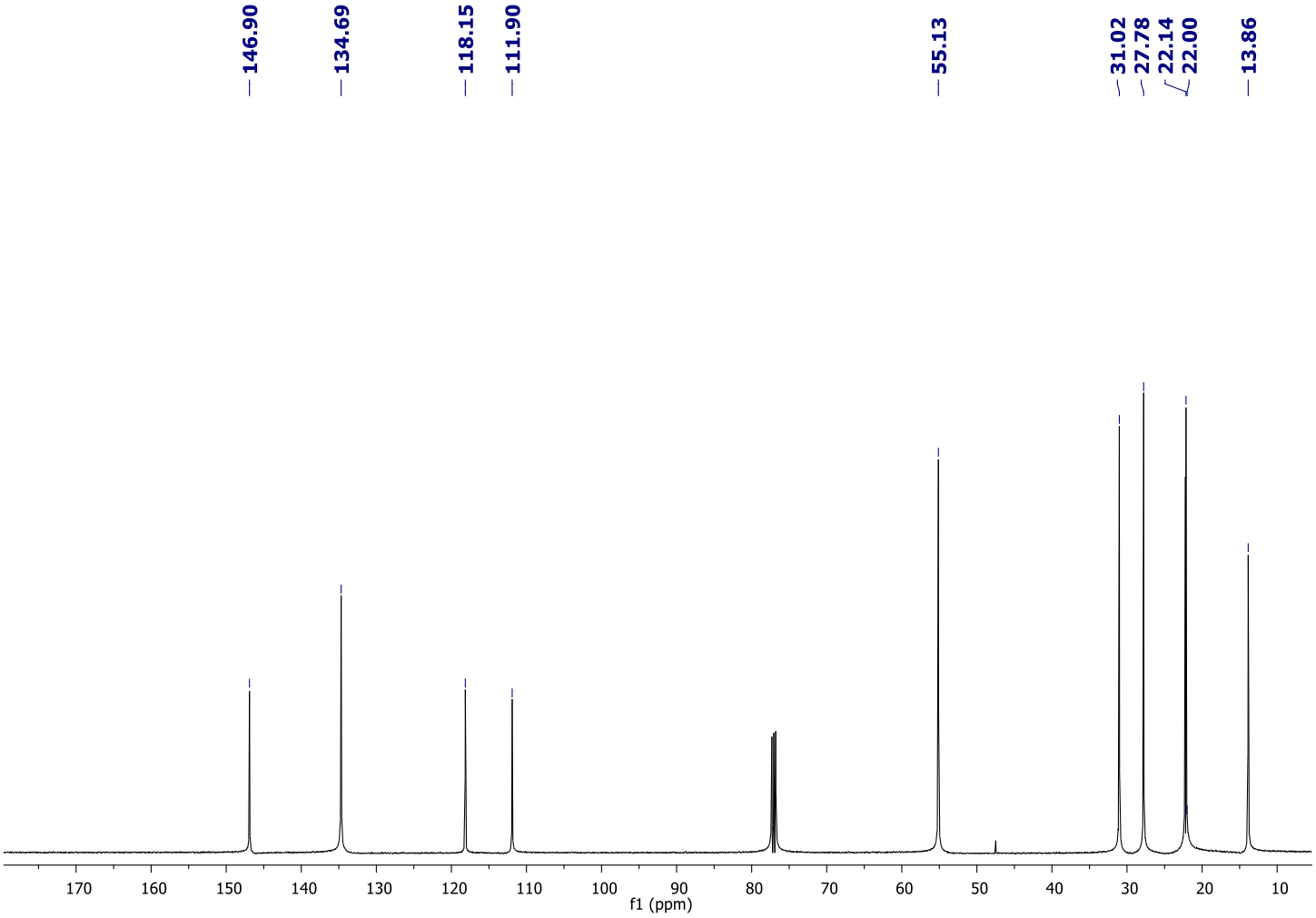

Figure A.13. ^{13}C NMR spectrum of compound **5**.

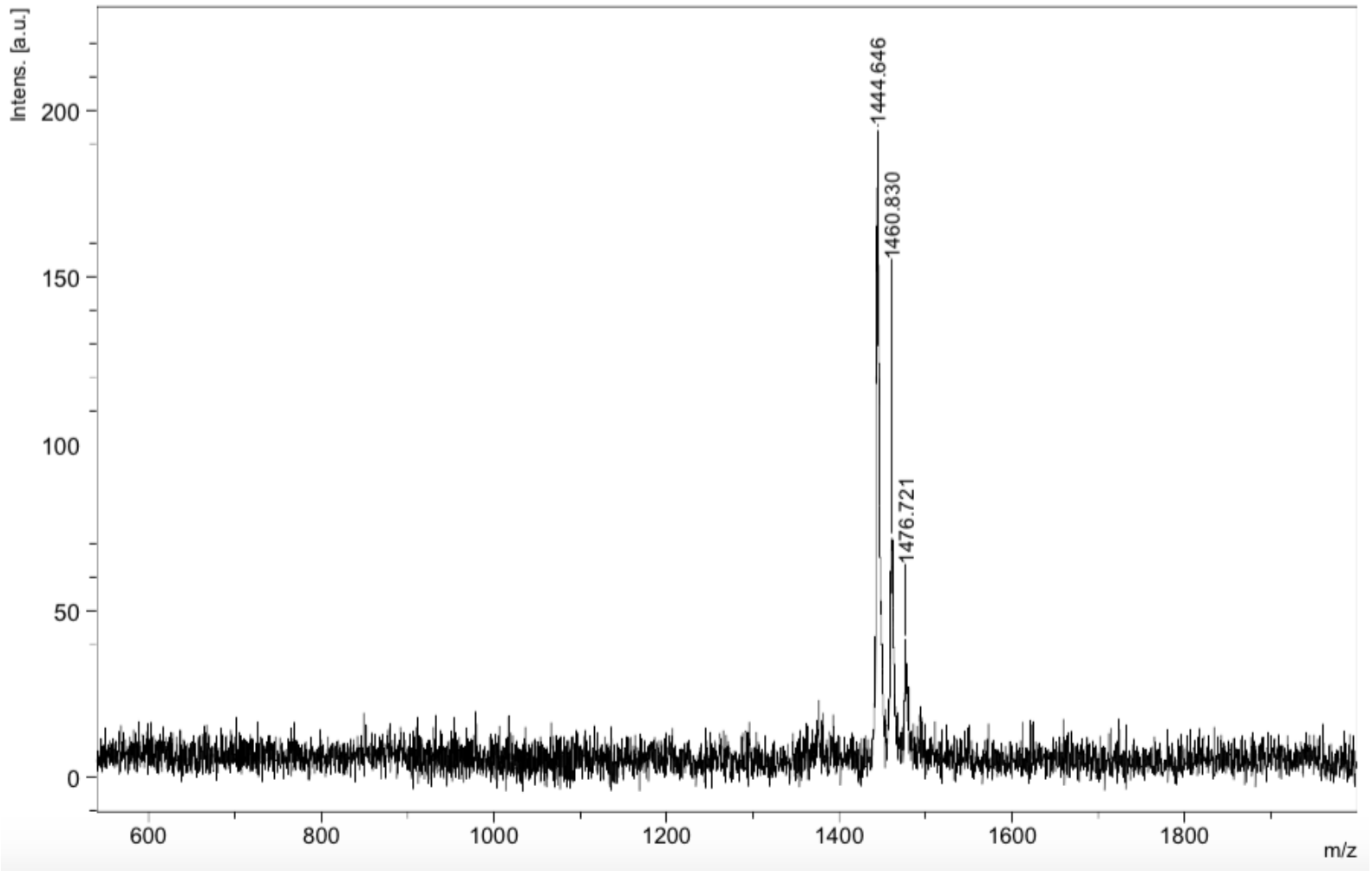

Figure A.14. Mass spectrum of compound **6**.

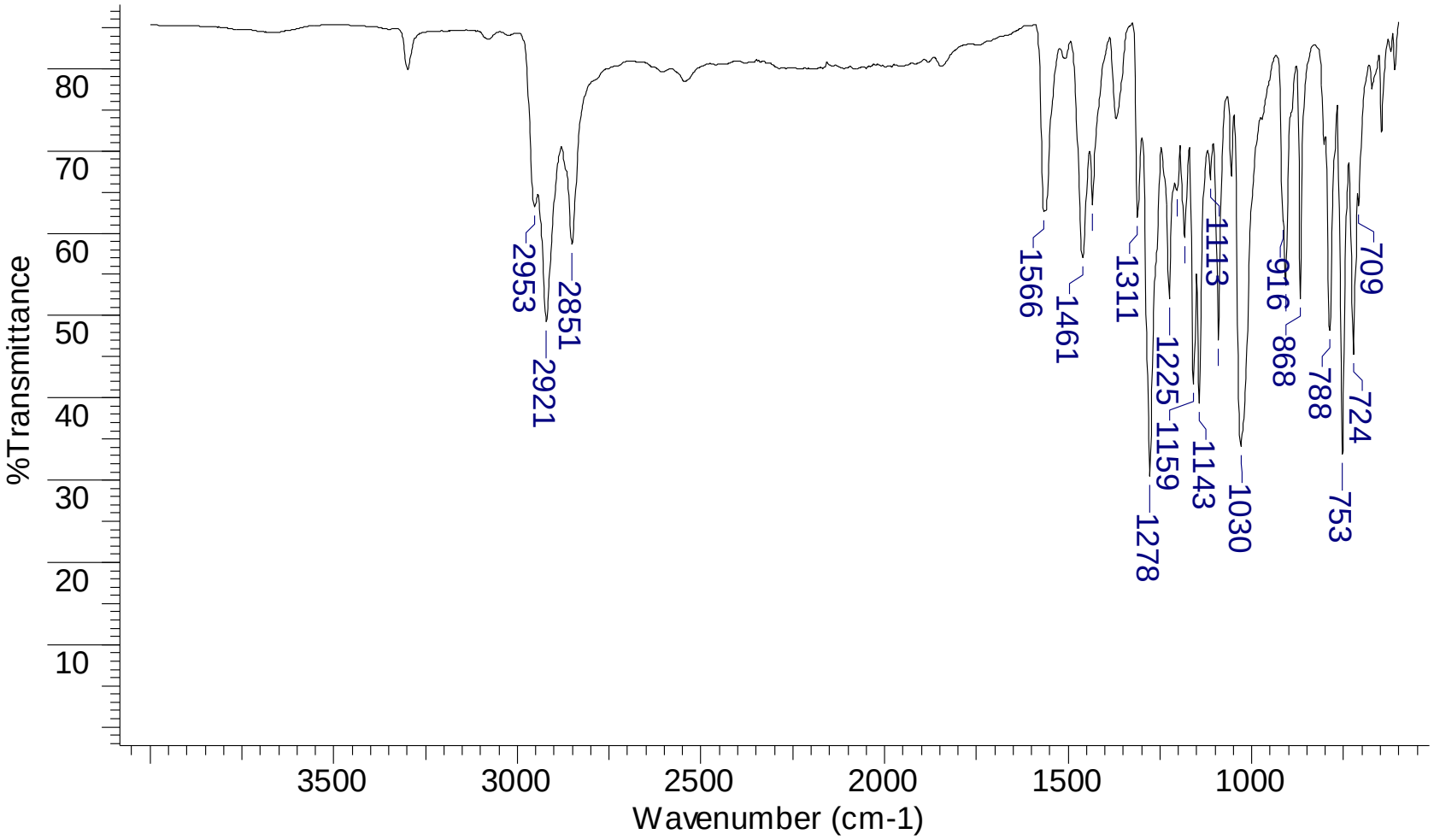

Figure A.15. ATR-IR spectrum of compound **6**.

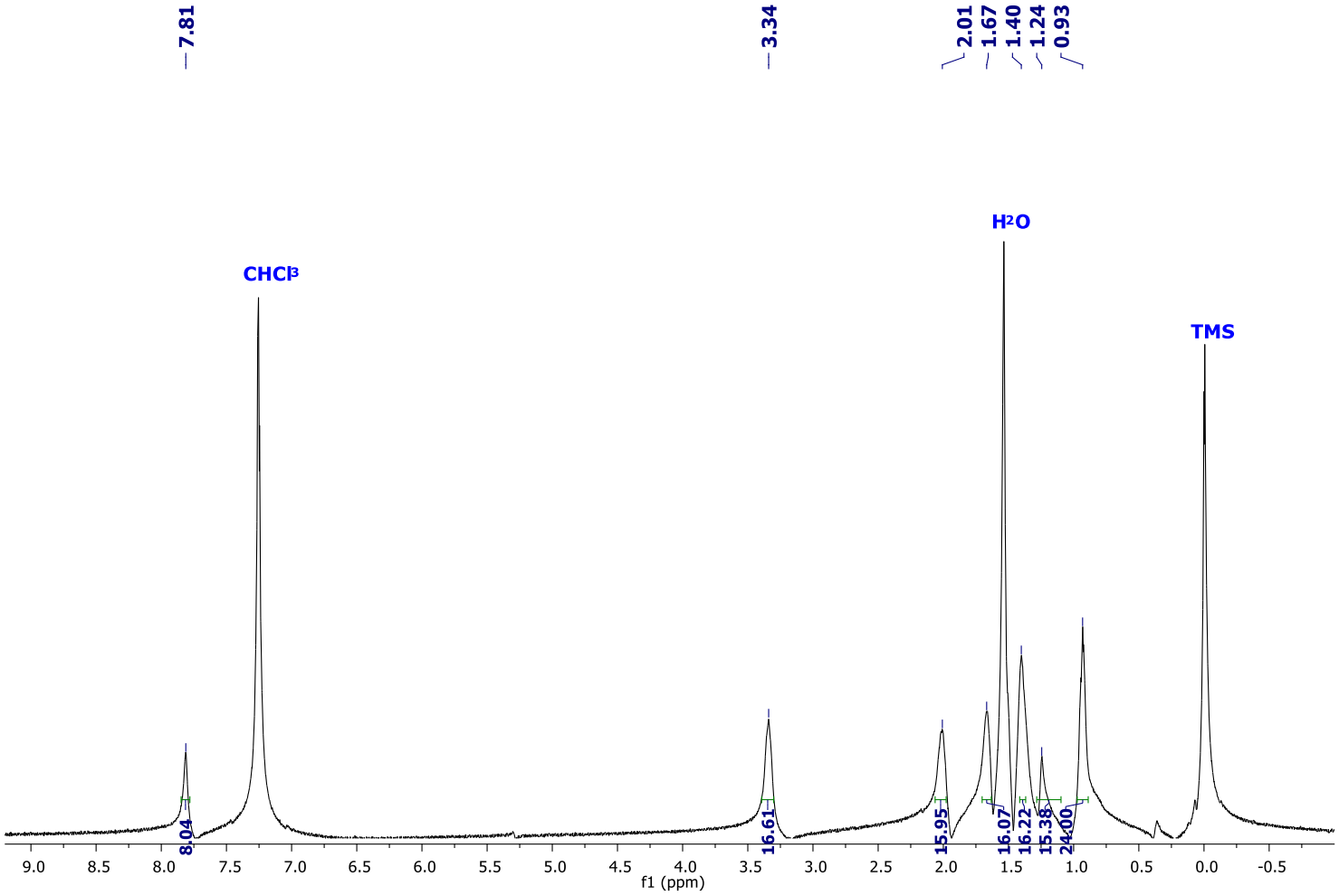

Figure A.16. ^{1}H NMR spectrum of compound **6**.

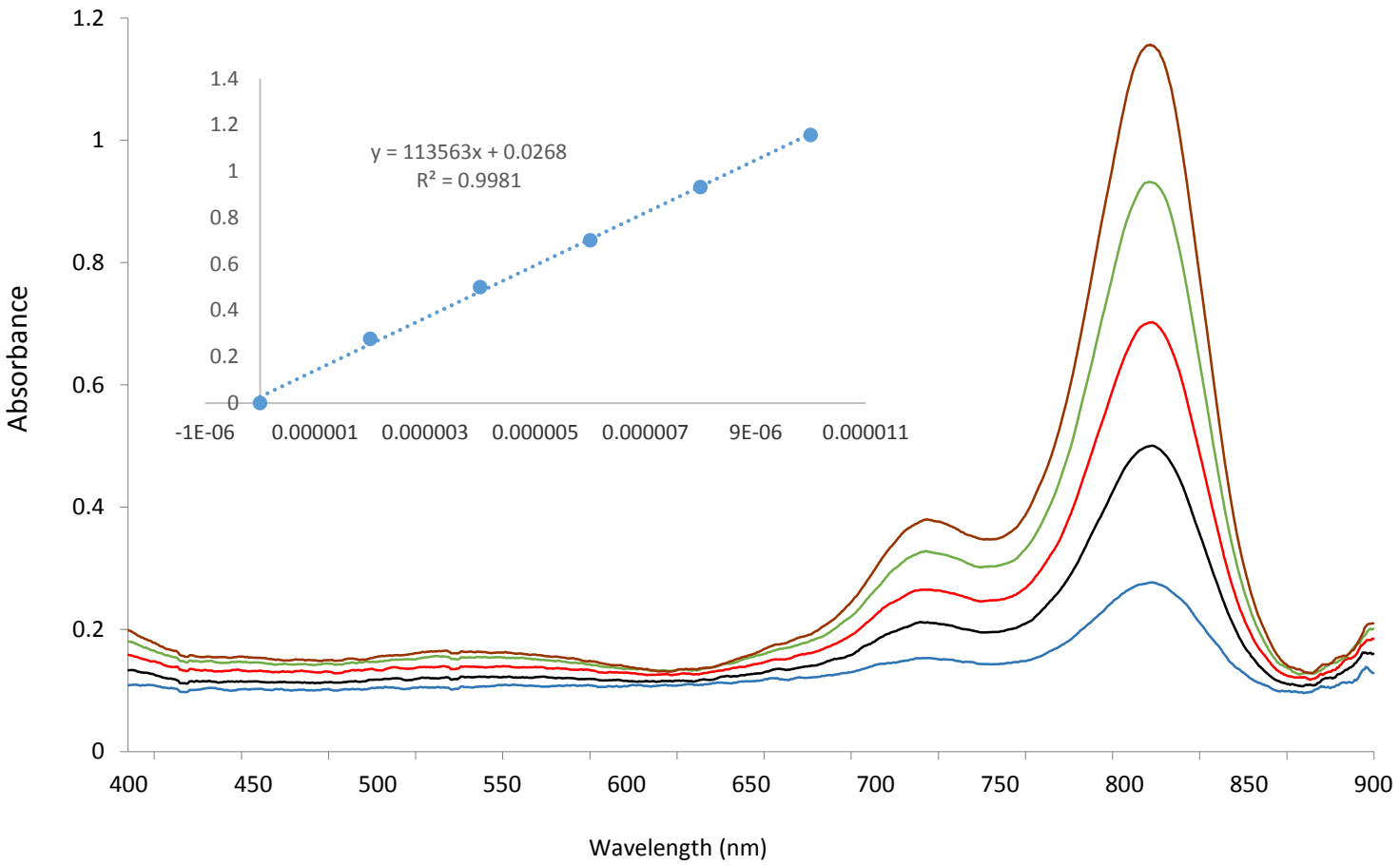

Figure A.17. UV-Vis spectrum of compound **6** in $CHCl_3$.

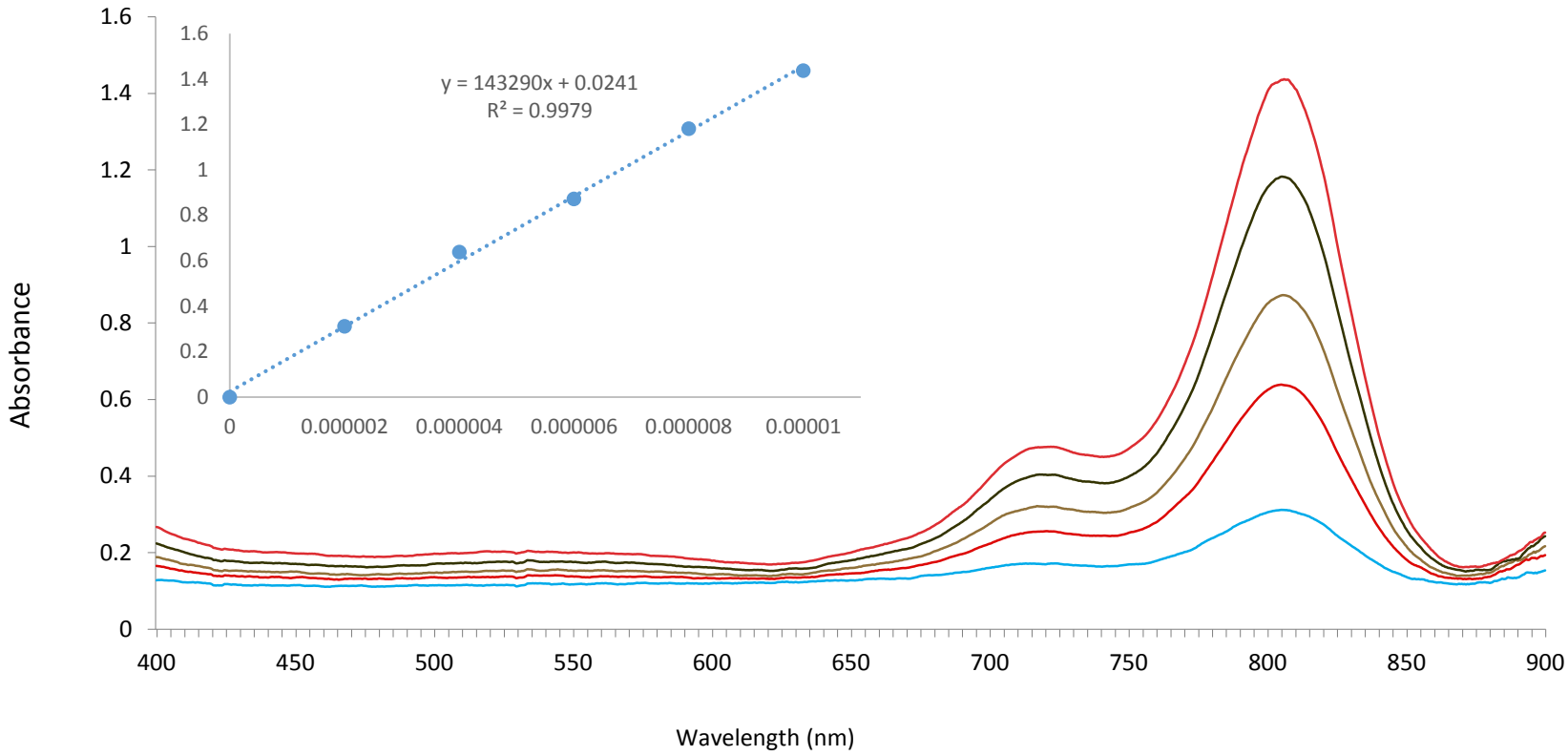

Figure A.18. UV-Vis spectrum of compound **6** in THF.

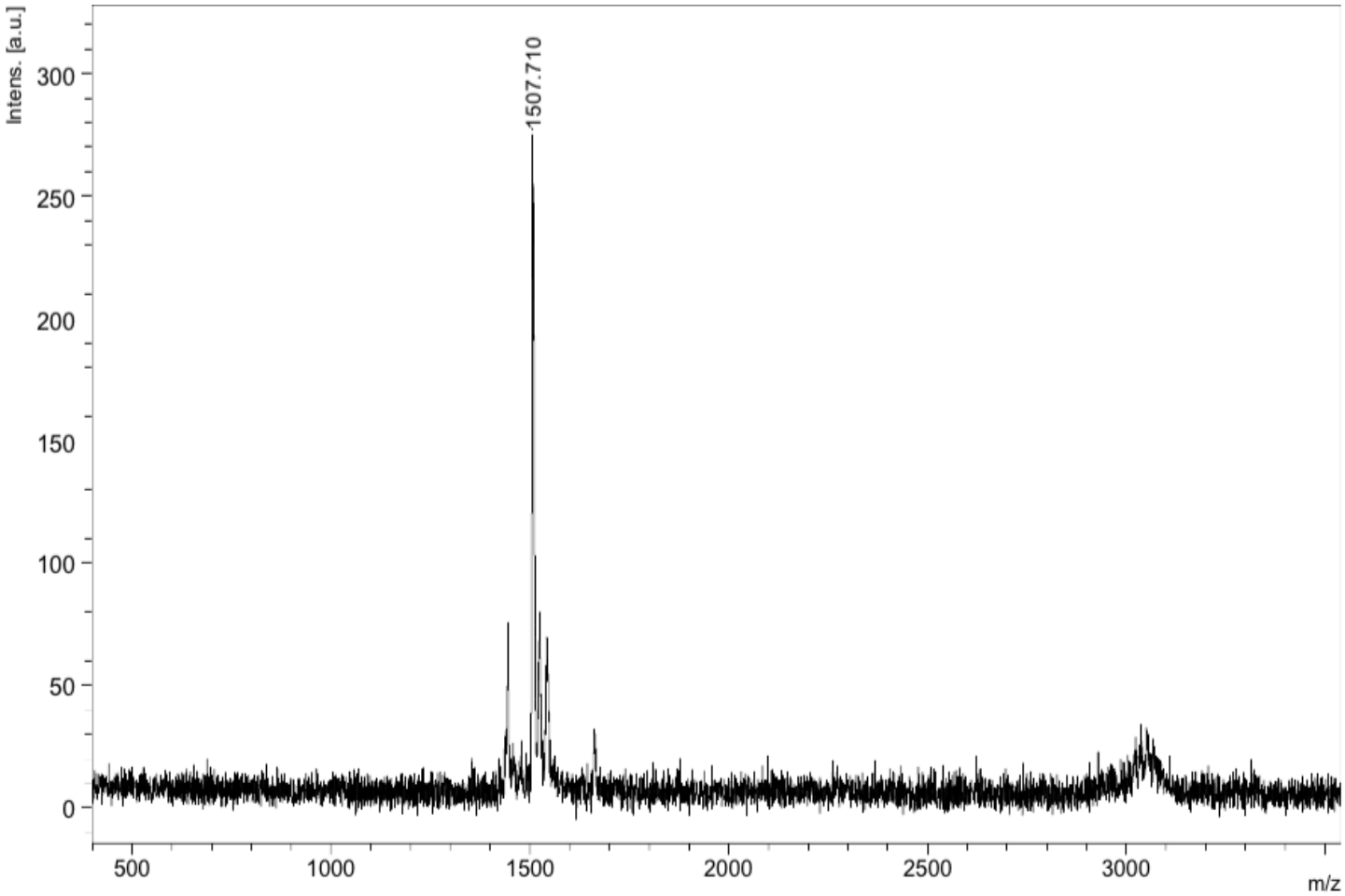

Figure A.19. Mass spectrum of compound **7**.

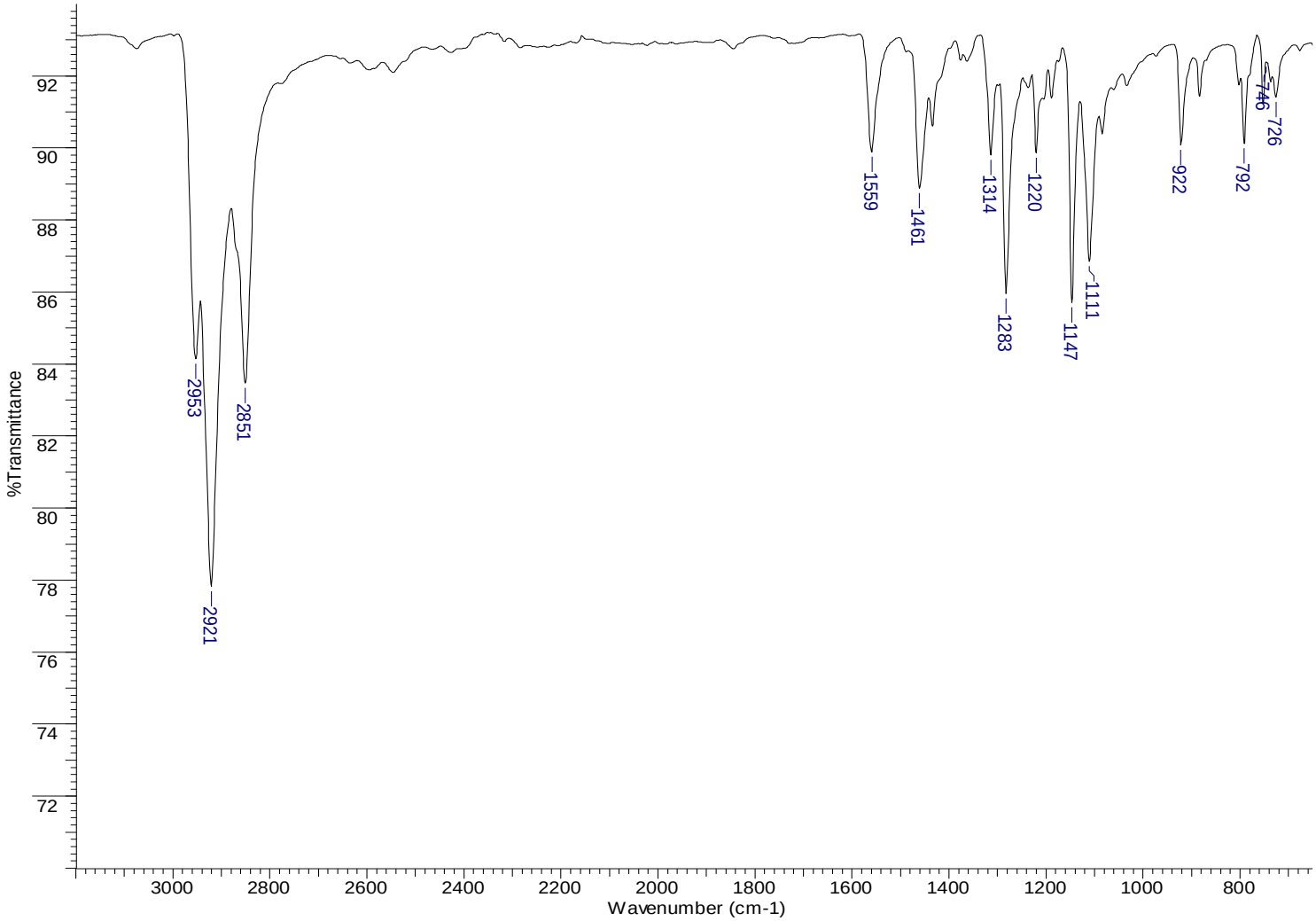

Figure A.20. ATR-IR spectrum of compound 7.

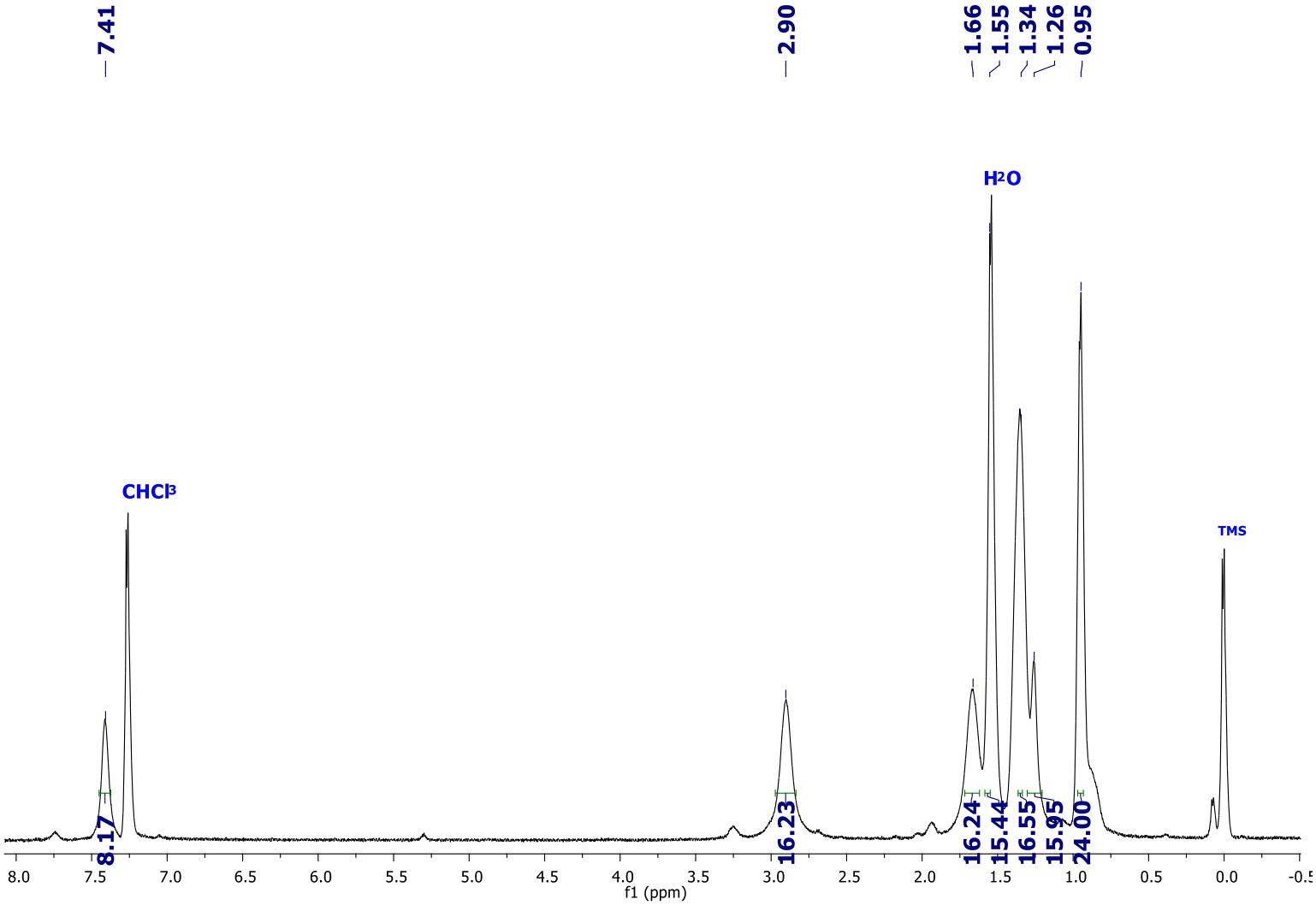

Figure A.21. ^{1}H NMR spectrum of compound **7**.

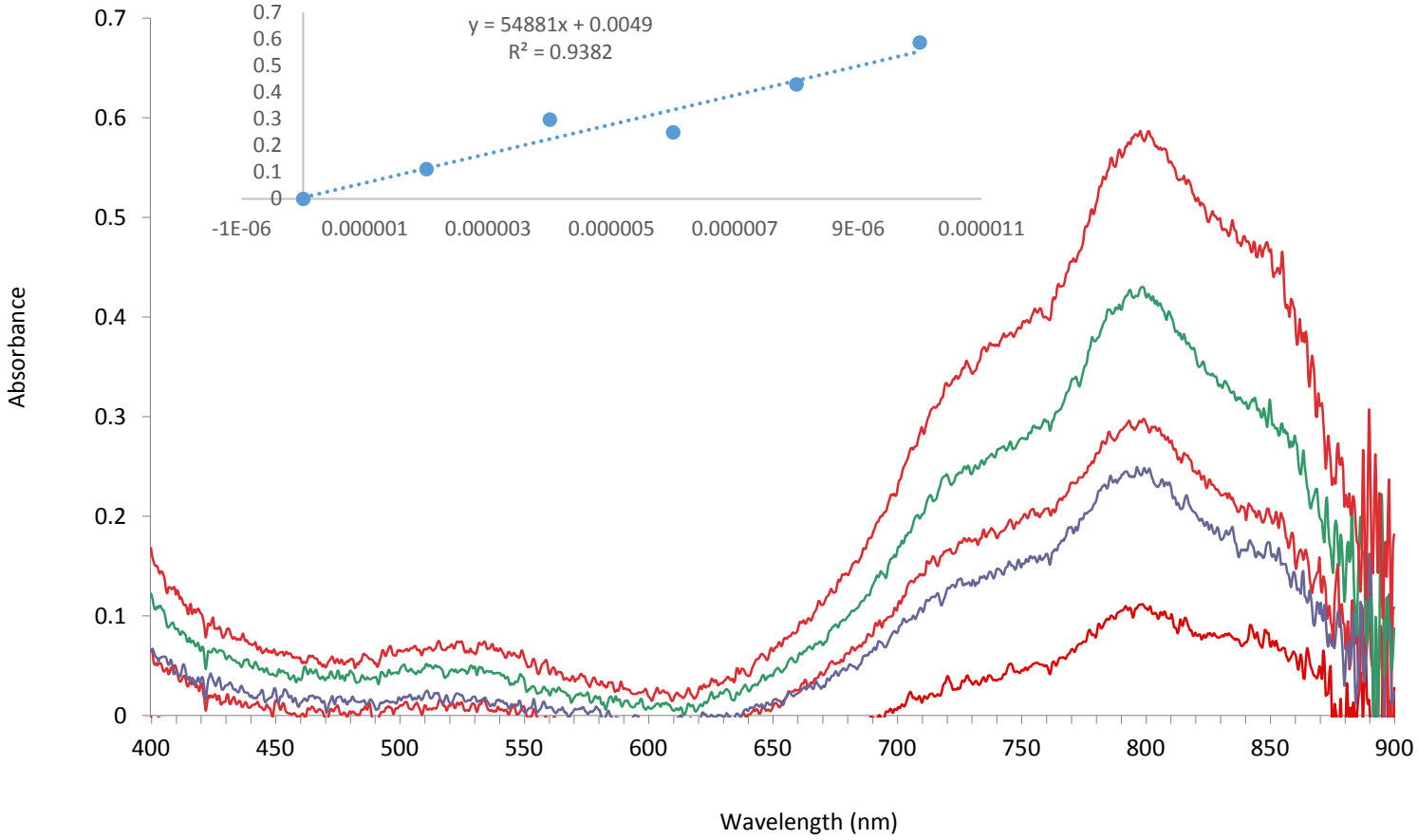

Figure A.22. UV-Vis spectrum of compound **7** in $CHCl_3$.

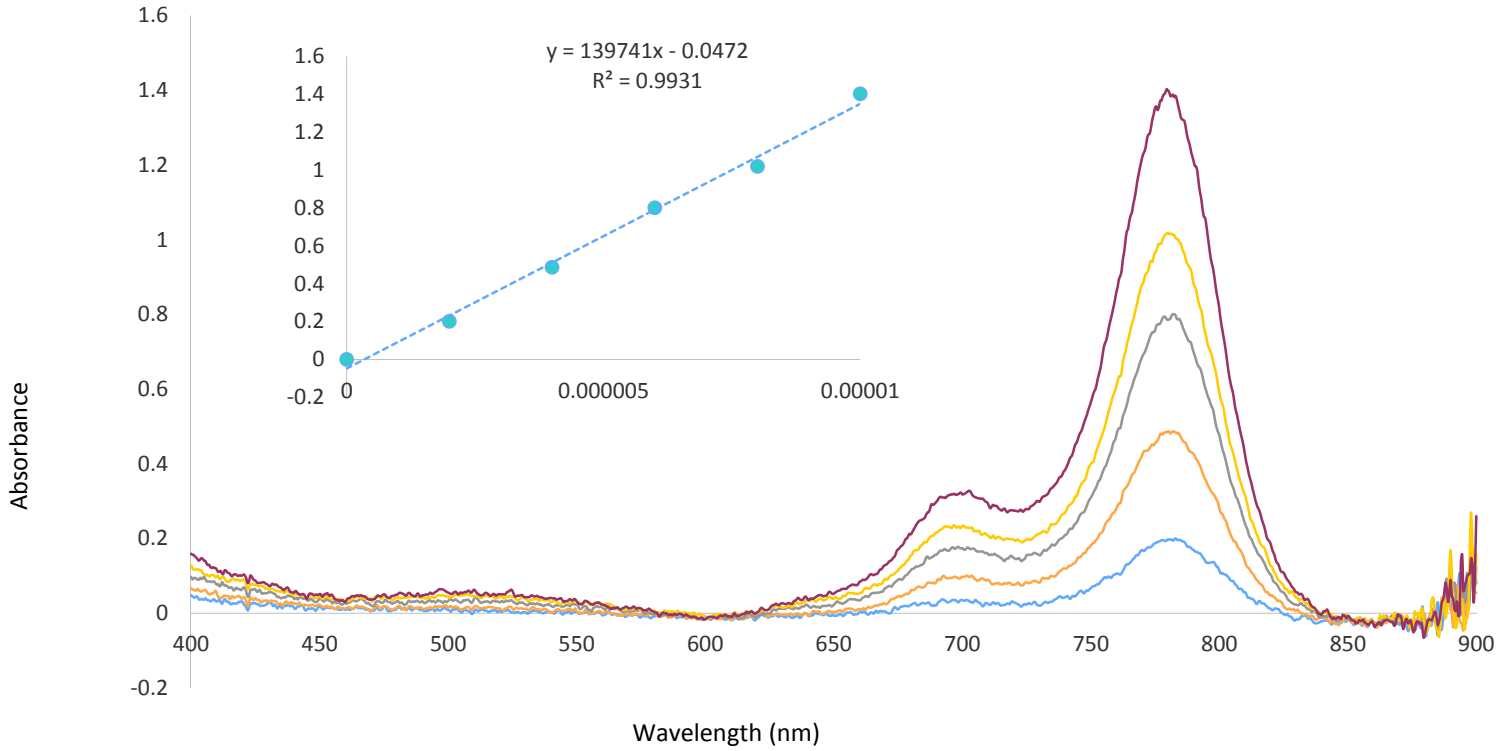

Figure A.23. UV-Vis spectrum of compound **7** in THF.

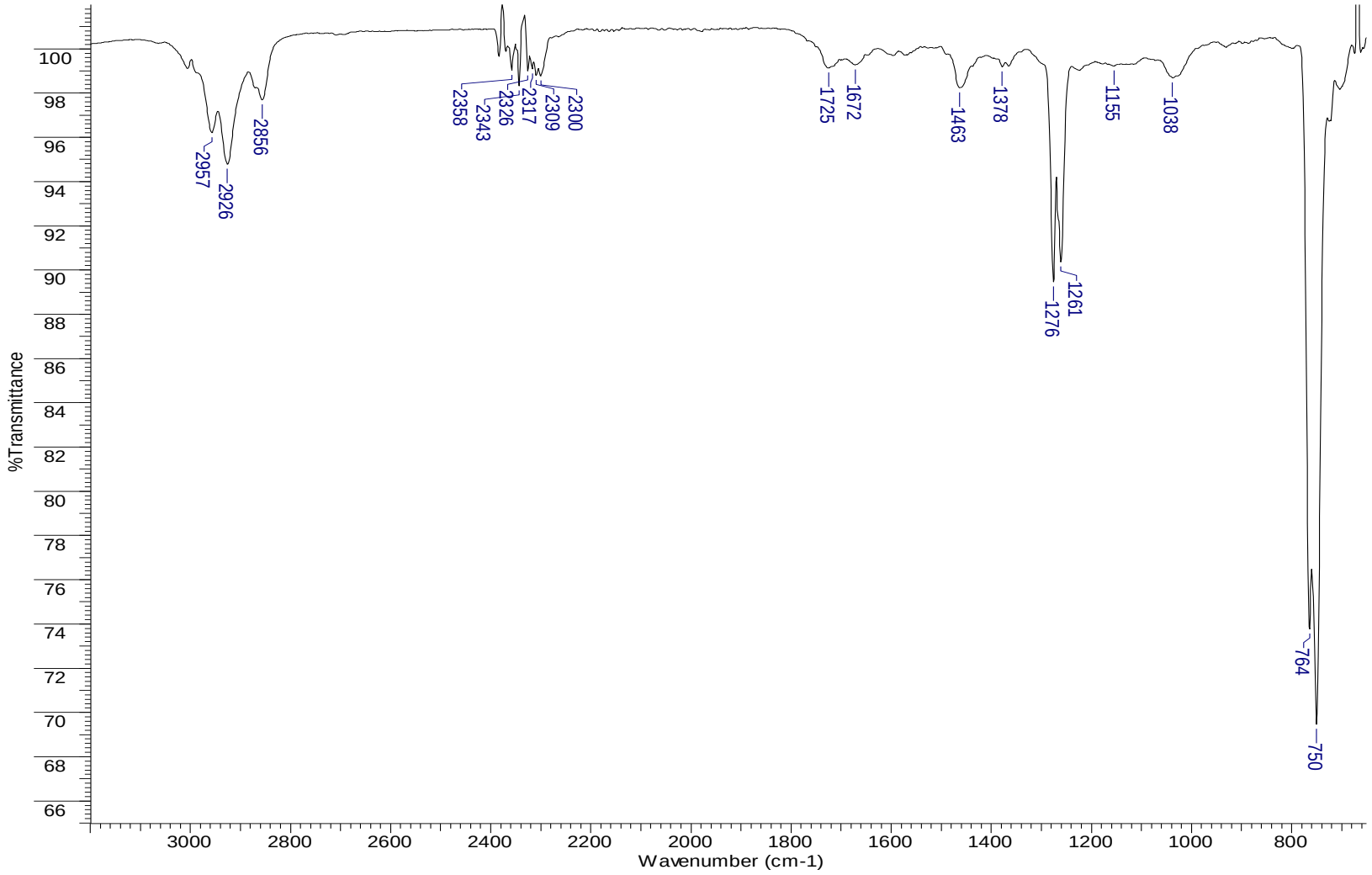

Figure A.24. ATR-IR spectrum of compound **8**.

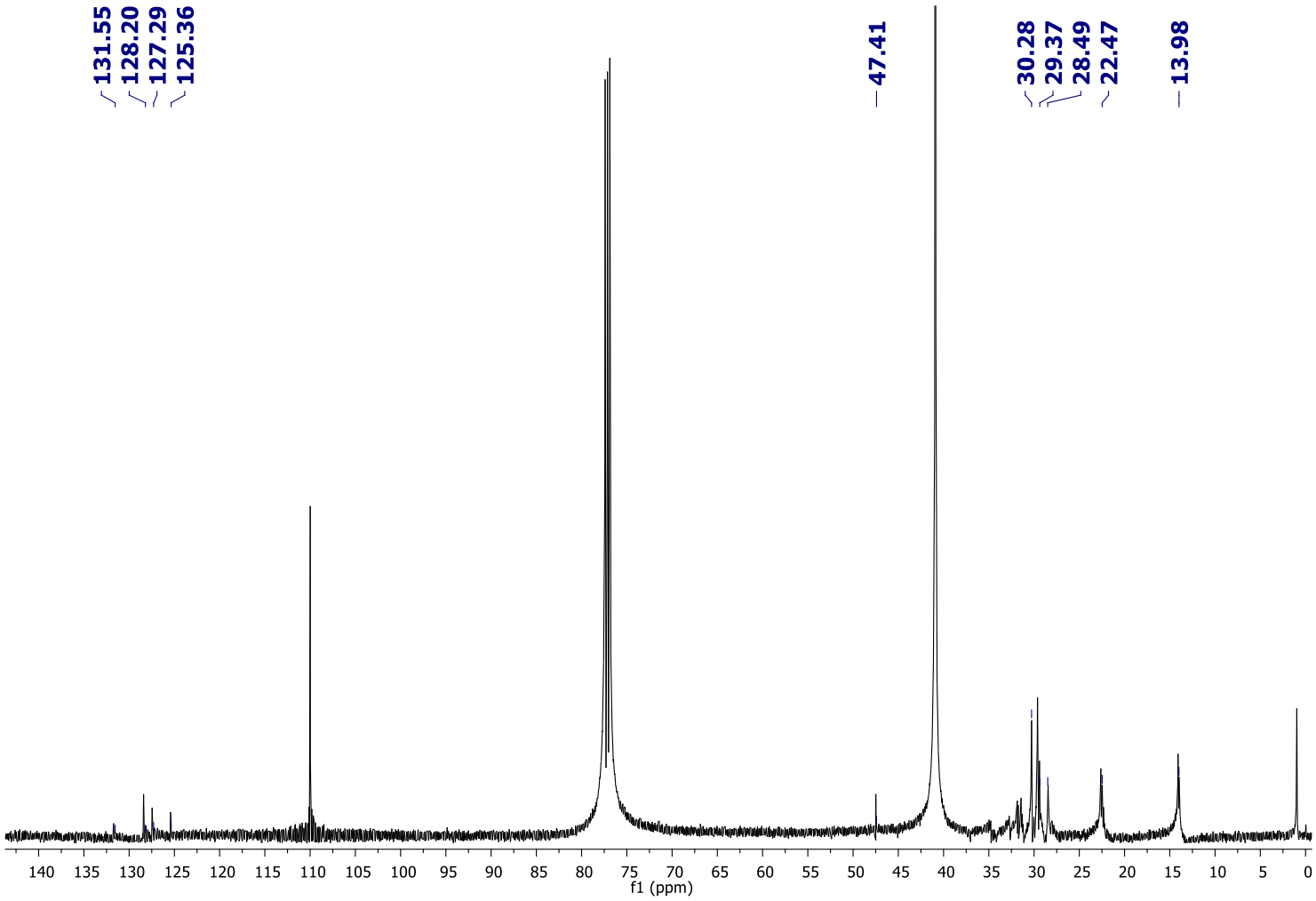

Figure A.25. ^{13}C NMR spectrum of compound **8**.

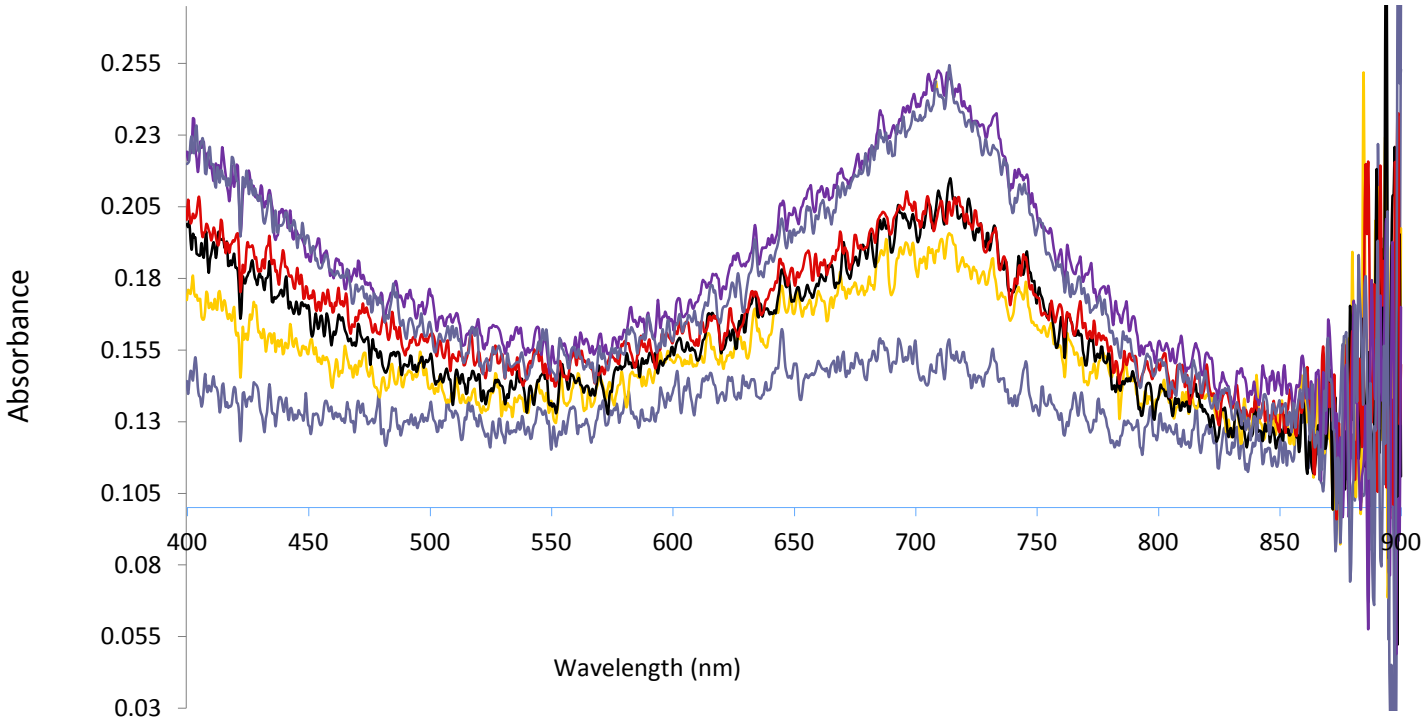

Figure A.26. UV-Vis spectrum of compound **8** in $CHCl_3$.

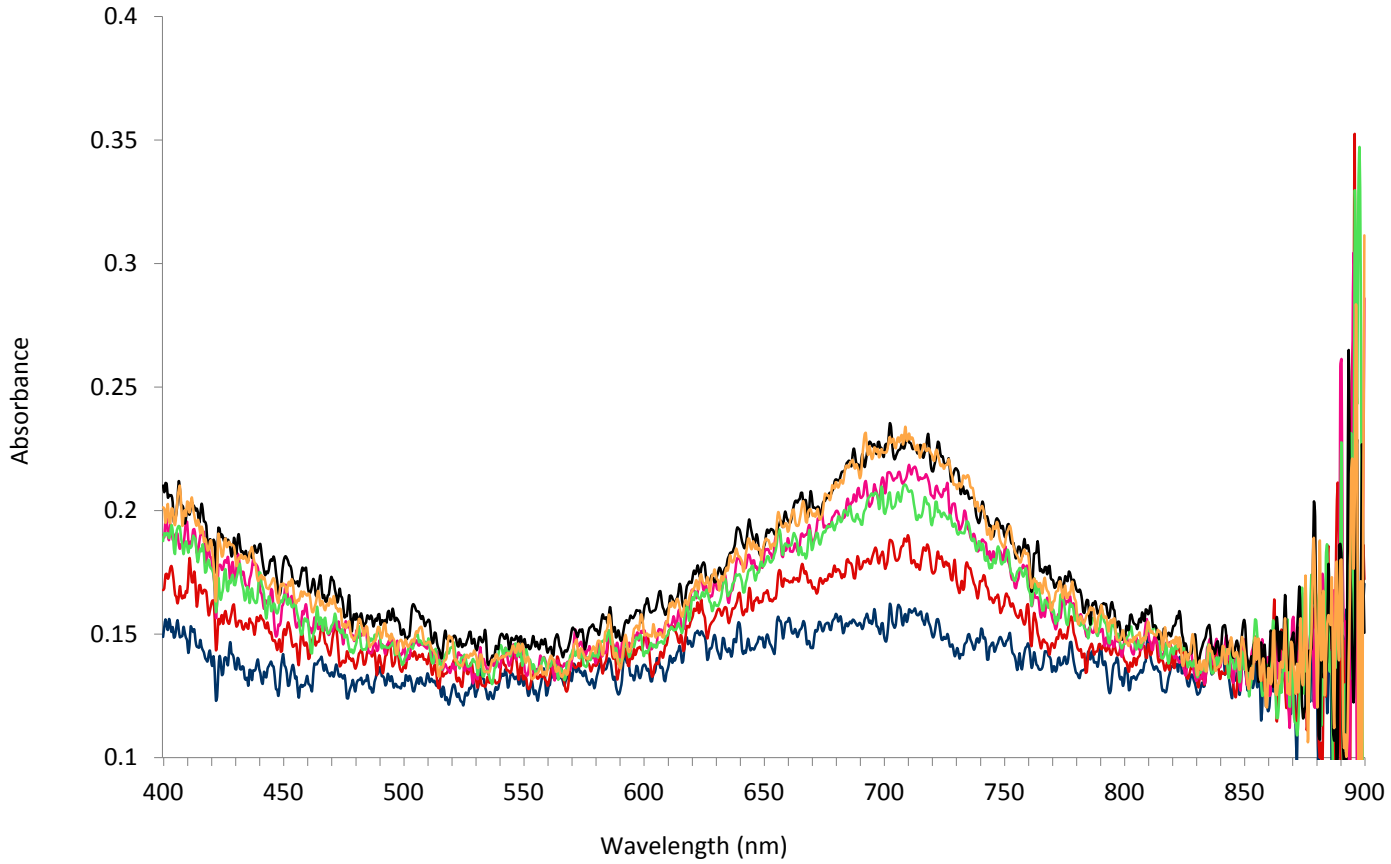

Figure A.27. UV-Vis spectrum of compound **8** in THF.

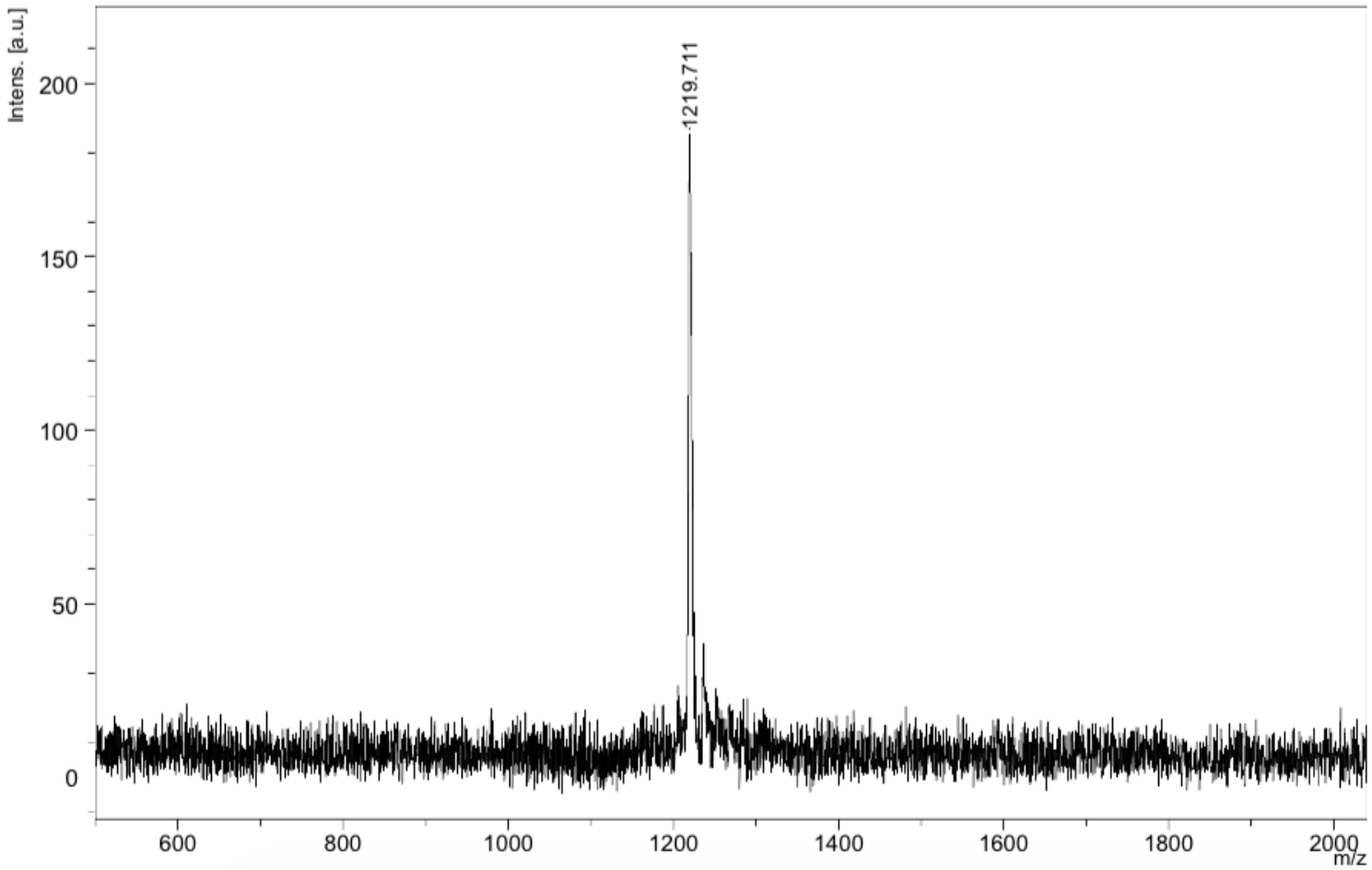

.

Figure A.28. Mass spectrum of compound **9**.

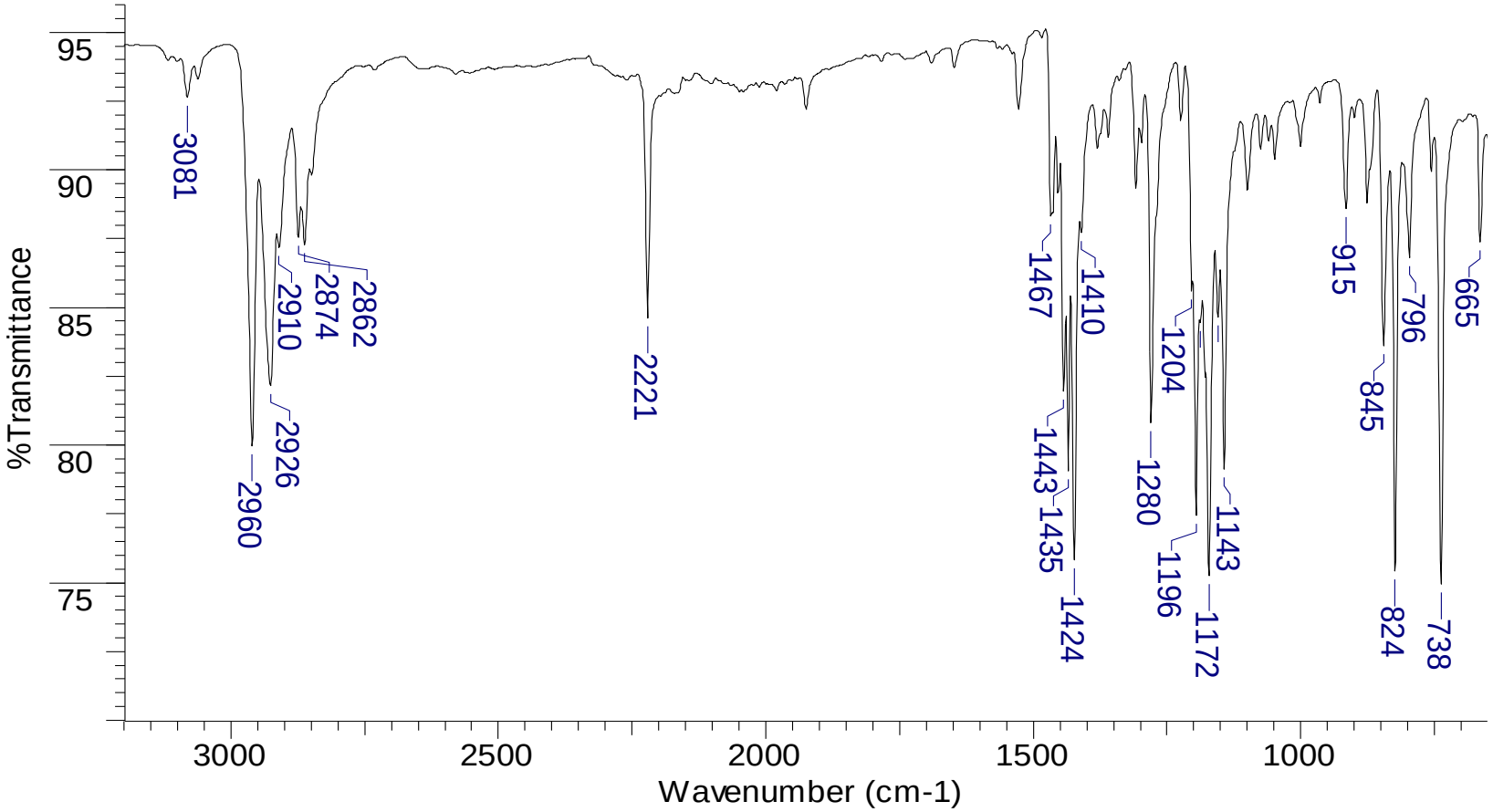

Figure A.29. ATR-IR spectrum of compound **9**.

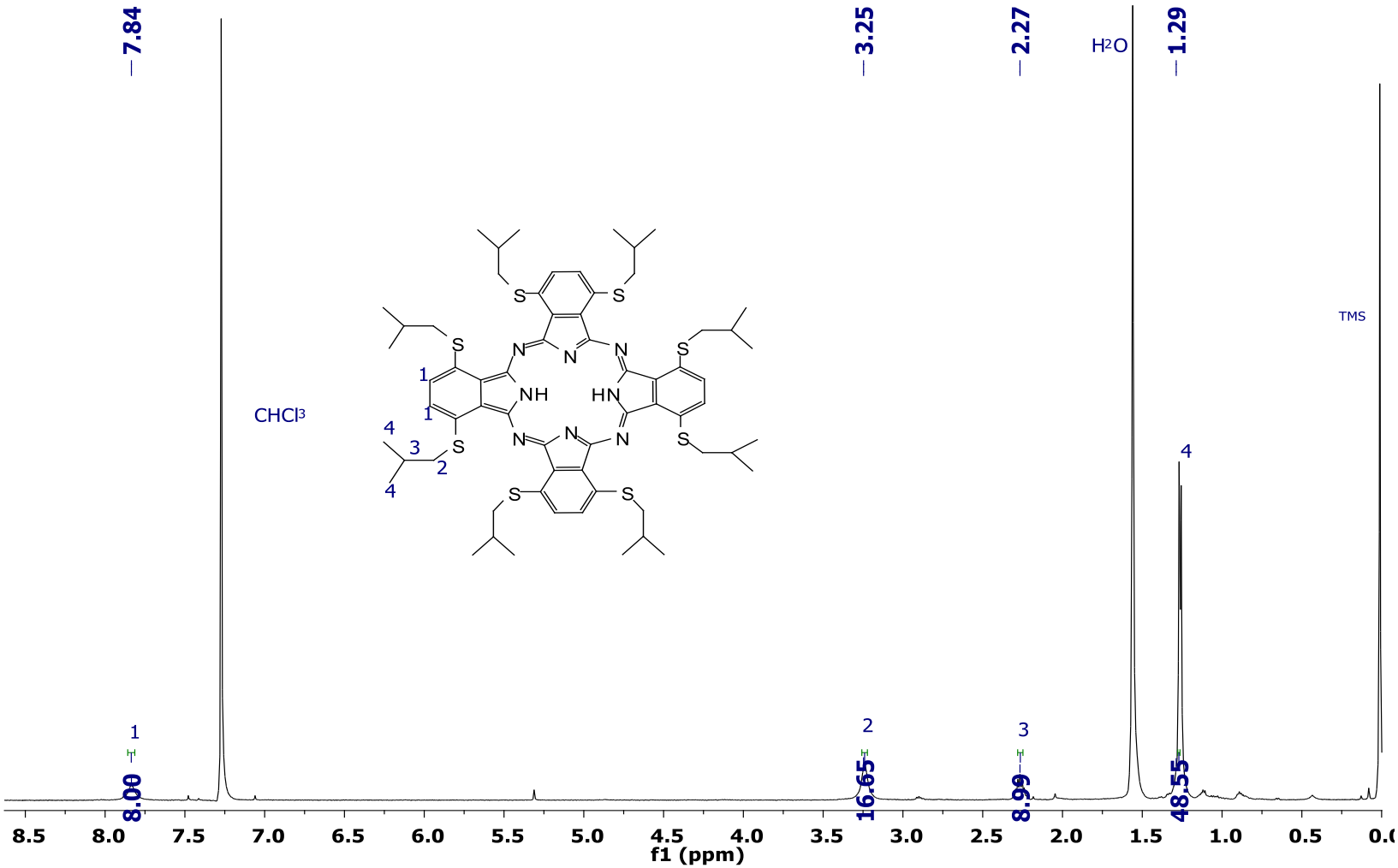

Figure A.30. ^{1}H NMR spectrum of compound **9**.

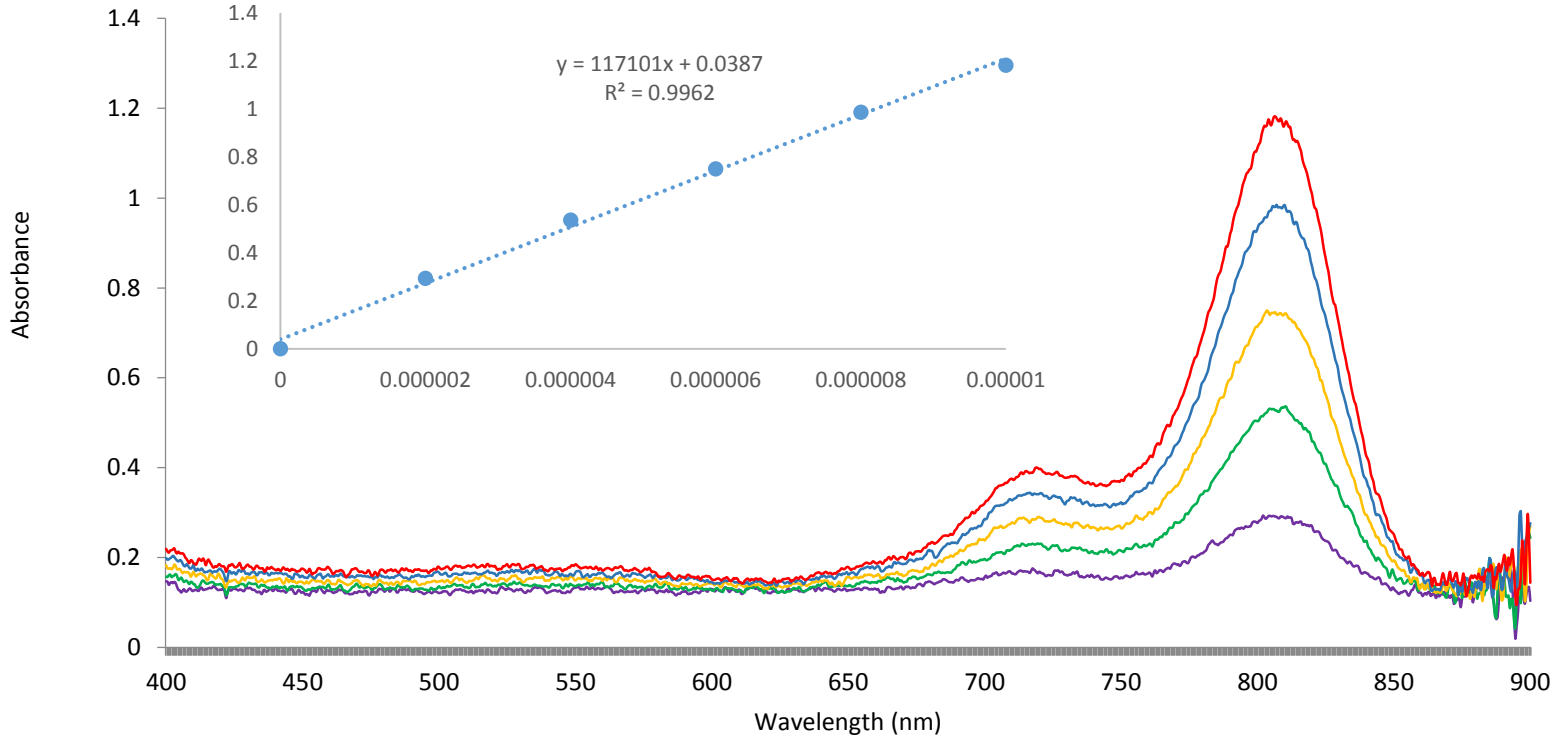

Figure A.31. UV-Vis spectrum of compound **9** in $CHCl_3$.

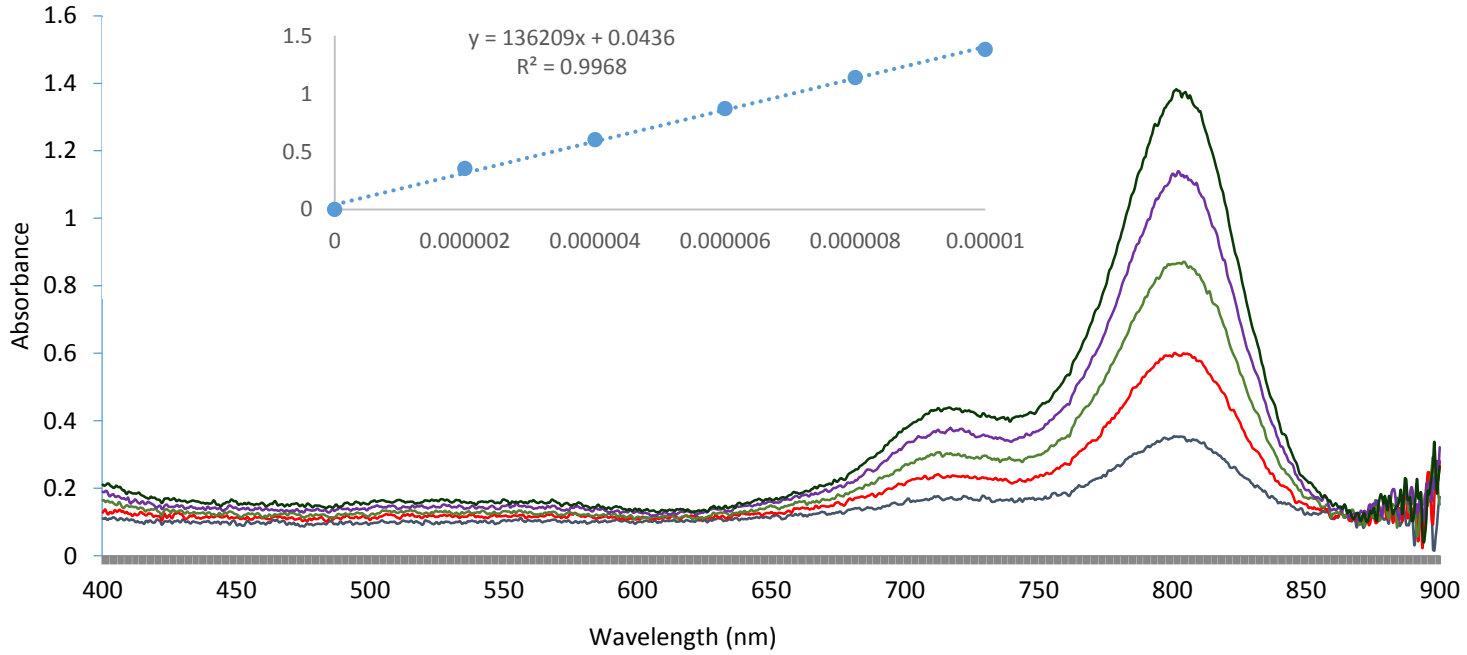

Figure A.32. UV-Vis spectrum of compound **9** in THF.

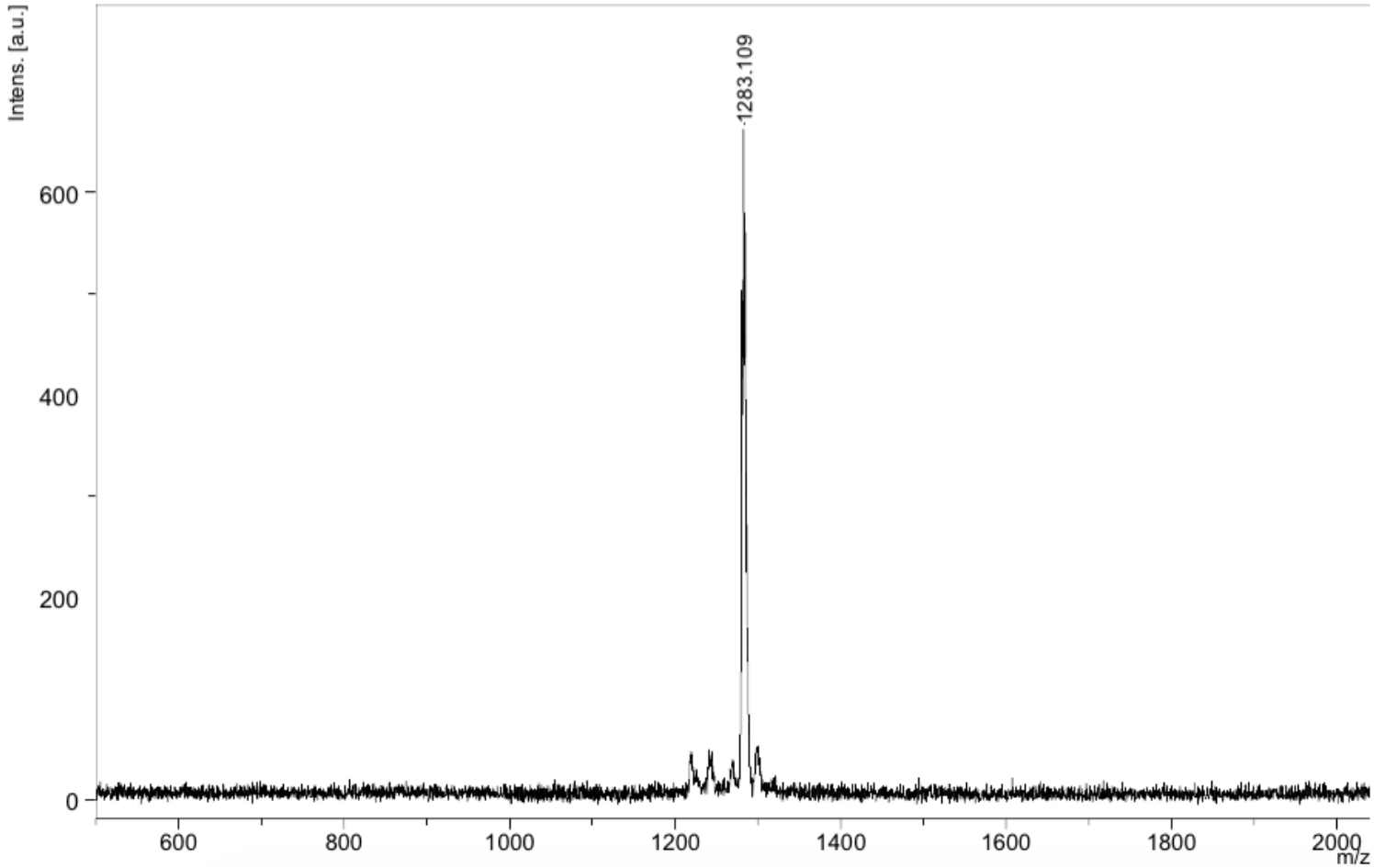

Figure A.33. Mass spectrum of compound **10**.

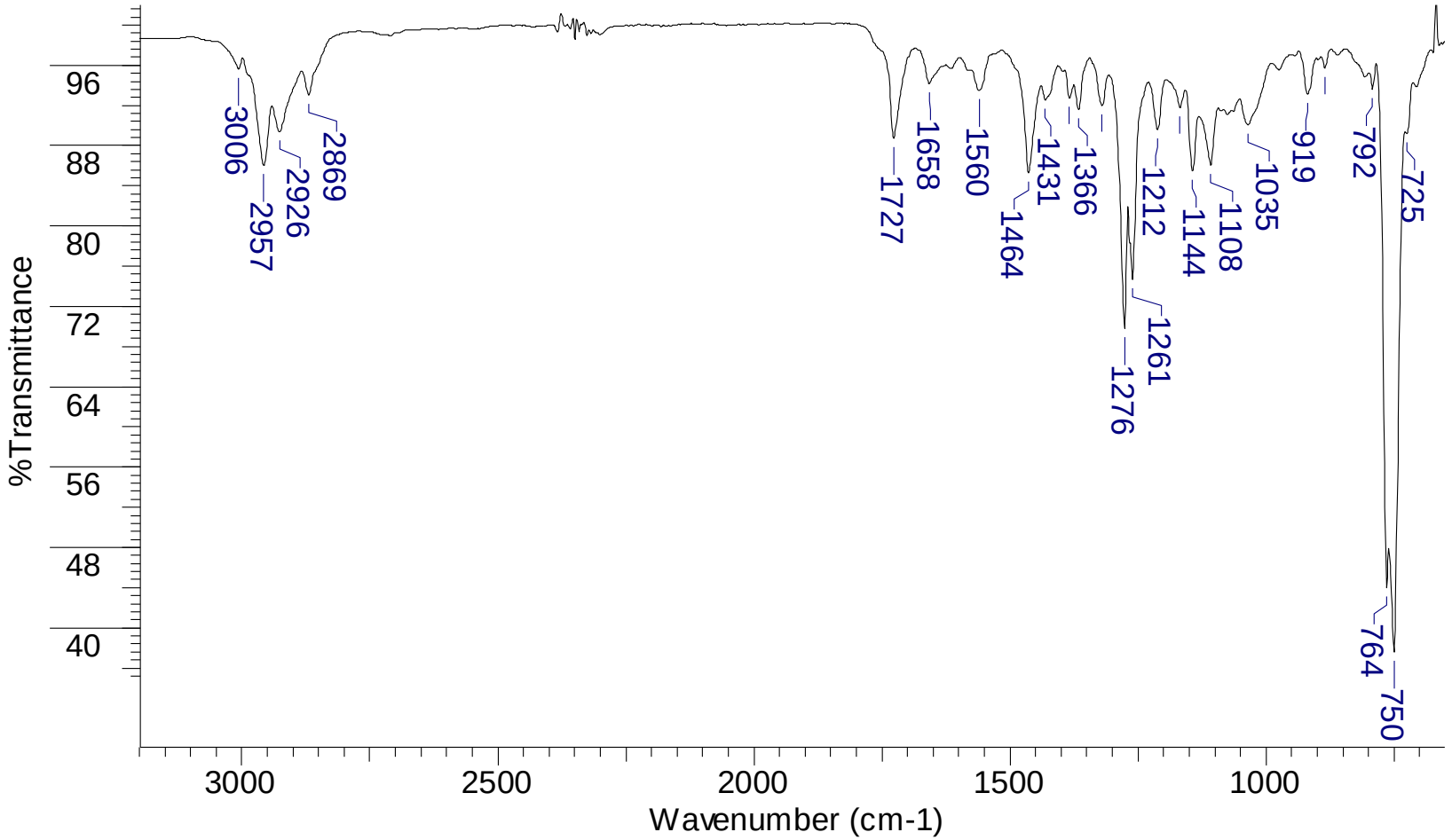

Figure A.34. ATR-IR spectrum of compound **10**.

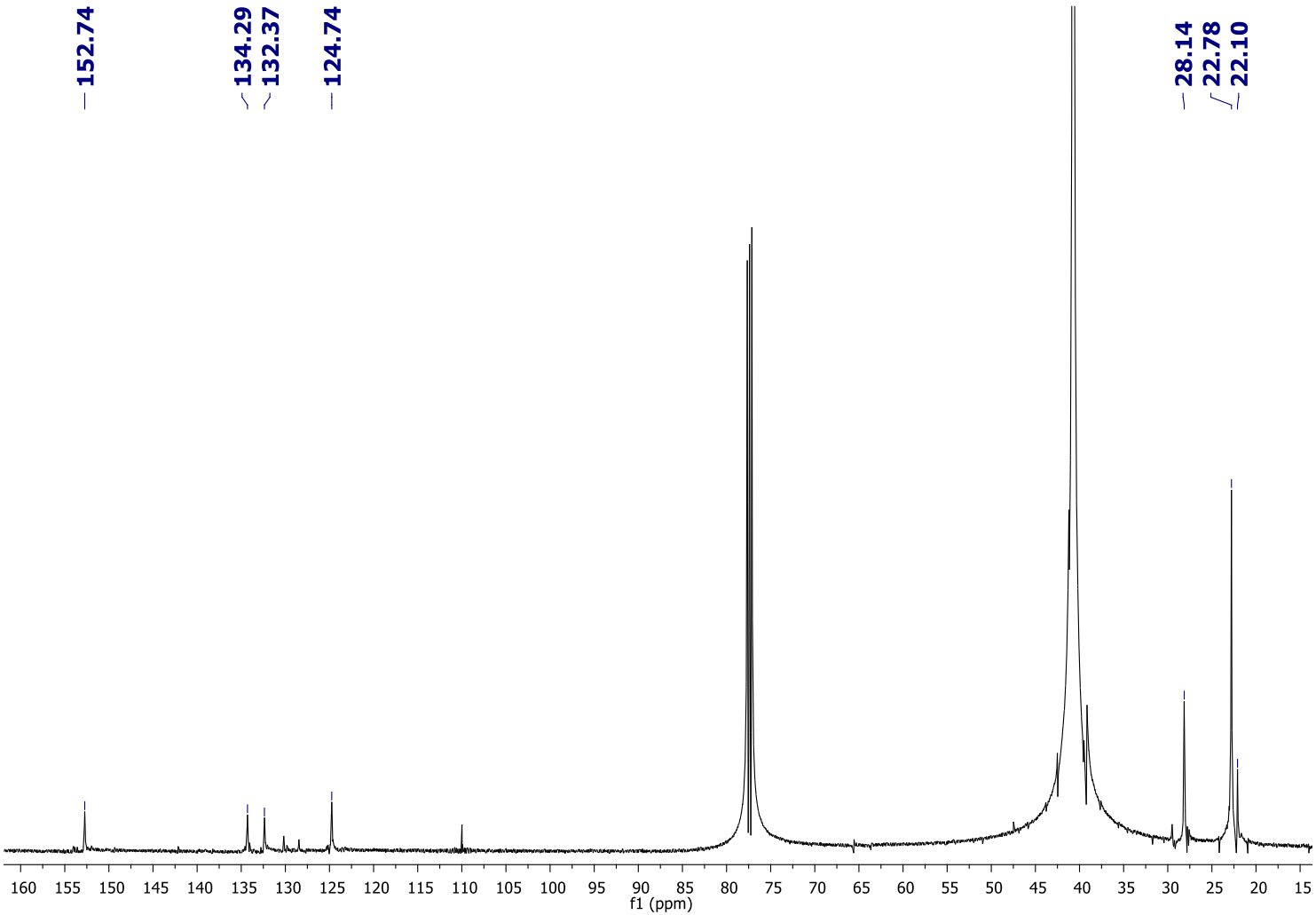

Figure A.35. ^{13}C NMR spectrum of compound **10**.

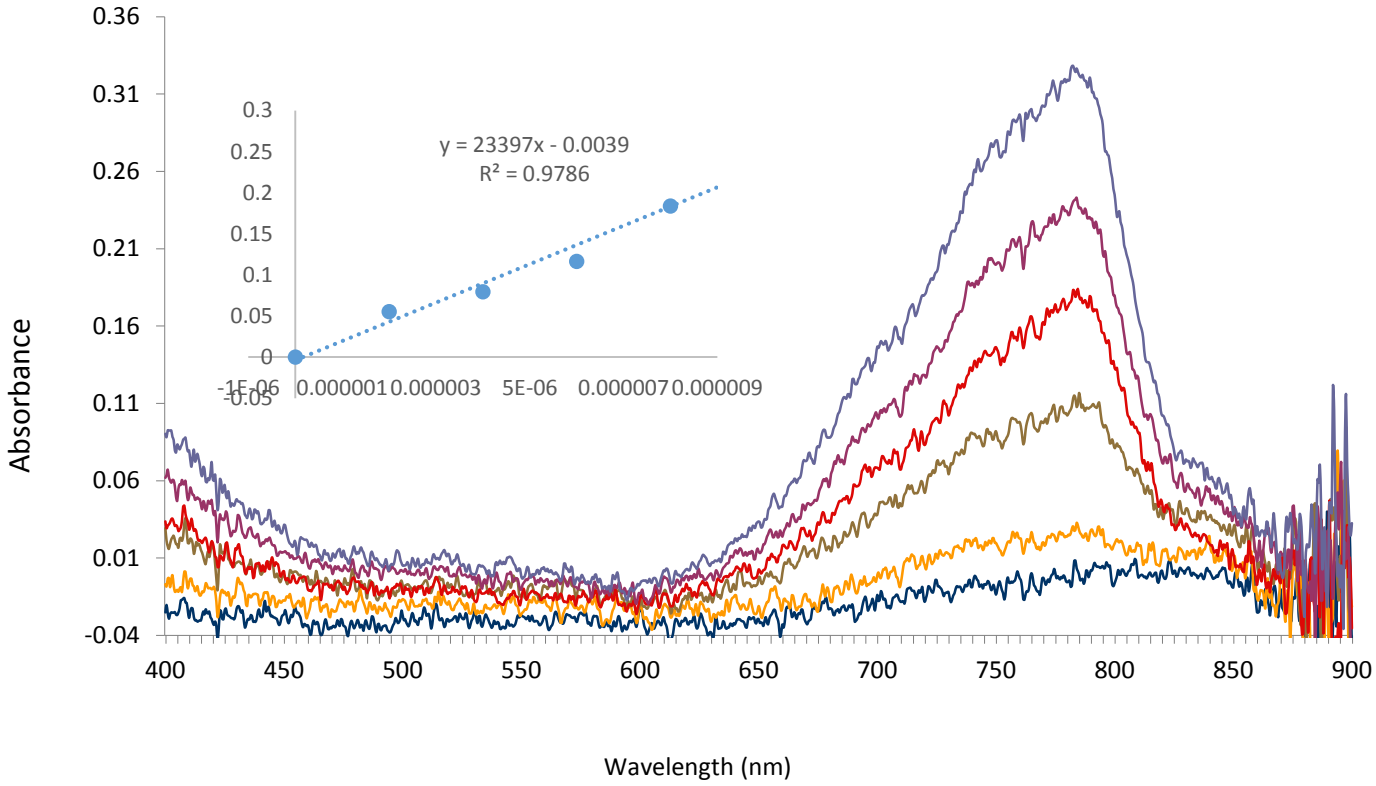

Figure A.36. UV-Vis spectrum of compound **10** in $CHCl_3$.

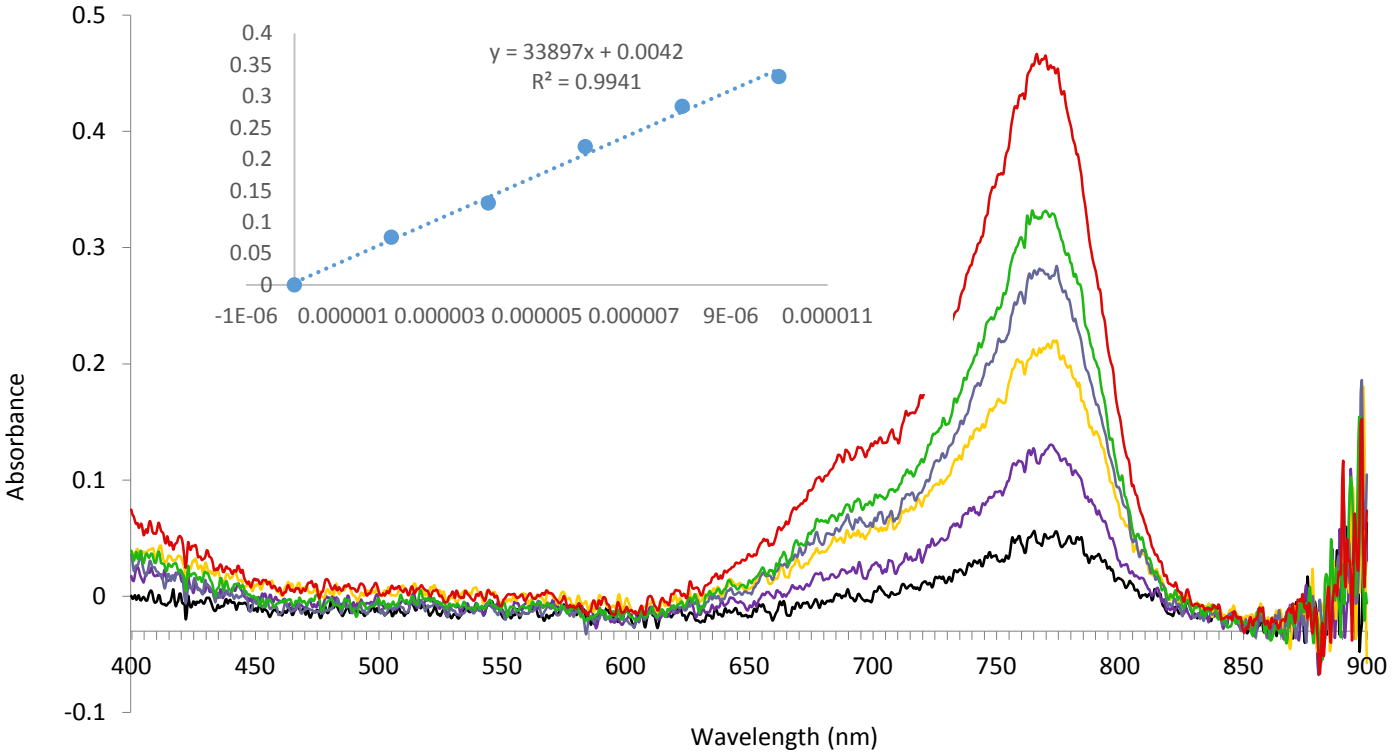

Figure A.37. UV-Vis spectrum of compound **10** in THF.

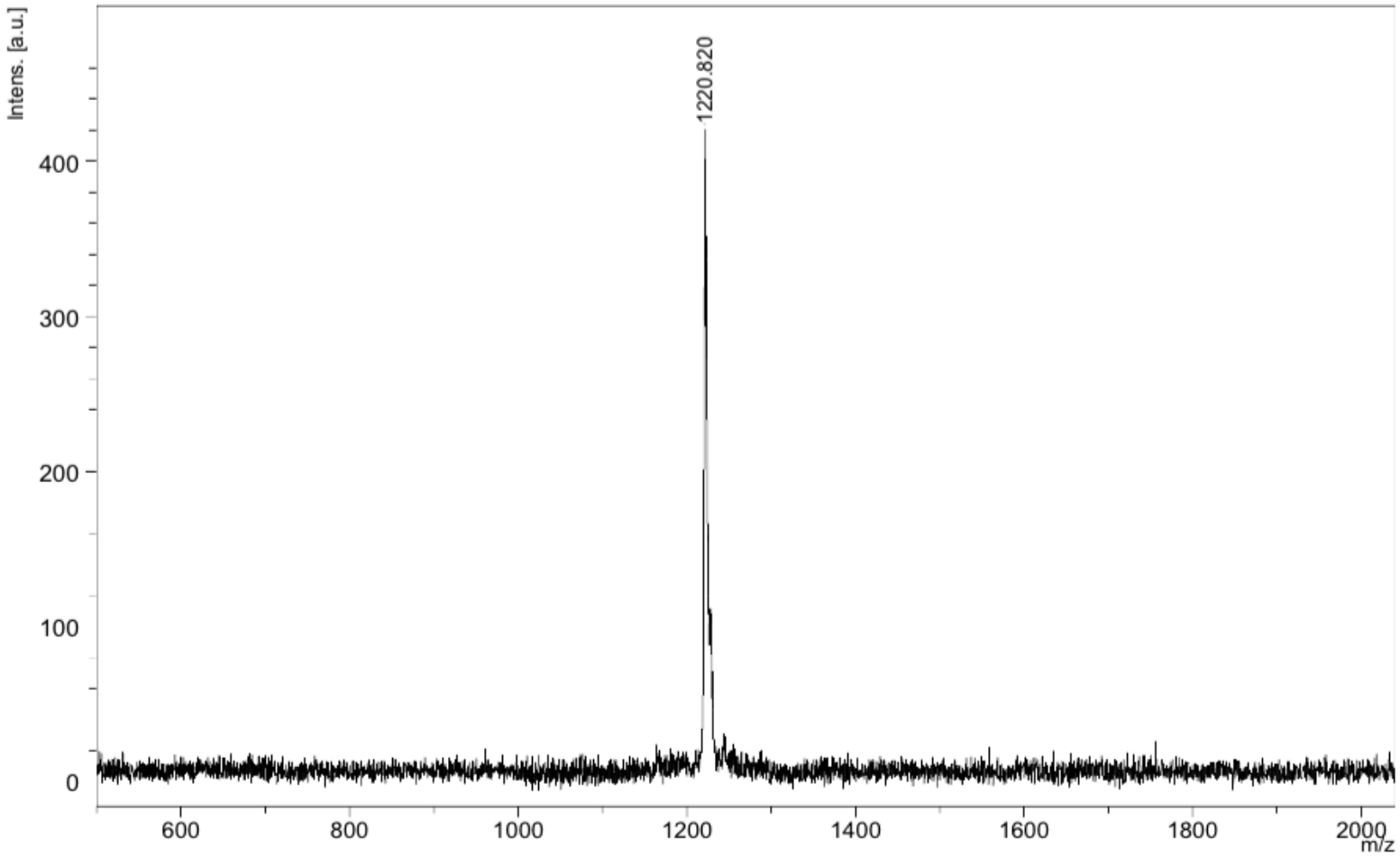

Figure A.38. Mass spectrum of compound **11**.

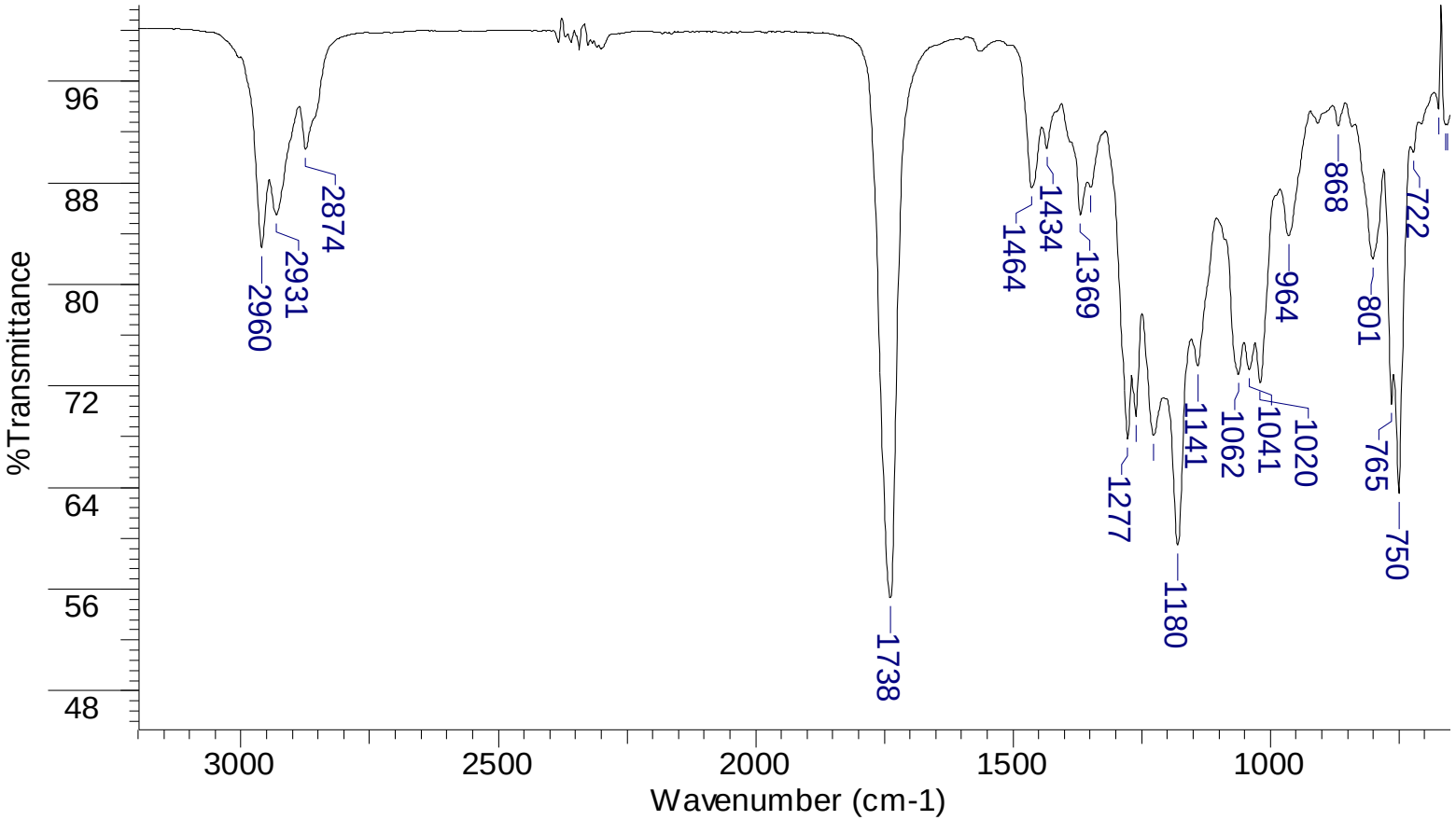

Figure A.39. ATR-IR spectrum of compound 11.

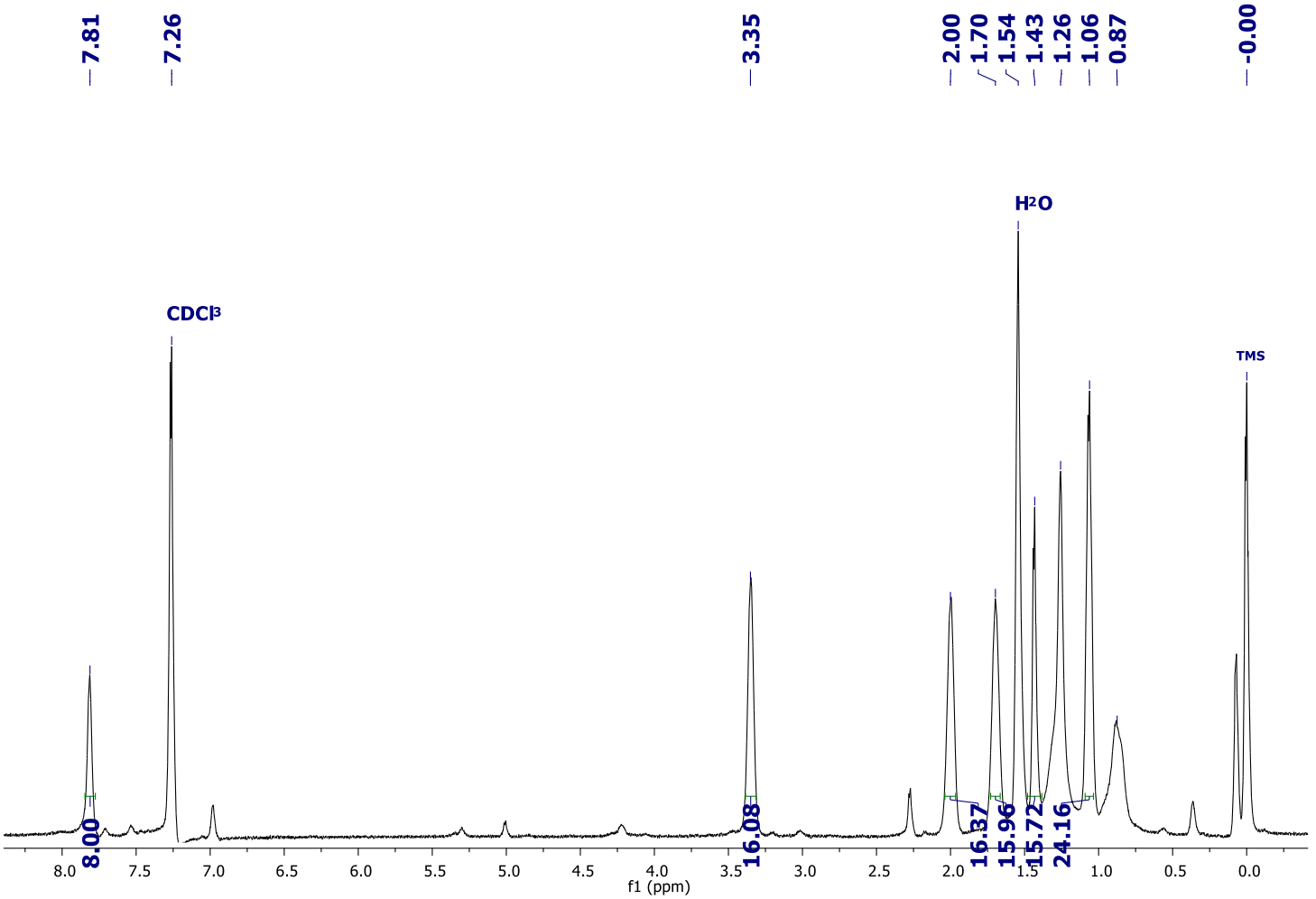

Figure A.40. ^{1}H NMR spectrum of compound **11**.

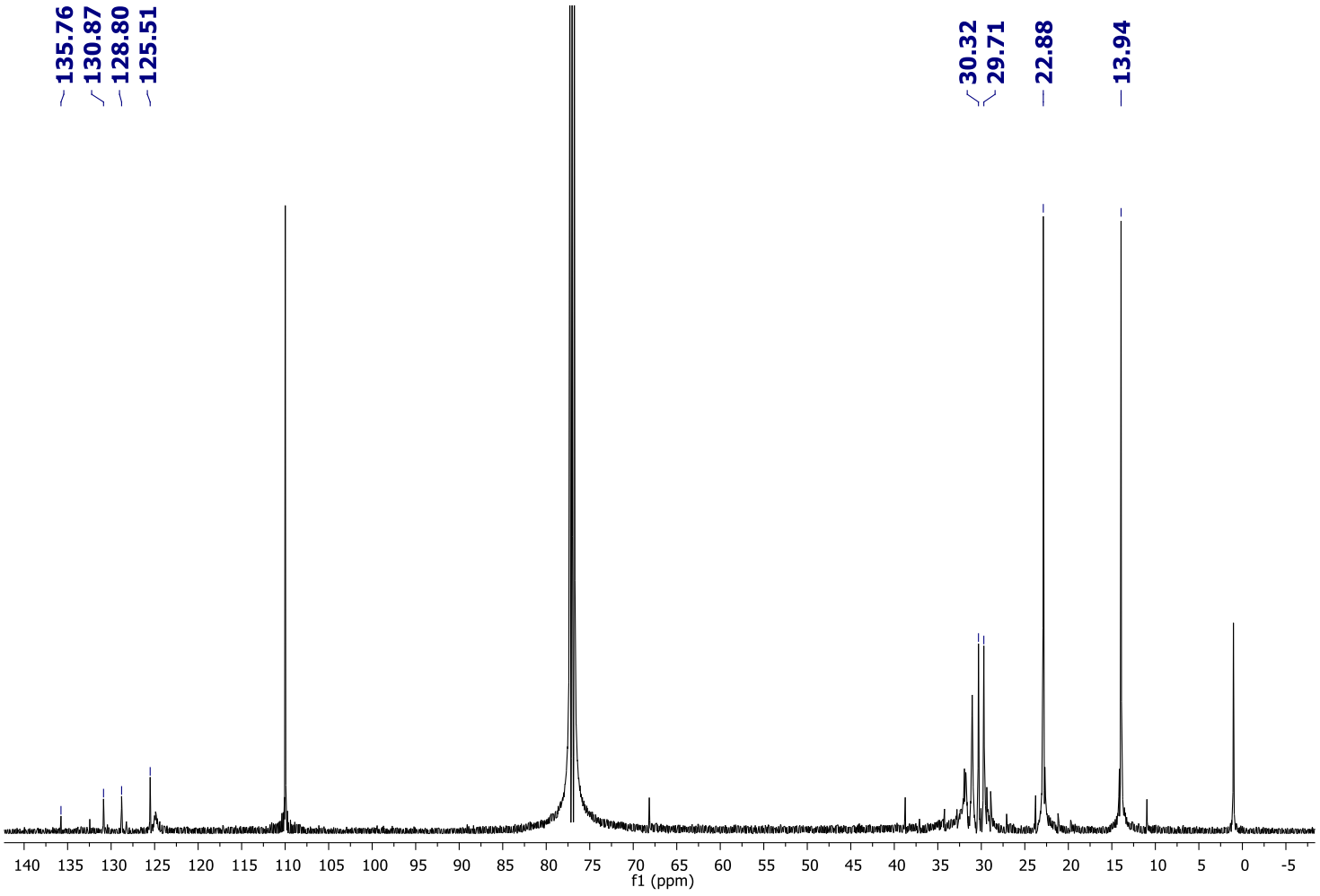

Figure A.41. ^{13}C NMR of compound **11**.

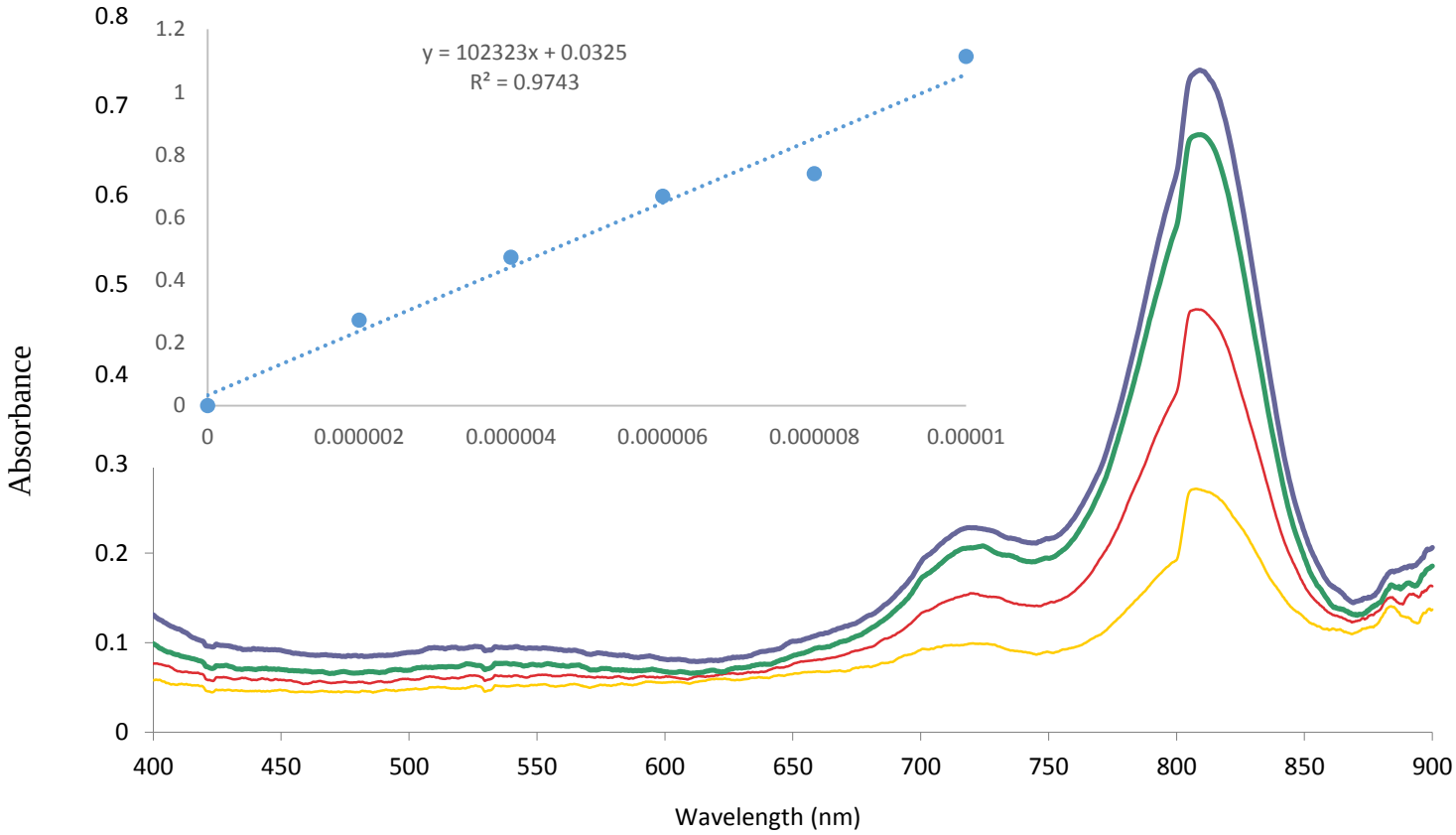

Figure A.42. UV-Vis spectrum of compound **11** in $CHCl_3$.

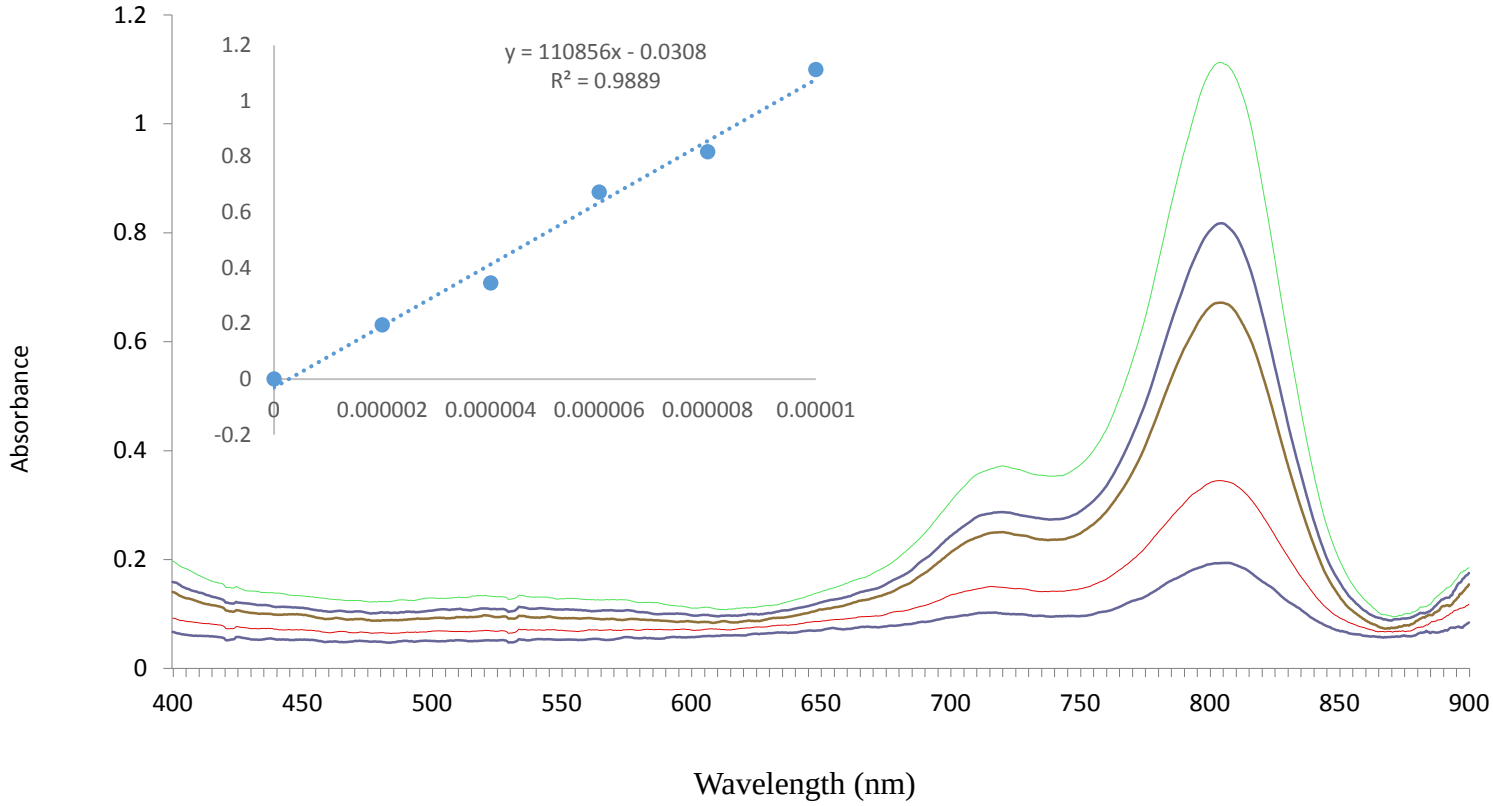

Figure A.43. UV-Vis spectrum of compound **11** in THF.

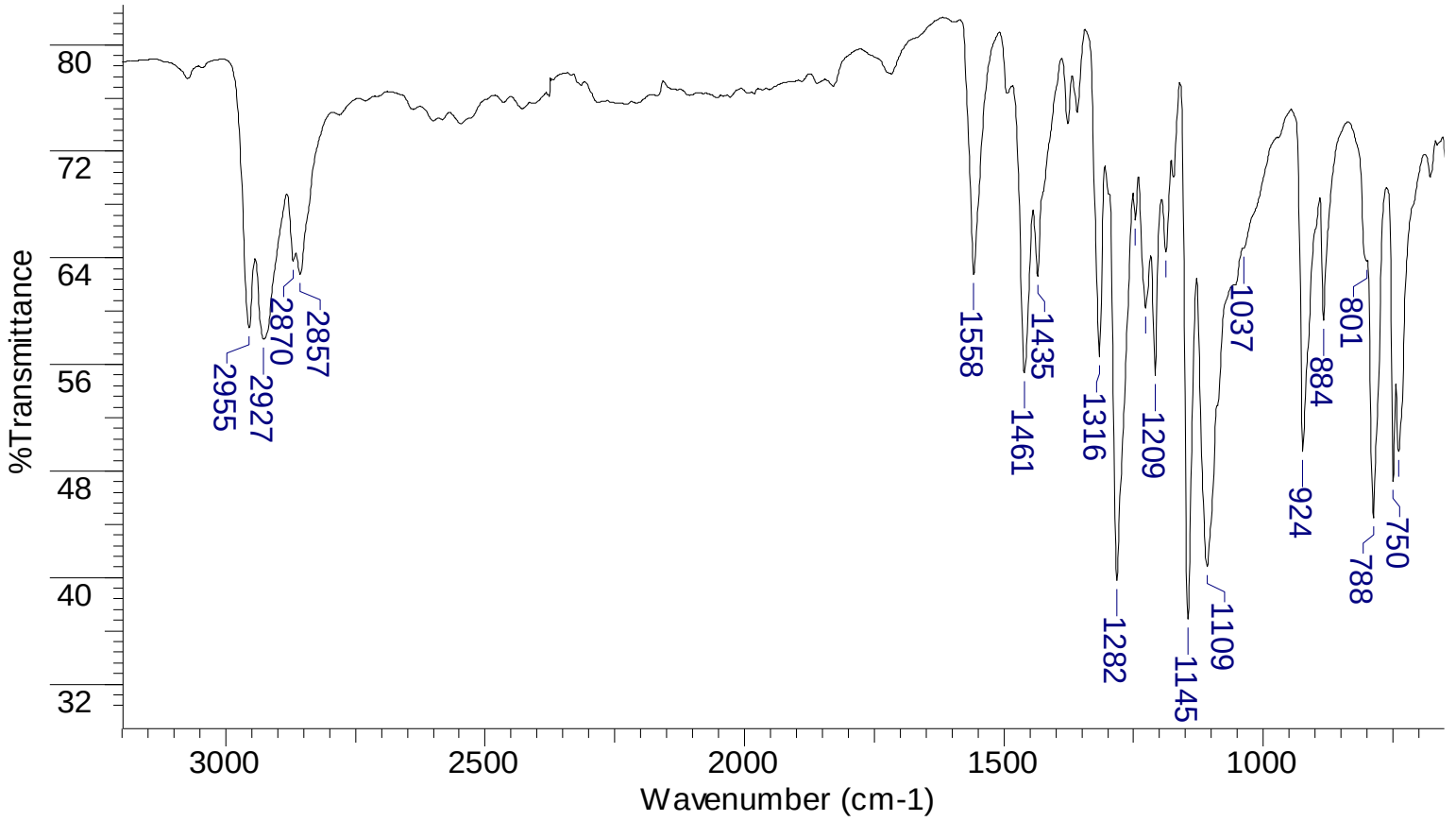

Figure A.44. ATR-IR spectrum of compound 12.

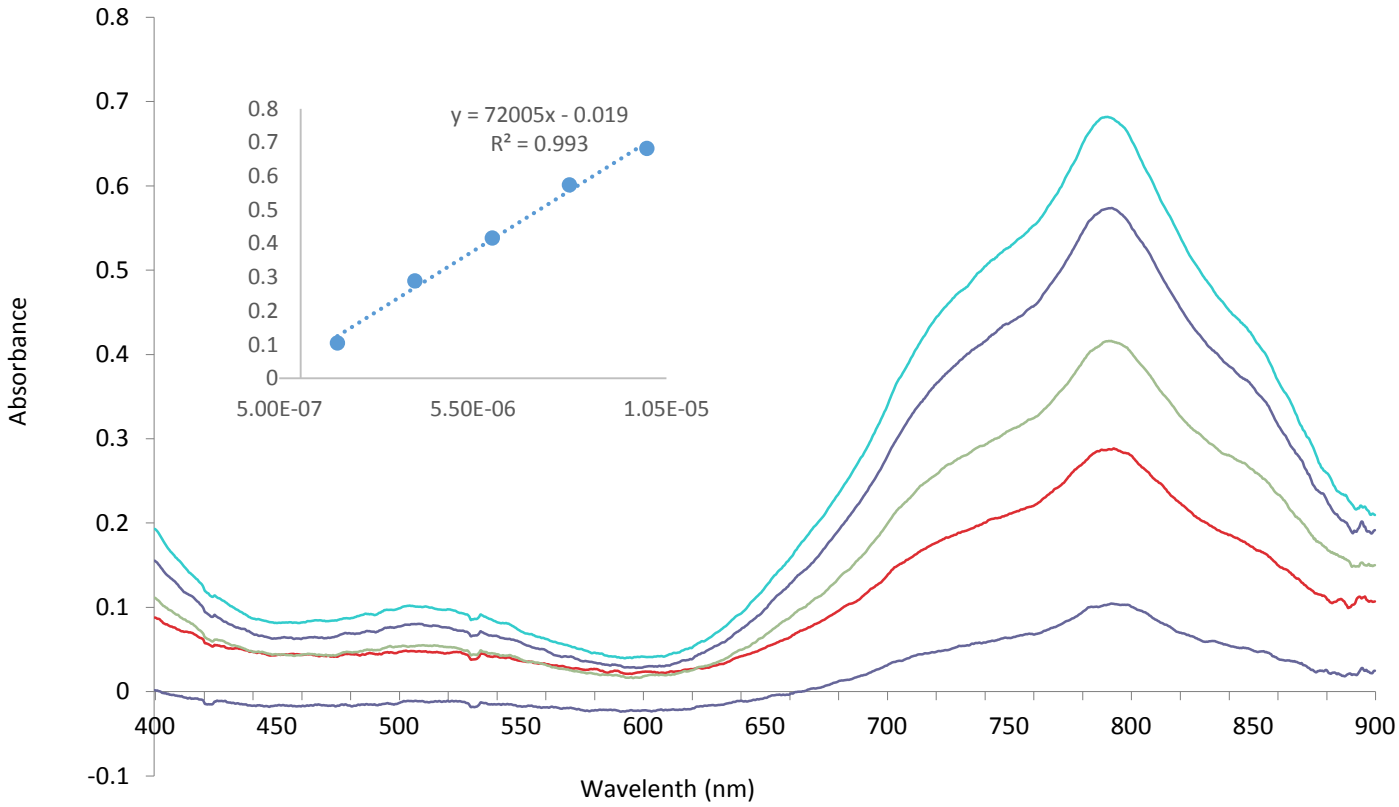

Figure A.45. UV-Vis spectrum of compound **12** in $CHCl_3$.

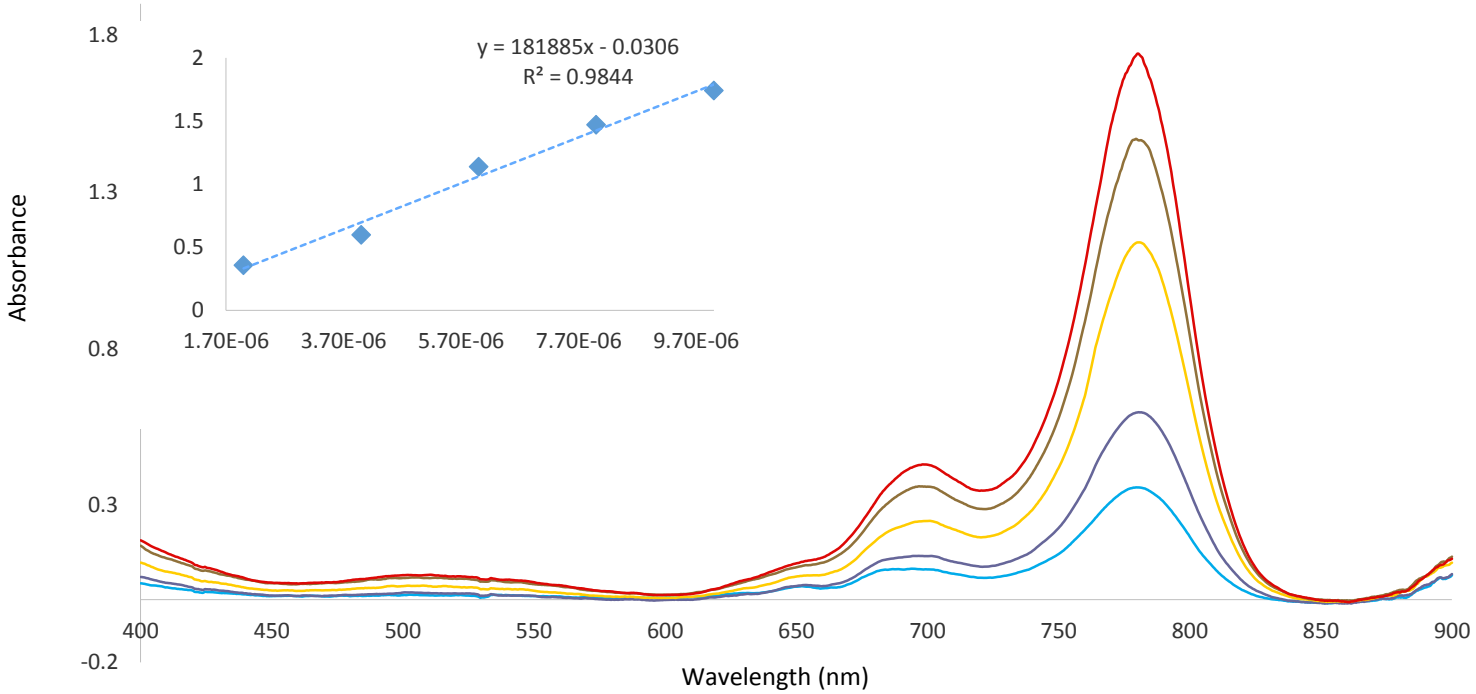

Figure A.46. UV-Vis spectrum of compound **12** in THF.

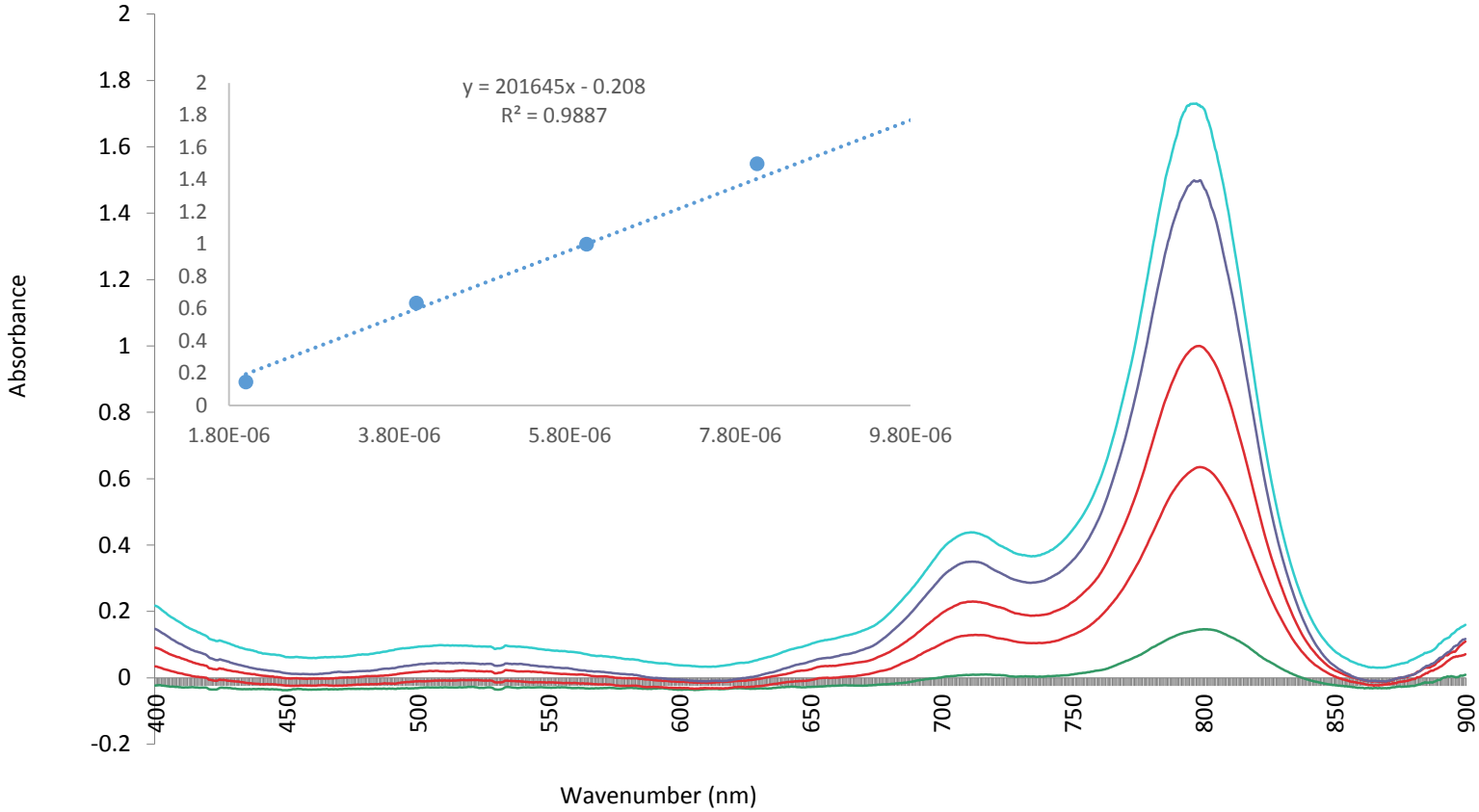

Figure A.47. UV-Vis spectrum of compound **12** in DMSO.

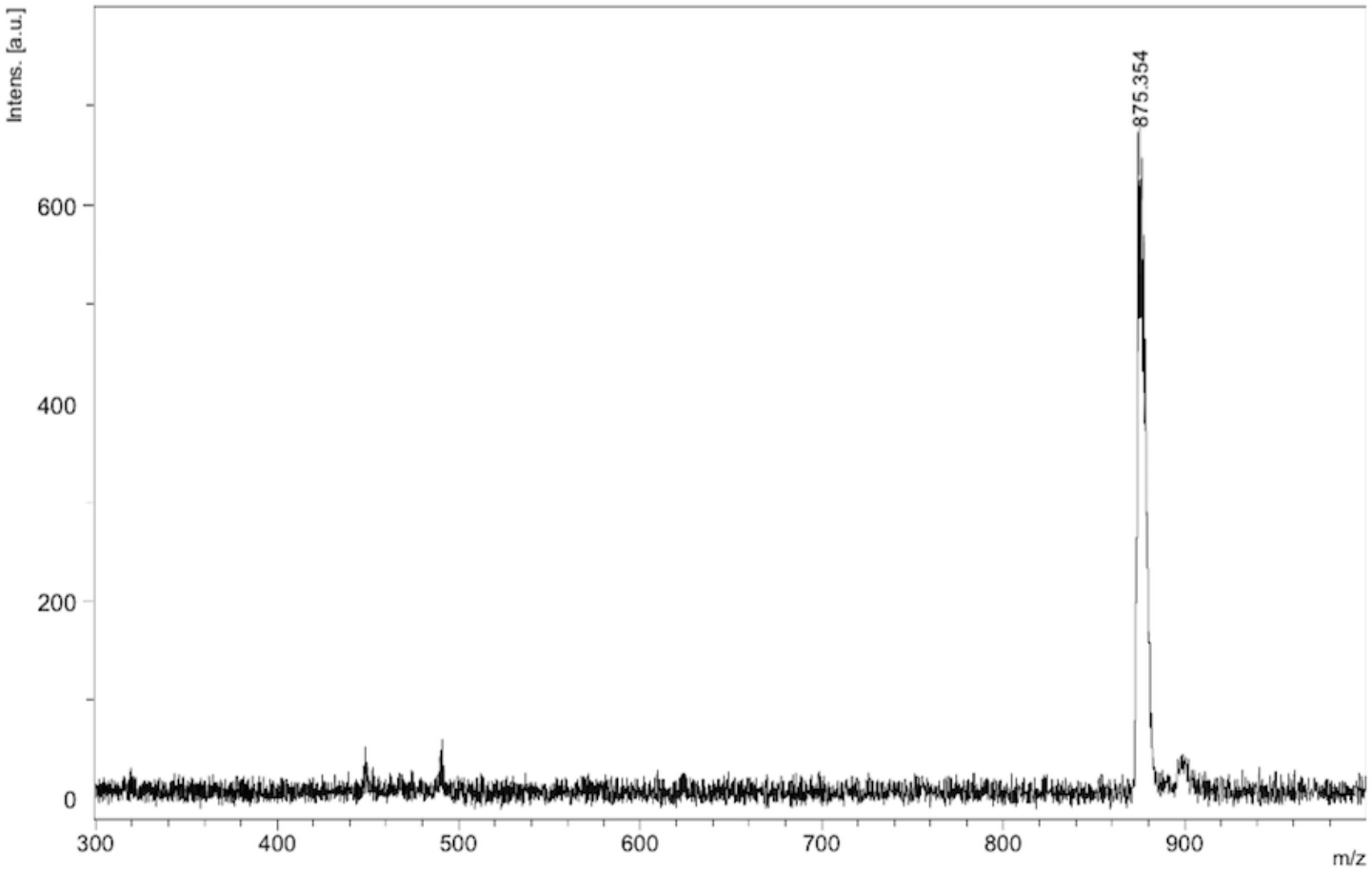

Figure A.48. Mass spectrum of compound **13**.

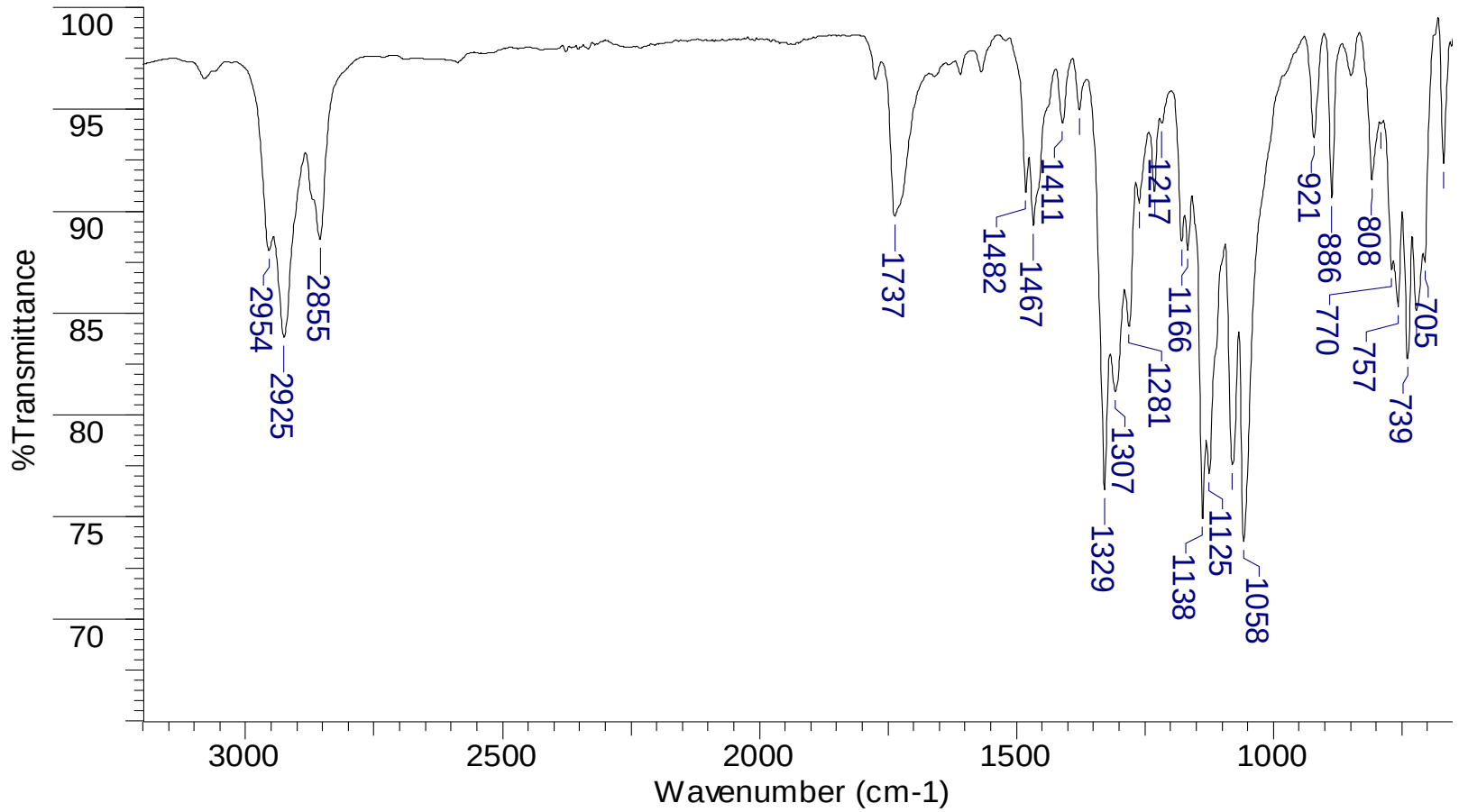

Figure A.49. ATR-IR spectrum of compound **13**.

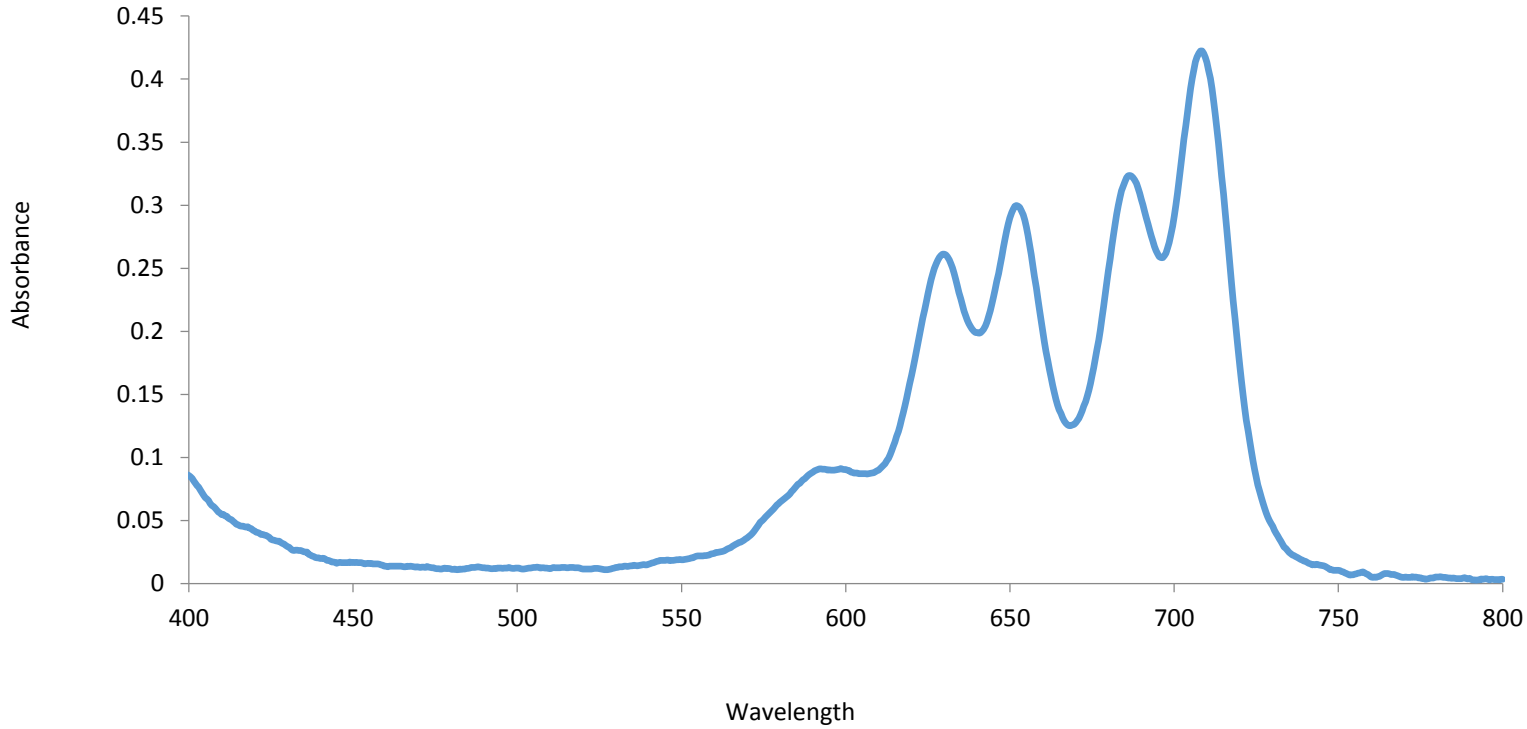

Figure A.50. UV-Vis spectrum of compound **13** (2 μM) in $CHCl_3$.